DISPLACEMENT OF ADSORBED POLYMERS

*A systematic study of
segment-surface interactions*

Gerrit van der Beek

DISPLACEMENT OF ADSORBED POLYMERS

A systematic study of segment-surface interactions

Proefschrift
ter verkrijging van de graad van doctor
in de landbouw- en milieuwetenschappen
op gezag van de rector magnificus,
dr. H.C. van der Plas,
in het openbaar te verdedigen
op woensdag 12 juni 1991
des namiddags te vier uur in de Aula
van de Landbouwuniversiteit te Wageningen.

aan mijn moeder

Stellingen

I

Als de geadsorbeerde hoeveelheid polymeer afneemt, kan onder bepaalde omstandigheden de hydrodynamische laagdikte juist toenemen.

Dit proefschrift, hoofdstuk 4.

II

Bij verstrooiingsexperimenten kan het versmerende effect van een golflengteverdeling juist bijdragen tot een verbetering van de resolutie.

III

Wanneer een aggregerend systeem ijle vlokken vormt, dan is het resulterende gel hydrodynamisch gezien relatief dicht.

Bremer, L. G. B., van Vliet, T., Walstra, P. *J. Chem. Soc., Faraday Trans. 1* **1989**, 85, 3359.

IV

Het constant zijn van de geadsorbeerde hoeveelheid in de tijd is een noodzakelijke doch onvoldoende voorwaarde voor het in evenwicht zijn van een polymeerlaag.

Dit proefschrift, hoofdstuk 3.

V

Voor de bepaling van de treindichtheid van geadsorbeerd polymeer is het aanzienlijk eenvoudiger de kernspinrelaxatie te meten van het oplosmiddel dan die van de treinen zelf.

Barnett, K. G.; Cosgrove, T.; Vincent, B.; Sissons, D. S.; Cohen Stuart, M. A. *Macromolecules* **1981**, 14, 1018.
Dit proefschrift, hoofdstuk 5.

VI

In hechtingsonderzoek hecht men te weinig waarde aan de intrinsieke (reversibele) wisselwerking tussen polymeersegmenten en oppervlakken.

VII

Voor microemulsies met een ionogene oppervlakte-actieve component wordt vaak ten onrechte verondersteld dat de zoutconcentratie in de waterrijke fase gelijk is aan die in de intiële electrolietoplossing.

Van Aken, G. A. In *The Structure, Dynamics and Equilibrium Properties of Colloidal Systems*; Bloor, D. M., Wyn-Jones, E., Eds.; NATO ASI Series; Kluwer Academic Publishers; Dordrecht, 1990; p 279.

VIII

Een laag onderzoeksbudget stimuleert de creativiteit van de onderzoeker.

IX

Een proefschrift behoort een smaakmaker te zijn voor verder onderzoek.

Leermakers, F. A. M., proefschrift, Wageningen, 1988, stelling XI.

Gerrit van der Beek
Displacement of Adsorbed Polymers
Wageningen, 12 juni 1991

Table of Contents

Chapter 1

Introduction

1.1. Flexible polymers

Linear polymer molecules can be conceptualized as long strings of repeating monomer units. For homopolymers all these units are identical. Polymers composed of chemically different segments are called copolymers.

In solution a flexible polymer molecule has a dynamically changing conformation which can be described as a random coil. The coil has the shape of a globular blob, with a size and density that depends on the solvent quality, the polymer concentration, and characteristics of the polymer chain like stiffness, length, branching, and composition of segments.

The spatial structure of a polymer molecule changes upon adsorption from solution onto a solid surface. The final conformation is a compromise between energetical factors (which tend to maximize the number of segment-surface contacts) and entropical ones (trying to maintain a relatively thick layer with many degrees of freedom). If there are many surface sites available the energy dominates and the polymer adopts a flat conformation (see Figure 1a). In this situation the surface is undersaturated.
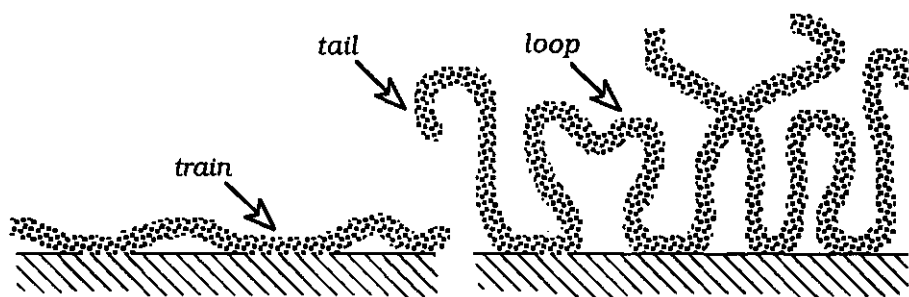
Figure 1. (a) undersaturated adsorbed polymer layer. (b) saturated adsorbed polymer layer.

As the polymer concentration in solution increases, more molecules will attach to the surface, and the entropical terms become more important. Due to the competition for surface sites, the fraction of bound segments per molecule decreases. Eventually, the surface is saturated. The amount of polymer at the surface and the conformation are then only weakly dependent on the polymer concentration. Such a saturated adsorbed layer is sketched in Figure 1b. Segments can be found in three different conformational states. Segments in *trains* are directly bound to the surface. A *loop* is a string of segments of which both ends are bound to the surface. *Tails* have only one bound end, the other end protrudes into the solution. Just as in the case of free polymer molecules, adsorbed ones should not be considered to have a static conformation. Segments may change their conformational state as a function of time. The molecular motion of entrained segments is more restricted and anisotropic than of loop and tail segments. In principle, tails, loops, and trains can be distinguished by the difference in mobility.

The conformation of a particular polymer adsorbed on a solid surface depends on the polymer concentration, the solvent quality, the segmental adsorption energy relative to the solvent, the density and distribution of active surface sites, and the geometry of the surface.

1.2. Applications of polymers at interfaces

Polymers at interfaces play a very important role in many industrial and biological products and processes. For instance, polymer adsorption onto colloidal particles in solution can either stabilize or destabilize dispersions.[1] Both effects depend on the polymer conformation at the surface.

The stabilizing effect of polymer adsorption occurs when particles have a thick adsorbed layer on a saturated surface. Such layers act as steric barriers for particle aggregation. Stabilization of dispersions is important in products as diverse as inks, foods, pharmaceuticals, pesticides, magnetic tapes, and paints.

Destabilization of dispersions may occur when the surface of particles is undersaturated with polymer. Long polymer molecules may then adsorb simultaneously onto two or more particles, which may cause flocculation. Flocs formed in this way are large, rigid, and open. The sediment consisting of such flocs can be easily filtrated. This destabilization effect of polymers is very helpful in water purification, soil structure improvement, paper manufacturing, mineral processing, etc.

Applications of polymers at interfaces where the strength of the polymer/surface contact plays a very important role are adhesives, coatings, and polymer composites. For instance, the mechanical properties of polymer composites is affected by the adhesion strength between polymer and reinforced filler.

Characteristic for polymers at interfaces is that one molecule may have many contacts with or in both phases. This feature of polymers increases the stability and quality of many products in which polymers at interfaces are involved.

For more examples of applications of polymers at interfaces, the reader is referred to a paper by Eirich.[2]

1.3. Free energy contributions for polymer adsorption

Polymer molecules only adsorb from solution onto a surface if the total Gibbs free energy for this process decreases. Solvents from which a polymer does not adsorb onto a substrate may be called *displacers* for that particular polymer/substrate system. Apparently, the total free energy for polymer adsorption from displacers increases. The following terms contribute to the free energy for the exchange of one polymer chain from the solution against solvent molecules at the surface.

1) The polymer *adsorption energy* with respect to the solvent. This is the driving force for adsorption. In theoretical treatments, the adsorption energy per segment is usually characterized by a χ_s parameter, first introduced by Silberberg[3]. This parameter is defined as the adsorption energy difference between a polymer segment and a solvent molecule, in units kT. The χ_s parameter is

counted positive if the polymer adsorbs preferentially from the solvent. The effective adsorption energy per polymer molecule is then equal to $-\chi_s kT$ times the number of adhered segments per molecule.

2) The loss of *conformational entropy* experienced by an adsorbed polymer molecule. Each segment in the surface layer has less orientational freedom than a segment in the bulk solution. This entropy loss inhibits polymer adsorption. The Gibbs free energy per segment which corresponds to this entropical effect may be called the critical adsorption energy $\chi_{sc} kT$. The χ_{sc} parameter represents the value of χ_s at the adsorption/desorption transition; long polymer molecules do not adsorb if $\chi_s < \chi_{sc}$.

3) The *mixing energy* per polymer molecule. The concentration of segments at the interface is higher than in the bulk solution. The exchange of a solvent molecule at the surface by a polymer segment leads to a change in mixing energy. The mixing energy may be expressed in terms of the Flory-Huggins χ-parameter.[4] This parameter is defined as the energy change (in units of kT) associated with the transfer of a polymer segment from the polymer melt to the pure solvent. Two special χ values may be considered: (i) $\chi = 0$ for athermal solvent behaviour, and (ii) $\chi = 0.5$ for theta conditions (solvent is ideally poor for the polymer). The polymer adsorption process is stimulated when the solvent quality is poor (i.e., $\chi > 0$). Values of χ for polymer-solvent contacts can be obtained from several observable properties, such as osmotic pressure, intrinsic viscosity, and light scattering.[5]

4) The *(de)mixing entropy* for the adsorption of a polymer chain and the concomitant desorption of solvent molecules. Polymer adsorption leads to a demixing of a homogeneous polymer solution into a concentrated surface phase and a more dilute solution. Hence, the mixing entropy decreases upon polymer adsorption and therefore counteracts this process.

Adsorbed polymers can be desorbed by adding a displacer. All energy terms given above may be affected by this addition. However, the decrease in segmental adsorption energy is in most cases

dominant. Figure 2 shows the displacement of adsorbed polymer by increasing the displacer concentration. At a certain solvent composition the polymer is completely desorbed. This displacer concentration may be called the *critical point.*

Adsorption of polymer segments onto a bare surface from a binary solvent mixture with a critical composition would not change the total free energy. Hence, there is no driving force for adsorption any more. Cohen Stuart *et al.*[6,7] have developed a model which relates critical solvent compositions to χ_s values relative to the individual solvent components. This model takes into account all the free energy terms discussed above. Hence, measuring critical displacer concentrations yields segmental adsorption energies, provided all the other interaction parameters are known. So far, this method is the only one that gives the Gibbs free energy for adsorption of polymer segments relative to that of solvent molecules. The method was first applied to poly(vinylpyrrolidone) adsorption on silica from water and from dioxane.[7]
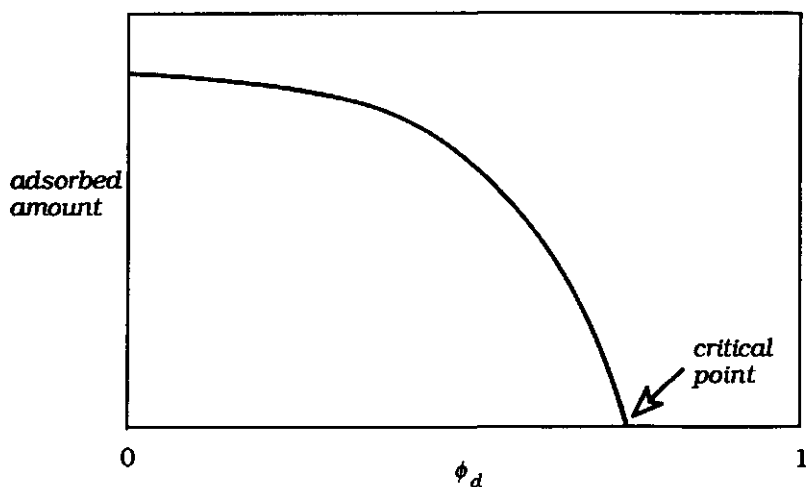
Figure 2. *The adsorbed amount of polymer as a function of the volume fraction ϕ_d of displacer.*

1.4. Work of adhesion

The adhesion strength of polymers on solid surfaces is usually determined in a macroscopic way as the work of adhesion. Examples of such kind of experiments are: peeling, fibre pull-out, and interlaminar shear stress (ILSS) tests.[8] In all these experiments the constituent phases are separated in an irreversible way, by mechanically breaking the contact. Consequently, two terms play a role for such adhesion strength measurements[1]:

- The intrinsic work of adhesion W_i. This term is the reversible (thermodynamic) part of the work of adhesion and is related to the segmental adsorption energy χ_s. It is often convenient to split the thermodynamic work of adhesion into two contributions, one for dispersive interactions, and one for specific interactions, such as acid-base interactions.

- The dissipation of viscoelastic energy W_v in the adhesive material. This energy loss occurs mainly around the crack tip where the strain rates and stresses are high. Viscoelastic energy dissipation usually dominates the adhesion strength and depends on the type of experiment (geometry), properties of the adhesive material, temperature, crack speed v, and the intrinsic adhesion strength (W_i).

The total work of adhesion W_t is equal to the sum of the terms given above, i.e.,

$$W_t = W_i + W_v \tag{1}$$

Maugis and Barquins[9,10] have proposed an equation for the dependence of W_v on W_i. This approach is based on the work of Gent and Schultz[11] and that of Andrews and Kinloch[12]. Kinetic energy is neglected in this concept. The viscoelastic energy dissipation is assumed to be proportional to the intrinsic adhesion:

$$W_v = \phi(a_T v) W_i \tag{2}$$

---

[1] We do not consider mechanical interlocking.

The proportionality factor $\phi(a_T v)$ is a function of the crack speed v, the temperature, and the glass temperature of the adhesive material. The latter two quantities are combined in the Williams-Landel-Ferry (WLF) shift factor a_T. Maugis et al.[9,10] showed that Eq. (2) holds for various glass/elastomer contacts and for different types of adhesion strength measurements. Hence, the total work of adhesion can be predicted using Eqs. (1) and (2), provided the thermodynamic work of adhesion and the function $\phi(a_T v)$ are known.

Although W_v may be much greater than W_i, the latter quantity is still very important because W_v is proportional to it. An increased thermodynamic work of adhesion leads to higher energies of dissipation and may therefore cause a remarkably increased apparent work of adhesion.

1.5. Objective of this work

The main object of this study is twofold: (i) to determine segmental adsorption energies (χ_s-values) of various homopolymers on inorganic substrates, using the model of Cohen Stuart et al.[6], and (ii) to investigate how these χ_s-values can be used to predict W_i for polymer/oxide interfaces. Special attention is given to the effect of the functional group and the chain structure on the adsorption energy. The chain structure is varied by changing either the alkyl end group linked to the functional group or the number of methylene groups between recurring functional groups in the main chain.

Another aspect is the difference between the adsorption energies of the same polymer on different substrates. We studied polymers with basic characteristics on silica, which is purely acidic, and on alumina, which is an amphoteric surface. Silica and alumina are both common substrates in many applications. Silica (glass) is of special interest for polymer composites. Almost all polymer composites are reinforced with glass fibres. Adhesion on alumina surfaces receives much interest in the aircraft industry. Many joints in aeroplane constructions are established with the help of adhesives. Anodic

surface oxidation of aluminium units is generally applied to improve adhesive bonding.

The derived object is to get more insight in the conformation of adsorbed polymer molecules as a function of the effective adsorption energy parameter χ_s. The question here is how the structure of adsorbed polymer chains is affected by the adsorption energy.

1.6. Determination of critical displacer concentrations

In order to determine segmental adsorption energies with the help of the model of Cohen Stuart et al.[6], critical displacer concentrations have to be measured. In this study, the following methods are used to determine critical points.

- Indirect measurement of the adsorbed amount of polymer by the depletion method. The adsorbed amount as a function of displacer concentration is determined by analyzing the polymer solution which is in equilibrium with the adsorbed polymer layer. Substrate particles with any possible adsorbed polymer must be first separated from the dispersion. The concentration of polymer in the supernatant is then analytically determined. The critical point is reached when the amount of polymer found in the equilibrium solution is equal to the total (initial) amount of polymer. This approach was adopted by Cohen Stuart et al.[7]

- Direct measurement of the adsorbed amount by using Attenuated Total Reflection (ATR) Fourier Transform Infrared (FTIR) Spectroscopy. These measurements are carried out in a cell that contains an internal reflection element (IRE). The infrared beam is totally reflected along the IRE/sample interface, producing an evanescent wave (i.e., an exponential decaying standing wave) which extends about one micron into the sample. Only the volume over which the evanescent wave extends is sampled. Polymer adsorption onto the IRE takes place within this volume and can therefore be directly determined.

- Measurement of the adsorbed layer thickness by means of Dynamic Light Scattering (DLS) on dilute dispersions of colloidal particles with and without polymer. The layer thickness of adsorbed

polymer is equal to the radius of particles coated with polymer minus that of bare particles. At the desorption point there is a sudden drop in the layer thickness. This method to determine critical points is new and first described in this thesis.

- Measurement of the amount of segments directly bound to the surface by means of nuclear magnetic resonance (NMR) relaxation of the solvent. Entrainment of segments at the surface can be viewed through the dynamics of the solvent in the system. The mobility of a solvent molecule in the solvation layer of a polymer segment can be separated in the motion of the solvent molecule with respect to the segment and the motion of the segment with respect to a fixed point. Adsorption of polymer segments leads to a reduction of the mobility of these segments and, hence, to a decrease in solvent mobility, which can be measured by magnetic relaxation. For the case of rapid exchange between immobilized solvent molecules and free molecules in the solution, an effective relaxation rate is measured, which is a weighted sum of the two contributions. With proper calibration, the amount of train segments can be extracted from this effective relaxation rate. Also this method is applied for the first time in this work.
- Measurement of interfacial residence time of polymer on a substrate by means of Thin-Layer Chromatography (TLC). The critical eluent composition is marked by the sudden transition between complete retention and no retention of polymer on the thin layer. This method constitutes a modification of the chromatographic studies by Glöckner et al.[13]

Each method has its limitations as far as applicability is concerned. For instance, DLS is only possible with stable dispersions, TLC works only if a suitable thin layer can be made which can be developed, and the depletion method can be hampered by analytical problems. However, critical points of many systems can be determined by one or more of the methods given above.

Each method gives not only the critical point but often also specific information about the conformational state of adsorbed

polymers. Combining these pieces of information yields a more complete picture of adsorbed polymer layers.

1.7. Outline of this study

Chapters 2 - 5 describe each of the respective techniques which we used to determine critical points. The last chapter (6) of this thesis provides an overview of segmental adsorption energies and adhesion strengths which were determined in this study. Every chapter can be understood without direct reference to previous ones. Readers who are only interested in the results can read chapter 6 independently.

Chapter 2 describes how TLC can be used to determine critical displacer concentrations. Adsorption/desorption transitions determined by this technique are compared with the same transitions obtained by the depletion method. All experiments were done with a model system (polystyrene on silica). This chapter also elaborates the relation between the chromatographic *solvent strength* defined by Snyder[14] and the χ_s parameter.

Chapter 3 deals with polymer adsorption and desorption studied by ATR-FTIR Spectroscopy. Polymers were desorbed using monomeric as well as polymeric displacers. We also considered the kinetics of polymer adsorption and desorption. Effects of the molecular weight and concentration of the adsorbing polymer, of the displacer concentration, and of the molecular weight of the displacer were investigated.

Chapter 4 discusses the measurement of the hydrodynamic thickness of adsorbed polymer layers by DLS. These measurements are sensitive to the tail density in the adsorbed layer. Effects of polymer concentration and the amount of added displacer were studied.

Chapter 5 presents a study of polymer adsorption and desorption by proton NMR relaxation of the solvent. For the systems we studied the rate of relaxation could be related to the amount of train segments. The density of train segments as a function of the displacer concentration was measured.

Chapter 6 gives a compilation of critical points and adsorption energies of five polymers with basic characteristics on both silica and alumina. The polymers are classified according to their adsorption energy.

The last part of this chapter discusses the relation between the adsorption energy and the thermodynamic work of adhesion. Both the thermodynamic work of adhesion and the contribution of specific interactions to it have been estimated for various polymers on silica.

1.8. References

1. *Polymer Adsorption and Dispersion Stability*; Goddard, E. D., Vincent, B., Eds.; ACS Symposium Series 240; American Chemical Society: Washington, D. C., 1984.
2. Eirich, F. R. *J. Colloid Interface Sci.* **1977**, 58, 423.
3. Silberberg, A. *J. Chem. Phys.* **1968**, 48, 2835.
4. Flory, P. J. *Principles of Polymer Chemistry*; Cornell University Press: New York, 1953.
5. Orwoll, R. A. *Rubber Chem. Technol.* **1977**, 50, 451.
6. Cohen Stuart, M. A.; Fleer, G. J.; Scheutjens, J. M. H. M. *J. Colloid Interface Sci.* **1984**, 97, 515.
7. Cohen Stuart, M. A.; Fleer, G. J.; Scheutjens, J. M. H. M. *J. Colloid Interface Sci.* **1984**, 97, 526.
8. *Adhesion and Adsorption of Polymers*; Lee, L. H., Ed.; Plenum Press: New York, 1980.
9. Maugis, D.; Barquins, M. In *Adhesion and Adsorption of Polymers*; Lee, L. H., Ed.; Plenum Press: New York, 1980; p 203.
10. Maugis, D. *J. Mater. Sci.* **1985**, 20, 3041.
11. Gent, A. N.; Schultz, J. *J. Adhesion* **1972**, 3, 281.
12. Andrews, E. H.; Kinloch, A. J. *Proc. R. Soc. Lond.* **1973**, A 332, 385.
13. Glöckner, G.; Kahle, D. *Plaste Kautsch* **1976**, 23, 338.
14. Snyder, L. R. *Principles of Adsorption Chromatography*; Marcel Dekker: New York, 1968.

Chapter 2

A Chromatographic Method for the Determination of Segmental Adsorption Energies of Polymers

Polystyrene on silica

Abstract

Polystyrene adsorption on a silica surface was studied by means of adsorption TLC. This is a very sensitive technique for detecting polymer adsorption/desorption transitions in binary solvent mixtures. Such transitions, which occur at a well-defined solvent composition (the so-called *critical point*) were earlier shown to be related to the segmental adsorption energy. In this chapter we derive a relation between the concept of chromatographic *solvent strength*, as defined by Snyder, and segmental adsorption energies. It turns out that solvent strength data, which are available in the chromatographic literature, can now also serve as a useful source of information for polymer adsorption and adhesion studies. Finally, we give some experimental results for the displacement of polystyrene from silica in two different solvents (carbon tetrachloride and cyclohexane) by various weakly adsorbing low molecular weight displacers. Using tabulated solvent strengths, we determined segmental adsorption energies for polystyrene on silica of 1.0 kT and 1.9 kT, from carbon tetrachloride and cyclohexane, respectively.

2.1. Introduction

Thin-layer chromatography, TLC, is frequently used to analyze polymer samples.[1-8] This technique has many advantages: simple instrumentation, high sensitivity, rapidity, and ease of detection of separated bands. TLC can be based on either adsorption (ATLC), size exclusion as in GPC (TLGPC), or dissolution-precipitation (extraction and precipitation TLC). These techniques permit the investigation of all kinds of polydispersity: polydispersity according to molecular

weight,[1-4] stereoregularity,[4-6] microstructure,[1,2] and chemical composition in copolymers.[1,4,7] It is even possible to separate isotopically different polymers by these techniques.[8]

We are interested in TLC as a technique to study the adsorption of polymers. Hence, we will exclusively consider ATLC. Polymer adsorption has many technological applications. The mechanical strength of polymer composites depends on the strength of adhesion between the matrix polymer and the reinforcing filler. Polymer adsorption can stabilize dispersions, which is important in products like paints, foods, pharmaceuticals, etc. It can also destabilize colloidal systems, which is useful in water purification and improvement of soil structure. The aim of this paper is to establish a relation between ATLC with polymers and polymer adsorption studies as done by Cohen Stuart et al. [10] More specifically, we will show how adsorption (thin-layer) chromatography experiments can be used in the determination of the segmental adsorption energy of polymers on a substrate.

Some years ago, Cohen Stuart et al.[9,10] proposed a method to estimate segmental adsorption energies, based on polymer adsorption/desorption transitions in binary solvents. Desorption of polymer from an adsorbent can be achieved by increasing the concentration of the more strongly adsorbing solvent component (which was termed *displacer*). At a certain critical composition, the polymer is fully desorbed by the displacer. The central result of the analysis of Cohen Stuart et al. is an equation which relates the critical displacer concentration to the difference in adsorption energy between a polymer segment and a solvent molecule. So far, this method is the only one that yields information on the adsorption energy of polymer segments on a surface.

A somewhat parallel development can be found in the chromatographic literature, where the *solvent strength* concept was introduced by Snyder[11,12] in order to characterize the interaction strength between solute and stationary phase in chromatographic separations. Snyder has given an equation from which one can calculate the solvent strength of an arbitrary binary solvent mixture from tabulated solvent strengths of pure solvents. By measuring polymer retention in ATLC, the critical composition or, in Snyder's

terminology, the critical solvent strength can be found. In this paper, we present a quantitative relation between the critical solvent strength and the segmental adsorption energy. The advantage of this relation is that chromatographic data available in the literature can serve as a useful source of information in the determination of segmental adsorption energies. We note in passing that some ideas relative to polymers at interfaces had already been introduced into the chromatographic approach.[2]

Finally, the relation between Snyder's solvent strength concept and the treatment of Cohen Stuart et al. is checked by experiments on the polystyrene/silica system, both with ATLC and with batch adsorption studies.

2.2. Theory

Cohen Stuart et al.[9,10] used the following simple model in their analysis of the polymer adsorption/desorption transition. The solution is described by means of a lattice adjacent to the solid surface. Each lattice site can accommodate either a solvent molecule (o), a displacer molecule (d), or a polymer segment (p). The coordination number of the lattice is z. Each site has $\lambda_o z$ neighbours in the same layer and $\lambda_1 z$ in each of the two adjacent layers. The sites in the surface layer have $\lambda_1 z$ contacts with the surface and $(\lambda_1 + \lambda_0)z$ contacts with the solution. The adsorption energy parameter χ_s^{po} was defined by Silberberg[13] as

$$\chi_s^{po} = -\left(u^p - u^o\right)/kT \tag{1}$$

where u^p and u^o are the interaction (free) energies of the solid surface with a polymer segment and a solvent molecule, respectively, with respect to a suitable reference state (e.g., bare solid surface + isolated monomer unit). Note that by this definition χ_s^{po} is counted positive if the polymer adsorbs preferentially from the solvent. The parameters χ_s^{do} (displacer from solvent) and χ_s^{pd} (polymer from displacer) are defined in an analogous way. These χ_s parameters are related in a cyclic way because of their exchange character:

$$\chi_s^{po} = \chi_s^{pd} + \chi_s^{do} \tag{2}$$

This relation follows immediately from the definition in Eq. (1).

In a polymer solution in contact with an adsorbent, not only contact energies with the surface (adsorption energy) but also nearest-neighbour interactions in the solution (solvent quality) play a role. These can be taken into account by using Flory-Huggins χ parameters. In our particular case, the relevant parameters are χ^{po} (polymer-solvent), χ^{pd} (polymer-displacer), and χ^{do} (displacer-solvent). We note that adsorption energies may also be expressed by a Flory-Huggins type parameter, if the adsorbent is considered as a separate component s.[14] However, in this paper we still use χ_s according to Silberberg's definition because it simplifies the equations.

The model of Cohen Stuart et al.[9,10] leads to relatively simple expressions for the free energy associated with changes in the surface layer composition, provided the simplifying assumption is made that in the neighbourhood of the critical point only the segment concentration in the surface layer is different from the bulk solution value (one-layer approximation). The final result of this treatment is a relation between the adsorption energy and the critical displacer volume fraction ϕ_{cr} in dilute polymer solutions. It can be written as

$$\phi_{cr} = \frac{\exp\left[\chi_s^{po} - \chi_{sc} - \Delta h^{po}/kT\right] - 1}{\exp\left[\chi_s^{do} - \Delta h^{do}/kT\right] - 1} \tag{3}$$

Here, Δh^{po} and Δh^{do} are the nearest neighbour interaction enthalpies corresponding to a polymer/solvent and a displacer/solvent contact. Expressions for these enthalpies in terms of solution concentrations and the various χ parameters are given in ref 9. The parameter χ_{sc} is the (dimensionless) critical adsorption energy: the minimum value of χ_s for which long chains adsorb from the solvent. It has an entropic origin because a bond connected to an adsorbed segment has less orientational freedom than a bond in a polymer molecule in the bulk solution. A simplified version of Eq. (3) is

obtained by neglecting the terms -1 and substituting Δh^{po} and Δh^{do}:[9]

$$\chi_s^{po} = \chi_s^{do} + \ln \phi_{cr} + \chi_{sc} - \lambda_1 \chi^{pd} - (1 - \phi_{cr})(1 - \lambda_1)\left(\chi^{po} - \chi^{pd} - \chi^{do}\right) \qquad (4)$$

This equation holds only for not too small χ_s^{po} and χ_s^{do} values. If we ignore all interactions other than those with the substrate (i.e., all χ parameters are zero), the result becomes very simple:

$$\chi_s^{po} = \chi_s^{do} + \ln \phi_{cr} + \chi_{sc} \qquad (5)$$

The picture presented by Snyder [11] closely resembles the one sketched above, so that a similar result may be anticipated. In chromatography, it is customary to characterize a solvent by means of its solvent strength ε, which is a measure of its (free) energy of interaction with an adsorbent. Values of ε are tabulated by Snyder with respect to the solvent pentane; i.e., the reference state is a surface fully covered by pentane. In order to characterize solvent mixtures of a given composition in the same way, Snyder derives an expression for the solvent strength of binary solvent mixtures, ε_m. The solvent strength is defined in such a way that $-2.303\alpha A \varepsilon^1$ is the adsorption energy of a solvent molecule, which occupies a surface area A on the adsorbent. The coefficient α, called *activity*, is a property of the substrate. It is determined by the type and density of active sites on the adsorbent surface. Apparently, the adsorption energy per unit area can be split into a factor representing the adsorbate (ε) and one which stands for the adsorbent (α). Snyder claims that this is reasonable, provided that a single type of interaction is largely responsible for the adsorption. The forces which account for the adsorption of a polymer on a silica surface (as in our experiments) are almost exclusively of the acid-base type. [15] Acid-base interactions have been described quantitatively by Drago *et*

---

1 The factor 2.303 arises because Snyder uses decimal rather than natural logarithms.

$al.$[16] These authors analyze the energies of such interactions in terms of a covalent and an electrostatic contribution, and show that each of them can be split into two factors, one for each molecule participating in the bond. Snyder[11] demonstrates that the adsorption energies of functional groups on polar substrates such as silica correlate fairly well with only the electrostatic contribution (the so-called "hard" interaction). This justifies the separation of the adsorption energy into a contribution of the substrate and one of the adsorbate.

We should note here that A is originally expressed in units of 8.5 $Å^2$, which corresponds to $A = 6$ for benzene. Since we prefer the more usual SI units, we write A in units of nm^2. If we define an activity α' as 27.1α, we can write the dimensionless molecular energy between a solvent molecule and the adsorbent as $-\alpha'A\varepsilon$. The numerical factor is $2.303/0.085 = 27.1 \ nm^{-2}$.

For the derivation of ε_m, Snyder assumed that the components of the solvent mixture have no interactions with each other (which is equivalent to neglecting the χ parameters) and that they occupy the same surface area. The solvent strength ε_m is expressed in the solvent strengths of the pure components by considering the average probability to create one vacant site on a surface covered with a mixed adsorbate (with fractions θ_d and $\theta_o = 1 - \theta_d$ for the components d and o, respectively). This average probability is simply written as a linear combination of Boltzmann factors. The effective solvent strength ε_m is now defined by expressing this average probability in one Boltzmann factor with an average potential $-\alpha'A\varepsilon_m$ in the surface layer:

$$\exp(-\alpha'A\varepsilon_m) = (1 - \theta_d)\exp(-\alpha'A\varepsilon_o) + \theta_d \exp(-\alpha'A\varepsilon_d) \tag{6}$$

The final assumption of Snyder is Langmuirian adsorption of component d from the solvent o:

$$\frac{\theta_d}{1 - \theta_d} = \frac{\phi_d}{1 - \phi_d}\exp[\alpha'A(\varepsilon_d - \varepsilon_o)] \tag{7}$$

Here, ϕ_d is the mole fraction of component d in the bulk solution. Combination of Eq. (6) and Eq. (7) leads to the main result of Snyder's treatment:

$$\varepsilon_m = \varepsilon_o + \frac{\ln\left\{\phi_d \exp\left[\alpha'A(\varepsilon_d - \varepsilon_o)\right] + 1 - \phi_d\right\}}{\alpha'A} \tag{8}$$

This equation can be rewritten in a form which resembles closely Eq. (3):

$$\phi_d = \frac{\exp\left[\alpha'A(\varepsilon_m - \varepsilon_o)\right] - 1}{\exp\left[\alpha'A(\varepsilon_d - \varepsilon_o)\right] - 1} \tag{9}$$

This similarity suggests strongly that a simple relation between the χ_s parameters used by Cohen Stuart et al.[9,10] and the solvent strengths defined by Snyder should exist, particularly if solute interactions are absent. Let us consider a polymer segment trying to adsorb from a mixture of solvent and displacer onto a substrate. At the critical point $\phi_d = \phi_{cr}$, the net free energy change just vanishes. In other words, the surface contact energy per polymer segment u^p plus the entropic contribution $\chi_{sc}kT$ is then equal to the average contact energy of the critical solvent mixture. If we denote the solvent strength of the critical solvent mixture by ε_{cr}, the segment surface contact energy can be written as

$$u^p/kT = -\alpha'A\varepsilon_{cr} - \chi_{sc} \tag{10}$$

For the monomeric components o and d, for which the bond entropy term χ_{sc} is absent, the surface contact (free) energy (with respect to pentane) can directly be written in terms of their solvent strengths:

$$u^o/kT = -\alpha'A\varepsilon_o \tag{11a}$$

$$u^d/kT = -\alpha'A\varepsilon_d \tag{11b}$$

Using the definition of the χ_s parameters as given in Eq. (1), we can express them in the solvent strengths ε_o, ε_d, and ε_{cr}:

$$\chi_s^{po} = \alpha' A(\varepsilon_{cr} - \varepsilon_o) + \chi_{sc} \qquad (12)$$

$$\chi_s^{pd} = \alpha' A(\varepsilon_{cr} - \varepsilon_d) + \chi_{sc} \qquad (13)$$

$$\chi_s^{do} = \alpha' A(\varepsilon_d - \varepsilon_o) \qquad (14)$$

Equations (12) - (14) constitute our central result. They show that effective adsorption energies of polymer segments can be related to tabulated solvent strengths of pure solvents (ε_o, ε_d) and the solvent strength (ε_{cr}) of the critical mixture of displacer and solvent. The latter quantity is obtained from the measured value of ϕ_{cr} through Eq. (8), after substitution of ϕ_{cr} for ϕ_d. In order to check the result for consistency, we substitute ε_{cr}, as given in Eq.(8), into Eq. (12):

$$\phi_{cr} = \frac{\exp\left[\chi_s^{po} - \chi_{sc}\right] - 1}{\exp\left[\chi_s^{do}\right] - 1} \qquad (15)$$

which is indeed the athermal version of Eq. (3). In other words, both theories lead to the same expression, at least in the absence of solvent/solute interactions. If the latter interactions do play a role, a variant of Eq. (4) can be used, combining Eq. (4) with Eqs. (5) and (12):

$$\chi_s^{po} = \alpha' A(\varepsilon_{cr} - \varepsilon_o) + \chi_{sc} - \lambda_1 \chi^{pd} + (1 - \phi_{cr})(1 - \lambda_1)\Delta\chi^{dop} \qquad (16)$$

where, for shortness of notation, $\Delta\chi^{dop}$ replaces $\chi^{pd} + \chi^{do} - \chi^{po}$. The advantage of the latter equation is that the experimental determination of χ_s^{do} from adsorption experiments, which is very time consuming and often rather inaccurate, can be avoided. Instead, tabulated solvent strengths (the well-known eluotropic series)[11,16] can be used.

An important question is how do the critical displacer concentration and the critical solvent strength depend on the activity of the substrate. Expressing the dimensionless surface contact energy for a polymer segment (u^p/kT), in the chromatographic terminology, as $-\alpha' A\varepsilon_p$ and using Eq. (10), we get

the relation between ε_{cr} and the "solvent strength" ε_p of a polymer segment:

$$\varepsilon_{cr} = \varepsilon_p - \chi_{sc}/\alpha'A \qquad (17)$$

The critical solvent strength depends only on α' by the term $\chi_{sc}/\alpha'A$. If there were no conformational entropic effects (i.e., $\chi_{sc} = 0$), ε_{cr} would be independent of α' and thus of the surface group density (which may vary with the kind of silica), provided the segment/surface bond type is always the same. Because $\chi_{sc}/\alpha'A$ is often small compared to ε_p, the critical solvent strength hardly depends on the kind of silica. Since the solvent strength of mixtures is not independent of the activity α' of the adsorbent (see Eq.(8)), the critical composition at a given ε_{cr} may vary with α'. However, if the solvent strengths of the components in the mixture do not differ very much (as in our experiments), the dependence of the critical composition on the activity is very small, especially when ϕ_{cr} is relatively high.

Obviously, the simple model presented above has its limitations. We discuss a few important cases.

1) An adsorbent surface may be heterogeneous with respect to some adsorbates. Polar and hydrogen bonding solvent molecules may preferentially attach to specific groups on an acidic surface. This selective process is caused by the difference in bonding energy between different surface groups, which increases for stronger interacting adsorbates. For such polar adsorbates, α' can be considered as an *effective* activity, which varies with coverage. At low coverage, α' could be higher than the activity at high coverage due to preferential adsorption onto the stronger groups. One might speculate that the presence of different surface sites will be less important for multifunctional (large) molecules if their area of contact with the surface is larger than the typical scale of heterogeneity, so that a kind of *averaging* occurs.[12] It is, however, not clear whether this would apply for a polymer near its adsorption/desorption transition.

2) For strongly adsorbing displacers the solvent strength is no longer a constant but depends on the displacer concentration.

Snyder[12,17,18] refers to this phenomenon as the *localization effect*. At low displacer concentrations, the surface is under-saturated with displacer. All displacer molecules may then be localized on the surface, i.e., have an optimal orientation with respect to surface sites. The tendency for localization increases as the interaction between displacer molecules and surface sites becomes stronger. At high concentrations of displacer molecules in the surface layer, molecules may become delocalized due to steric hindrance between the adsorbed molecules. The adsorption energy (solvent strength) for delocalized adsorbed molecules is lower than for localized ones. Two properties of the substrate affect the localization effect: (*i*) the distribution of active sites on the surface, and (*ii*) the rigidity of the position of sites. According to Snyder, localization on silica is only observed for solvents with $\varepsilon > 0.3$.[12] In order to avoid this complication, we chose polystyrene for our experimental test. This polymer has no strong polar or strongly hydrogen-bonding groups and can therefore be displaced from an acidic silica surface by means of weakly polar or apolar solvents ($\varepsilon \leq 0.3$).

3) The theory describes displacement on the basis that displacer molecules are more strongly adsorbed on the substrate than polymer molecules. However, displacement is also possible by molecules which have a stronger specific interaction with the polymer rather than with the adsorption sites on the surface. For example, for a basic polymer adsorbed on an acidic surface, displacement can occur by either a basic or an acidic displacer (i.e., by inactivation of either the adsorbent surface or the polymer).[15] In the latter case, the concentration of displacer molecules which occupy sites on the polymer will be higher than the concentration in the bulk, ϕ_d. The displacement theory above can not handle displacement by solvents which bind specifically to polymer segments, since at best *average* interactions in solution are taken into account through the χ parameters in Eq. (16). Hence, before using the theoretical description of displacement and concomitant determination of the adsorption strength of a polymer in a particular system, we have to make sure that we are

dealing with displacement by inactivation of the adsorbent surface instead of the polymer.

2.3. Experimental

2.3.1. Batch adsorption

Batch adsorption experiments were carried out at room temperature with dispersions of silica. Both silica scraped off the TLC sheets and aerosil (ox 50 ex Degussa) were used. The surface area of silica in the dispersions was 0.19 m^2/mL, and the equilibrium polystyrene (PS) concentration (without displacer) was about 100 ppm. The adsorbed amount as a function of the solvent composition was determined by the depletion method. After the dispersions (silica with polymer) were rotated end-over-end for about 15 h, the samples were centrifuged for 1 h at 20,000 rpm. A given amount of the supernatant was evaporated under reduced pressure at 60 °C. The residue was then redissolved in a known amount of carbon tetrachloride. The absorbance of this solution was measured at a wavelength of 262.5 nm with a Beckman 3600 spectrophotometer.

2.3.2. TLC

For the chromatographic experiments, we have used TLC plastic sheets with a silica layer (Kieselgel 60 F_{254}, Merck) of 0.2 mm thickness. The plates contained a fluorescent indicator for visualizing the polystyrene spots after elution. Before use, the plates were dried in air at 120 °C for at least 10 h. Spots of polystyrene were deposited along a line, 2 cm from the lower edge of the adsorbent layer, by evaporating droplets of PS in carbon tetrachloride (4000 ppm). The plates were then placed above the eluent of the appropriate composition in a closed thermostatted cylindrical tank for 45 minutes, in order to establish equilibrium between the vapour phase, the liquid phase, and the adsorbed phase on the silica. This vapour pretreatment of the silica layer suppresses the undesirable solvent demixing during the development. The upward elution was started

by lowering the plates just into the eluent, at a temperature of 25 °C. After elution the plates were dried and the polystyrene spots were visualized by short-wave U.V. illumination. The R_f values in most of the runs were either 1 or 0. The transition between these two extremes was scanned by changing the eluent composition stepwise, using very small variations in composition. Polystyrene is soluble in all solvent mixtures used, so that retention of PS by precipitation did not play any role. All solvents were analytical grade and used as such, with the exception of chloroform, which was washed with purified water in order to remove the stabilizing agent ethanol. After the chloroform fraction was dried with magnesium sulphate, it was kept in the dark as much as possible to prevent photochemical reactions. Since ethanol is a very strong displacer, concentrations as low as 0.1% cause complete PS desorption from a silica surface. Indeed, significant differences between the critical points of systems with pure and ethanol containing chloroform were found.

The PS samples used in this study are listed in Table 1. We have chosen high molecular weight samples because the retention behaviour of high molecular weight polymers $(M_w > 10\,kg/mol)$ is known to depend little on molecular weight or molecular weight distribution.[8] We did indeed find no significant differences in the R_f values for the samples tabulated.

Table 1. *Polymer samples*

sample	M_w (kg / mol)	M_w/M_n
PS (Ega-chemie)	320	3.8
PS (Polymer Laboratories)	105	1.05
PS (Polymer Laboratories)	530	1.06

2.4. Results and discussion

In Figure 1, we compare the result of a TLC experiment (triangles) with adsorption experiments on the same silica (open circles) and on a different silica (aerosil) (filled circles) for PS in carbon

tetrachloride with toluene as a displacer. It can be seen that the transition in the chromatographic experiments is much steeper. Hence, TLC is a much more sensitive technique for detecting the critical point than batch adsorption experiments. The basic reason for this is that polymer mobility (as measured in TLC experiments) is negligible as long as the total adsorption energy per polymer chain exceeds a few kT. Since the number of adsorbable monomers (N) in a chain is so high ($\sim 10^3$) it follows that this is always the case as long as χ_s^{po} exceeds χ_{sc} by even a small amount. An additional factor is that the fraction of bound monomers p increases also with χ_s^{po}. Thus, R_f, which follows $\exp\left(-Np\chi_s^{po}\right)$ switches very rapidly between 1 and 0 when χ_s^{po} passes through χ_{sc}. The adsorbed mass, on the other hand, increases gradually with χ_s^{po} because of the lateral interaction between the polymer molecules. The critical points for both kinds of silica, determined with either TLC or batch adsorption experiments, do not differ very much, as expected.
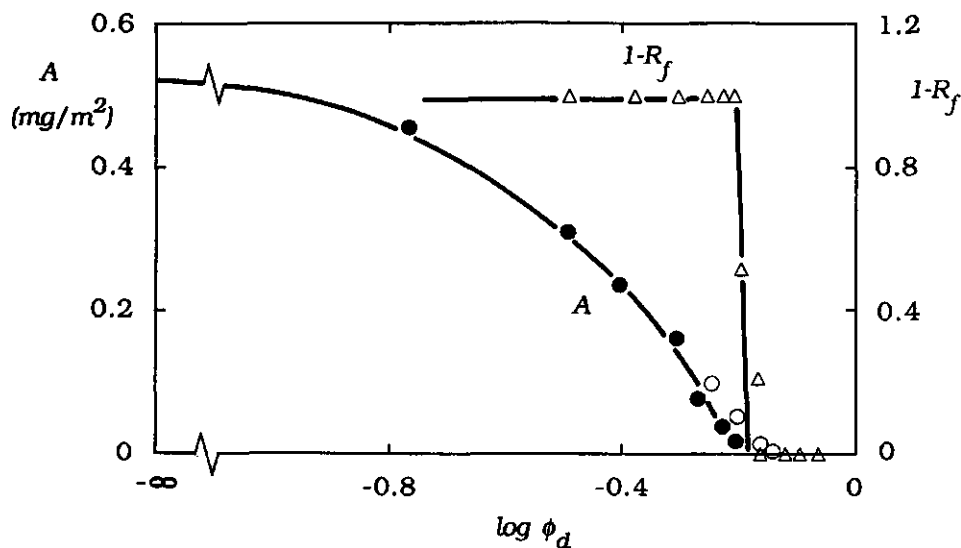

Figure 1. *The adsorbed amount A and retention, expressed as* $1-R_f$, *for PS in the solvent mixture carbon tetrachloride-toluene as a function of the logarithm of the volume fraction* ϕ_d *of toluene:* ●, *Batch adsorption experiment with aerosil;* ○, *Batch adsorption experiment with silica scraped off TLC plates;* Δ, $1-R_f$ *(TLC experiment).*

Figures 2 and 3 show the retention of PS on the silica thin layer as a function of the displacer volume fraction for several displacers in the solvents carbon tetrachloride and cyclohexane, respectively. The order of the various displacers is the same in both cases, but the critical points ϕ_{cr} are higher in the solvent cyclohexane. Apparently, polystyrene adsorbs more strongly from cyclohexane than from carbon tetrachloride. The critical solvent strength ε_{cr} for each of these solvent mixtures can be calculated from Eq. (8). The required solvent strengths ε_o and ε_d and the molecular areas A as taken from Snyder[17] are given in Table 2. The molecular area of an adsorbate is defined as the specific area of the adsorbent, divided by the number of adsorbed molecules per unit weight of the adsorbent in a fully occupied monolayer. For the determination of the activity α, we have used the procedure described by Snyder.[18] This method is essentially a calibration of the silica with a series of compounds with known $A\varepsilon$ values (tabulated by Snyder). For these compounds, the
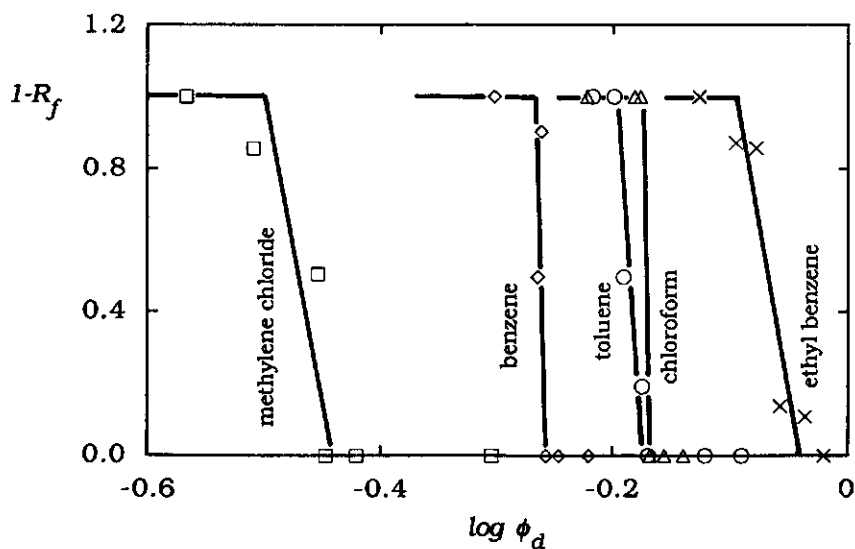
Figure 2. *Displacement of PS from silica into carbon tetrachloride/displacer mixtures, determined by ATLC, as a function of the logarithm of the volume fraction ϕ_d of various displacers: □, methylene chloride; ◇, benzene; ○, toluene; △, chloroform; ×, ethyl benzene.*
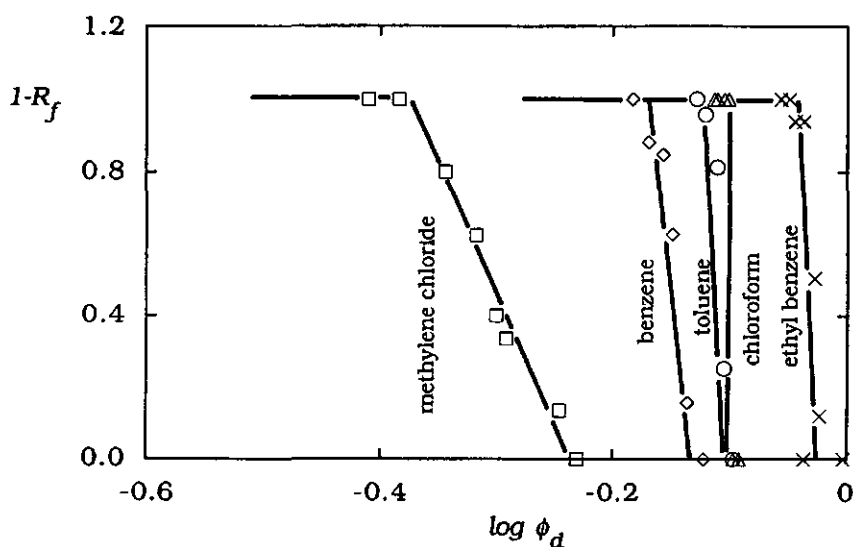
Figure 3. *Displacement of PS from silica into cyclohexane/displacer mixtures, determined by ATLC, as a function of the logarithm of the volume fraction ϕ_d of various displacers:* □, *methylene chloride;* ◊, *benzene;* ○, *toluene;* Δ, *chloroform;* ×, *ethyl benzene.*

R_f values on this particular silica have to be measured, with pentane as the eluent. For the chromatographic silicas used here, α turned out to be equal to 0.65 ($\alpha' = 17.6$ nm^{-2}).

Table 2. *Solvent strengths and molecular areas*[17]

solvent	$\varepsilon_o, \varepsilon_d$		A / nm^2
cyclohexane	(o)	0.04	0.51
carbon tetrachloride	(o)	0.11	0.43
toluene	(d)	0.22	0.58
benzene	(d)	0.25	0.51
chloroform	(d)	0.26	0.43
methylene chloride	(d)	0.30	0.35

In the theory, we have assumed that the components of the solvent mixture occupy equal molecular areas. Table 2 shows that this assumption is not completely true. However, the variation in the A values does not affect significantly the calculated critical solvent strengths. The critical values determined for the various systems are given in Table 3. As explained in the previous section, ε_{cr} should be independent of the solvent and displacer used, expressing the interaction between the segments and the surface (see Eq. (10)). This is not strictly true, as can be seen from Table 3. The differences are probably caused by solvency effects,[19] which were not considered in the derivation of Eq. (10).

The critical solvent strengths for cyclohexane mixtures are slightly higher than those for carbon tetrachloride mixtures. Carbon tetrachloride $(\chi^{po} = 0.396)$ is a better solvent for PS than cyclohexane $(\chi^{po} = 0.505)$.[20,23] When the solvent quality is poor, adsorption (the demixing of a homogeneous polymer solution into a concentrated surface phase and a more dilute solution) is stimulated. In that case, more displacer is needed to displace the polymer from the substrate, leading to higher ε_{cr} values.

Table 3. *Critical volume fractions and solvent strengths for PS on silica for two solvents and five displacers*

solvent	displacer	ϕ_{cr}	ε_{cr}
carbon tetra-chloride	methylene chloride	0.35	0.23
	benzene	0.55	0.21
	toluene	0.68 (C), 0.63 (batch)	0.20 (C)
	chloroform	0.68	0.23
	ethyl benzene	0.92	-
cyclohexane	methylene chloride	0.58	0.26
	benzene	0.71	0.21
	toluene	0.80	0.21
	chloroform	0.80	0.24
	ethyl benzene	0.93	-

Chloroform is a relatively acidic solvent. A notable specific interaction with the relatively basic phenyl groups of the polymer can then be expected. Fowkes also reports this effect for chloroform and basic polymers.[15] Hence, displacement by polymer inactivation could play a role in this case. However, the critical solvent strengths for the mixtures with chloroform are not significantly lower than for the other systems. This indicates that preferential solvatation of the polymer by chloroform does not play a significant role.

From the ε_{cr} and ϕ_{cr} data given in Table 3, χ_s parameters can be calculated using Eq. (16), provided the relevant χ parameters are known. Literature data for χ are given in Table 4. The theoretical value of χ_{sc} in a lattice model is $-\ln(1-\lambda_1)$. For a hexagonal lattice ($\lambda_1 = 0.25$), $\chi_{sc} = 0.288$. The experimental χ_{sc} might be lower than this value because rotational entropy loss is not taken into account in the lattice model. In special cases, the rotational entropy loss for an attached monomer with respect to the bulk solution might be so much greater than for an adsorbed polymer segment that χ_{sc} may even become negative.[10] When the monomer unit of the polymer is used as the displacer, it seems a logical first approximation to assume $\chi_s^{po} = \chi_s^{do}$, $\chi^{po} = \chi^{do}$, and $\chi^{pd} = 0$. Equation (4) leads then to $\chi_{sc} = -\ln\phi_{cr}$. If this reasoning holds, the χ_{sc} value for PS could be determined by displacement with ethyl benzene, which can be considered as the monomer unit of PS. From the displacement isotherms with ethyl benzene (Figures 2 and 3), we find χ_{sc} values of 0.08 and 0.07, respectively. However, ref 23 gives a Flory-Huggins parameter for the interaction of ethyl benzene with PS of 0.450. This means that the assumption $\chi^{pd} = 0$ is not justified, and a value $\lambda_1\chi^{pd} = 0.11$ should be added to χ_{sc} values given above. The term $(1-\phi_{cr})(1-\lambda_1)\Delta\chi^{dop}$ in Eq. (4) is probably still small if the monomer unit of the polymer is used as the displacer. Hence, a reasonable value for χ_{sc} could be 0.2 for PS from carbon tetrachloride and cyclohexane. Clearly, this value is only approximate. Moreover, a small experimental error in ϕ_{cr} affects the value $\ln\phi_{cr}$ considerably due to the fact that ϕ_{cr} lies mostly in the vicinity of 1 if a polymer is displaced by its own monomer. It is perhaps interesting to note that χ_{sc} is still positive in this weakly polar system.

For small χ_s^{po} values Eq. (3), instead of Eq. (4) has to be used to calculate the χ_{sc} value. However, there is no significant difference between χ_{sc} values calculated by Eq. (3) and by Eq. (4) for small χ_s^{po} values if the critical volume fractions are close to unity (as in our case).

Table 4. *Flory-Huggins interaction parameters*

component a	component b	χ^{ab}	ref
carbon tetrachloride	toluene	-0.05	21
	benzene	0.19	22
	PS	0.396	20
cyclohexane	toluene	1.01	21
	benzene	1.29	22
	PS	0.505	20
polystyrene	toluene	0.432	20
	benzene	0.438	20

The molecular area A is also needed for the calculation of χ_s. We used the average surface contact area of the solvent molecule, the displacer molecule, and the PS segment. According to ref 24, the contact area of a PS segment (A_p) is equal to 0.57 nm^2. The calculation of χ_s is more sensitive to differences in A than the calculation of ε_{cr} This indicates that we should be careful to determine χ_s values from systems with components of different molecular size. Since methylene chloride has a low molecular area $(A = 0.35 \ nm^2)$ compared to the A values of the solvents used and the PS segment, the χ_s values from the systems with methylene chloride are less reliable than from systems with components of (nearly) the same molecular area.

Table 5 gives the calculated χ_s values and the mean contact areas for the various systems studied. We have done the calculations for the athermal case $(\chi^{pd} = \chi^{po} = \chi^{do} = 0)$ and, for those systems where all χ parameters are known, also for the nonathermal case. The χ_s^{po} values

for either carbon tetrachloride or cyclohexane as the solvent, determined with the displacers methylene chloride, benzene, toluene, and chloroform, are in excellent agreement. In spite of the differences in molecular size for the systems with methylene chloride, the χ_s values are apparently not affected. The average values for the "nonathermal" χ_s^{po} parameters for the solvents carbon tetrachloride and cyclohexane are 1.0 and 1.9, respectively. According to the exchange character of χ_s (Eq. (2)), the difference between these values, which is 0.9, should be equal to $\chi_s^{c,h}$ for carbon tetrachloride adsorbing on silica from cyclohexane. We can check the internal consistency of the procedure by calculating $\chi_s^{c,h}$ from the solvent strengths of the pure components (Eq. (14)), using $A = 0.53$ nm^2, the average value of the relevant contact areas given in Table 5. We find $\chi_s^{c,h} = 0.7$. The agreement between these two values for $\chi_s^{c,h}$ is within experimental error.

Table 5. Calculated χ_s^{po} values for PS and mean molecular areas

solvent	displacer	χ_s^{po}		A/nm^2
		nonathermal	athermal	
	methyl. chl.	-	1.1	0.45
carbon tetra-	benzene	1.0	1.1	0.50
chloride	toluene	0.9	1.0	0.53
	chloroform	-	1.2	0.47
	methyl. chl.	-	2.0	0.48
	benzene	1.9	1.8	0.53
cyclohexane	toluene	1.9	1.8	0.55
	chloroform	-	1.9	0.50

As can be seen in Table 5, the solvent interaction parameter terms $\lambda_1 \chi^{pd}$ and $(1 - \phi_{cr})(1 - \lambda_1)\Delta\chi^{dop}$ in Eq. (16) contribute only ± 0.1 to the value of χ_s^{po}. The effect of taking these interaction parameters into account can also be seen in Figure 4. This figure shows calculated displacement isotherms of PS in cyclohexane-benzene mixtures as a function of the volume fraction of benzene. These calculations were done with the self-consistent-field theory of Scheutjens-Fleer, which

is based on a multilayer model.[25,26] Hence, this model is more general than the one-layer approximation, used by Cohen Stuart *et al.*[9] for the calculation of the critical point and gives complete isotherms.
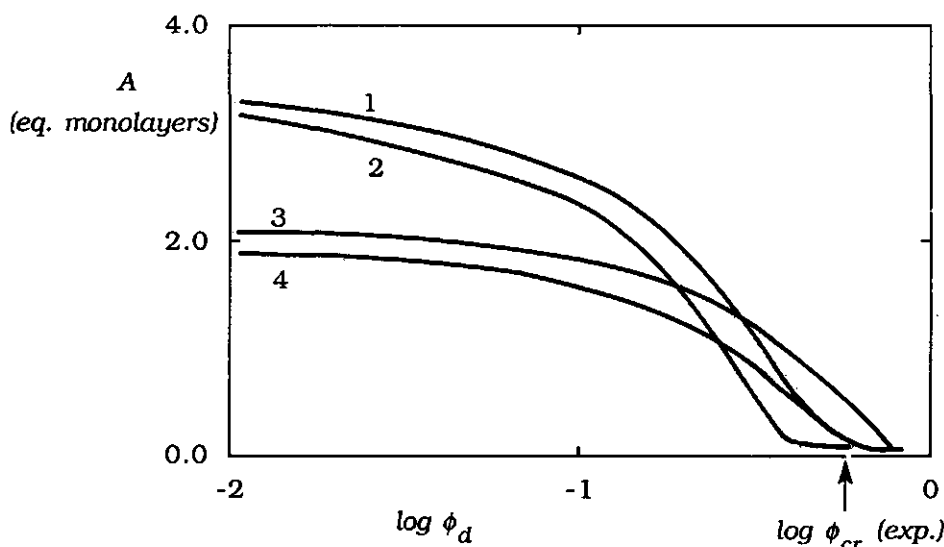

Figure 4. *Theoretical displacement isotherms (calculated by the Scheutjens-Fleer theory) for PS in the solvent mixture cyclohexane-benzene. Parameters:* $\lambda_0 = 0.5$, r *(number of polymer segments)* = 100, ϕ_p *(volume fraction of polymer in the bulk solution)* = 10^{-3}.
1, $\chi_s^{po} = 2.0$ *(non-athermal)*, $\chi_s^{do} = 1.88$, $\chi^{po} = 0.505$, $\chi^{pd} = 0.438$, $\chi^{do} = 1.29$; *2*, $\chi_s^{po} = 1.9$ *(athermal)*, $\chi_s^{do} = 1.88$, $\chi^{po} = 0.505$, $\chi^{pd} = 0.438$, $\chi^{do} = 1.29$; *3*, $\chi_s^{po} = 2.0$ *(non-athermal)*, $\chi_s^{do} = 1.88$, $\chi^{po} = \chi^{pd} = \chi^{do} = 0$; *4*, $\chi_s^{po} = 1.9$ *(athermal)*, $\chi_s^{do} = 1.88$, $\chi^{po} = \chi^{pd} = \chi^{do} = 0$.

The adsorbed amount of PS in Figure 4 is expressed in equivalent monolayers. Because the computer program used had a standard value for χ_{sc} of 0.288, we have done the calculations with χ_s^{po} parameters based on this value instead of 0.2. Therefore, the χ_s values in the last line of Table 5 were incremented by 0.1. Figure 4 shows four isotherms. For the curves labeled 1 and 3, we have taken χ_s^{po} values from Table 5, determined for nonathermal solvent mixtures. The isotherms 2 and 4 are calculated with χ_s^{po} values,

based on athermal behaviour of the solvent mixtures. Displacement isotherms 1 and 2 are the results of computer calculations done with literature values for χ, given in Table 4. For the curves 3 and 4, we have taken all χ parameters equal to zero (athermal). The experimental critical point is also indicated in the Figure. Only the critical points of the calculated curves 1 (completely nonathermal) and 4 (completely athermal) correspond with each other and with the experimental value. Curves 2 and 3, where solvent effects were either omitted from the theory or from the experimentally obtained value of χ_s^{po}, show deviating critical points. This implies that the simplified model of Cohen Stuart *et al.* and the solvent concept of Snyder are consistent with the extended model of Scheutjens and Fleer, as long as a consistent procedure for the determination of χ_s^{po} is used. The influence of the solvent-polymer, displacer-polymer, and displacer-solvent interactions on the critical point is shown by the shifted isotherms 2 and 3. Clearly, solvency effects have to be taken into account for a correct determination of the segmental energy.

2.5. Conclusions

Adsorption thin-layer chromatography is a very sensitive technique for determining the critical point in polymer adsorption experiments. The chromatographic solvent strength concept of Snyder is very useful in polymer adsorption studies. The segmental adsorption energy can be easily determined with the help of the well-known eluotropic series (tables of solvent strengths). In the case of strongly adsorbing components, the segmental adsorption energy determination is more complicated because solvent strengths become then a function of the concentration (*localization effect*). Specific interactions between polymer and displacer do not play a significant role in the displacement of polystyrene from silica by chloroform. The effective adsorption energy for PS on silica is 1.0 kT in carbon tetrachloride and 1.9 kT in cyclohexane, respectively. These values correspond, within experimental error, to the

difference in adsorption energy between cyclohexane and carbon tetrachloride.

2.6. References

1. Glöckner, G. *Polymer Characterization by Liquid Chromatography*; Elsevier: Amsterdam, 1987.
2. (a) Belenkii, B. G.; Gankina, E. S. *J. Chromatogr.* **1977**, 141, 13; (b) Belenkii, B.G. *Chromatography of Polymers*; English Ed.; Elsevier: Amsterdam,1983
3. Otocka, E. P. *Macromolecules* **1970**, 3, 691.
4. Inagaki, H. *Adv. Polym. Sci.* **1977**, 24, 189.
5. Buter, R. Ph. D. Thesis, University Groningen, 1973, p133.
6. Miyamoto, T.; Inagaki, H. *Macromolecules* **1969**, 2, 554.
7. Glöckner, G.; Kahle, D. *Plaste Kautsch* **1976**, 23, 338.
8. Tanaka, T.; Donkai, N.; Inagaki, H. *Macromolecules* **1980**, 13, 1021.
9. Cohen Stuart, M. A.; Fleer, G. J.; Scheutjens, J. M. H. M. *J. Colloid Interface Sci.* **1984**, 97, 515.
10. Cohen Stuart, M. A.; Fleer, G. J.; Scheutjens, J. M. H. M. *J. Colloid Interface Sci.* **1984**, 97, 526.
11. Snyder, L. R. *Principles of Adsorption Chromatography*; Marcel Dekker: New York, 1968.
12. Snyder, L. R.; Glajch, J. L. *J. Chromatogr.* **1981**, 214, 1.
13. Silberberg, A. *J. Chem. Phys.* **1968**, 48, 2835.
14. Evers, O. A. Ph. D. Thesis, Agricultural University, Wageningen, 1990.
15. Fowkes, F. M. *J. Adhesion Sci. Technol.* **1987**, 1, 7.
16. Drago, R. S.; Vogel, G. C.; Needham, T. E. *J. Am. Chem. Soc.* **1971**, 93, 6014.
17. Snyder, L. R. In *High-performance liquid chromatography*, 3rd ed.; Horvath, C., Ed.; Academic Press: New York, 1983; p 186.
18. Snyder, L. R.; Glajch, J. L. *J. Chromatogr.* **1982**, 248, 165.
19. Cohen Stuart, M. A.; Scheutjens, J. M. H. M; Fleer, G. J. In *Polymer Adsorption and Dispersion Stability*; Vincent, B.,

Goddard, E. D., Eds.; ACS Symposium Series 240; American Chemical Society: Washington, D.C., 1984; p 53.

20. Bristow, G. M.; Watson, W. F. *Trans. Faraday Soc.* **1958**, 54, 1742.

21. Fuchs, R.; Peacock, L. A.; Stephenson, W. K. *Can. J. Chem.* **1982**, 60, 1953.

22. Sharma, S.C.; Lakhanpal, M.L.; Rumpaul, M.L. *Indian J. Chem.* **1981**, 20A, 770.

23. Orwoll, R. A. *Rubber Chem. Technol.* **1977**, 50, 451.

24. Glöckner, G. *J. Polym. Sci. Polym. Symp.* **1980**, 68, 179.

25. Scheutjens, J. M. H. M.; Fleer, G. J. *J. Phys. Chem.* **1980**, 84, 178.

26. Scheutjens, J. M. H. M.; Fleer, G. J. *J. Phys. Chem.* **1979**, 83, 1619.

Chapter 3

Polymer Desorption by Monomeric and Polymeric displacers, as Studied by Attenuated Total Reflection FTIR Spectroscopy

Abstract

Attenuated total reflection FTIR is used to study polymer adsorption and desorption on/from an oxidized silicon surface. The advantages of this technique are that the measurements can be done *in situ*, and that different species on the surface can be detected simultaneously. For monodisperse polymers, we find that under stationary conditions a constant adsorbed amount is established within a few minutes. For polydisperse polymers, exchange processes between small and big molecules may slow down the kinetics to a time scale of hours.

A measure for the segmental adsorption energy can be obtained from the concentration of a low molecular weight displacer needed to displace a polymer entirely from the surface. The rate of polymer desorption by such a displacer is much more rapid (i.e., within a few minutes) than the rate of desorption by a displacing polymer. The latter process may have time scales of the order of weeks. Polymer desorption by a more strongly adsorbing polymer seems to occur segment-by-segment.

3.1. Introduction

Many spectroscopic techniques, such as Infrared Spectroscopy (IR),[1,2] Reflectometry,[3-5] Ellipsometry,[6] Fluorescence Spectroscopy,[7,8] Photon Correlation Spectroscopy (PCS),[9] Small Angle Neutron Scattering (SANS),[10] Nuclear Magnetic Resonance (NMR),[11] and Electron Spin Resonance (ESR)[12] are currently used to study polymer adsorption. Infrared Spectroscopy was already applied for this purpose by Fontana and Thomas[13] in 1960. These authors were able to estimate, for a silica dispersion with a poly-

(alkyl methacrylate), the amount of bound polymer segments from the spectral shift of the carbonyl vibration associated with the hydrogen bond formation with the surface silanol groups.

Since then, considerable progress has been made in infrared spectroscopy. By the advent of Fourier transform instrumentation, the accuracy of quantitative measurements has improved remarkably. Fourier transform infrared spectroscopy in combination with Attenuated Total Reflection (ATR) enables one to characterise very thin surface films.[14] The ATR technique is based on the presence of an evanescent wave (i.e., an exponentially decaying standing wave) which is produced upon total reflection. Only the region over which the evanescent wave extends is sampled.[15,16] Chittur *et al.*[17] have shown that ATR-FTIR Spectroscopy is a very useful technique to study (bio)polymer adsorption from solution.

A particularly useful ATR-IR accessory is the Cylindrical Internal Reflectance Cell for Liquid Evaluation (CIRCLE). This cell contains an internal reflection element (IRE) which is made of a material with a high refractive index, such as germanium (n=4.0), silicon (n=3.43), or zinc selenide (n=2.40). The IRE has the shape of a pencil sharpened at both ends. The infrared beam is reflected about 10 times along the rod at the IRE-sample interface, each time producing an evanescent wave into the sample. The CIRCLE has increased the analysing capability of infrared light for homogeneous solutions because of the very small path length (of the order of a micron) which is sampled. Therefore, it is possible to measure IR spectra of components in strongly infrared-absorbing solvents, such as water and ethanol. The CIRCLE can also be a very powerful tool to monitor surface processes in solution.[18] Changes in the concentration of species at the interface which react or interact with the IRE can be fairly easily determined. Chemical modification or coating of the IRE surface increases the potentiality of this technique for studying surface processes. Using a recently developed step-scan interferometer with adequate detector and electronics, time resolution of less than a microsecond should be possible. This utility makes the ATR technique very capable to study the kinetics of surface processes. One advantage of all spectroscopic techniques, is

that measurements can be done *in situ.* The big advantage of ATR infrared spectroscopy is, however, that different species can be detected simultaneously. Kuzmenka and Granick[20] were the first to apply the CIRCLE for a study of the kinetics of (homo)polymer adsorption. They investigated the exchange process between poly(methyl methacrylate) molecules in the bulk solution and in the polymer layer adsorbed on a germanium crystal, using protonated and deuterated polymers.

Most polymer adsorption studies, both theoretical and experimental, are dealing with equilibrium conditions. In recent experiments more attention is paid to the kinetics of polymer adsorption.[4,5,20-26] Several processes may play a role in polymer adsorption kinetics, such as transport towards the surface, attachment and reconformation of polymer molecules at the interface, and exchange of small molecules by large ones. The first process can be more or less controlled by choosing well defined hydrodynamic conditions.[4] The last process can be excluded by taking monodisperse polymer. Several kinetic studies of homopolymer adsorption in the literature seem to claim that attachment and reconformation of polymer molecules occur on a time scale of the order of seconds or minutes.[23-25] But for other systems, such as the block copolymers studied by Leermakers *et al.*[5], one finds time effects of the order of weeks.

In this study, we used the CIRCLE to obtain more insight into the time scales which are relevant for both a̲d̲sorption and d̲e̲sorption processes of polymers. Therefore, we first report some results on polymer adsorption as a function of time for different molecular weights and polymer concentrations. The second part of this chapter deals with polymer desorption by using a low molecular weight displacer as well as more strongly adsorbing polymers. The concentration of low molecular weight displacer needed to entirely displace a polymer from the surface (i.e., the critical point) is a measure for the adsorption energy of the segments.[27,28] We applied the ATR-FTIR technique also to measure these critical displacer concentrations.

3.2. Experimental

3.2.1. Determination of surface excess from absorbance

Harrick[15] has defined the penetration depth of the evanescent wave as the distance where the electric field component at the interface has dropped by a factor e (i.e., 36.8% of its value at the interface). This penetration depth is given by

$$d_p = \frac{\lambda}{2\pi n_1 \sqrt{\sin^2 \theta - (n_2/n_1)^2}}$$ (1)

where λ is the wavelength of the infrared radiation in vacuum, n_1 and n_2 are the refractive indices of the IRE (crystal) and the medium, respectively, and θ is the angle of incidence. The penetration depth of the evanescent wave may be affected by energy transfer due to absorption. Müller et al.[29] give an expression for the penetration depth in this case. However, the difference between the penetration depth calculated by Eq. (1) and the expression given by Müller et al. is negligible for not too strong absorbances.

The Beer-Lambert law can be applied by using an *effective path length*. However, this path length is different for the two polarisations because the electric field amplitudes of the polarisations at the interface are different for equal incident amplitudes of the perpendicular and parallel polarisation. The path length for parallel polarisation is always greater than that for perpendicular polarisation.[15] If one has either parallel or perpendicular polarisation, weak absorptions, and a thickness of the more transparent medium which is much greater than the penetration depth, the effective path length is given by

$$d_e = Q \int_0^\infty \exp(-2z/d_p) dz$$ (2)

where Q stands for $n_2 E_0^2 / n_1 \cos\theta$, with E_0 the amplitude of the electric field vector at the IRE/medium interface, and z is the

distance normal to this interface. Using the Beer-Lambert law, the absorbance A can be written as

$$A = QN\varepsilon \int_0^\infty c(z)\exp\left(-2z/d_p\right)dz \qquad (3)$$

where N is the number of reflections, ε the molar absorption coefficient, and $c(z)$ the concentration of the absorbing component as a function of z. The penetration depth (and the absorbance) is not very sensitive to small changes in n_2. Therefore, it is allowed to assume that the penetration depth does not significantly depend on $c(z)$.

When polymer adsorbs onto the crystal, the absorbance consists of two contributions, one due to the excess (adsorbed) polymer on the surface (A_a) and the other due to the free polymer in the solution (A_f). The absorbance can now be written as

$$A = QN\varepsilon\left[\int_0^\infty \Delta c(z)\exp\left(-2z/d_p\right)dz + c_0 \int_0^\infty \exp\left(-2z/d_p\right)dz \right] \qquad (4)$$

where c_0 is the free polymer concentration and $\Delta c(z)$ the excess (adsorbed) polymer concentration as a function of z. The integration of the second integral can simply be carried out, giving $A_f = QN\varepsilon d_p c_0 / 2$. Note that A_f is proportional to the penetration depth of the evanescent wave which is a function of λ. The exponential factor in the first integral is essentially constant over the region where Δc is finite because the extension of the adsorbed layer is much smaller than d_p. This integral is then reduced to the zeroth order moment of the adsorbed layer which is equal to the adsorbed amount per surface area Γ. So, the contribution of the adsorbed polymer to the total absorbance is $A_a = QN\varepsilon\Gamma$. Due to the fact that the extension of the adsorbed layer is much smaller than the penetration depth, no information about the shape of the adsorbed polymer concentration profile can be obtained by this technique. Shorter wavelengths (e.g., visible light) would be needed to obtain second or higher moments.[30] Dividing the expression for A_a by the one for A_f, one obtains an explicit expression for Γ:

$$\Gamma = \tfrac{1}{2}S^{-1}A_a d_p \tag{5}$$

Here, the parameter S equals A_f/c_0. So, if the contributions A_a and A_f in an adsorption experiment can be separated, the adsorbed amount can be calculated.

When non-polarised light is used, the absorbed intensity is the polarisation-ratio-weighted addition of parallel and perpendicular absorbed intensities. The absorbance is then of course not a simple weighted average of $A_\perp$ and $A_\parallel$. Ohta et al.[31] have shown that the difference between the observed absorbances measured by non-polarised light and polarised light, respectively, depends on the magnitude of the absorbance. For isotropic samples, this difference is negligible if the absorbance of a band is less than 0.5. This means that the formulas derived above can also be used for non-polarised light, provided the absorbance of the band under investigation is not too strong.

3.2.2. Materials

All measurements were carried out with analytical grade chemicals. The polymers used in this study were poly(tetrahydrofuran) (PTHF), poly(butyl methacrylate) (PBMA), and poly(methyl methacrylate) (PMMA). Table 1 gives the molecular weight and the polydispersity index M_w/M_n of the polymer samples. The ratio M_w/M_n does not characterise the sample fully. For the highly polydisperse PBMA sample, with $M_w/M_n = 2.5$, we also give the molecular weight distribution (Figure 1), as measured by gel permeation chromatography. The distribution is quite broad and ranges from a molecular weight of about 3.8 to 2400 kg/mol. We used carbon tetrachloride, toluene, and dioxane as solvents for the polymers given above.

3.2.3. Spectra

The IR measurements were carried out with a single beam Bruker IFS 85 Fourier transform infrared spectrometer equipped with a fast recovery DTGS (deuterated-triglycerine-sulphate) detector. We have

Table 1. *Polymer samples*

sample		M_w (kg / mol)	M_w/M_n
PTHF 4	PL	4.00	1.12
PTHF 10	PL	9.50	1.08
PTHF 15	PL	15.0	1.09
PTHF 38	PL	37.6	1.07
PTHF 107	PL	107	1.07
PTHF 258	PL	258	1.13
PTHF 415	PL	415	1.18
PTHF 690	PL	690	1.25
PBMA	Aldrich	240	2.5
PMMA	Aldrich	93	2.0

PL: Polymer Laboratories
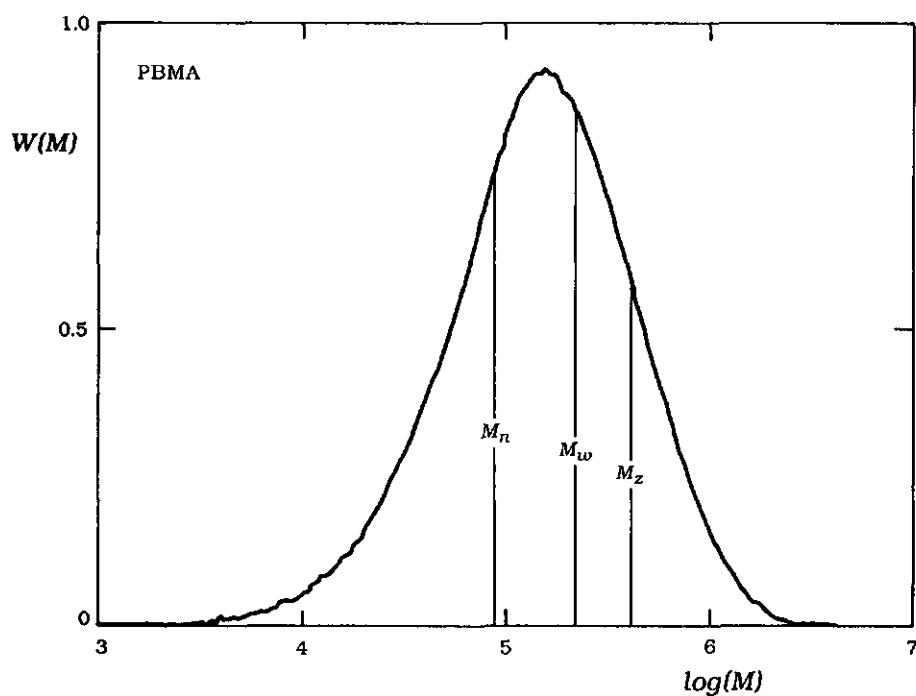
Figure 1. *The molecular weight distribution of PBMA. The different averaged molecular weights (M_n, M_w, and M_z) are indicated.*

to note here that probably more accurate results could be obtained with a more sensitive MCT (mercury-cadmium-telluride) detector but this was not available in our laboratory. The CIRCLE optics were purchased from Spectra-Tech Inc. We have used the macro-volume (about 10 mL) "open boat" cell with a silicon rod. The interferograms were recorded with non-polarised light, a nominal resolution of two wavenumbers, and a triangular apodization function. Although we obtained good results with these settings, nowadays other apodization functions such as Norton-Beer and Blackman-Harris are recommended for quantitative analyses.[32] Most spectra were based on a collection of 1000 interferograms, which took about a quarter of an hour sampling time. The number of scans was reduced to 100 for kinetic studies at short times. The temperature was kept constant within 0.5 °C during the measurement. The sample compartment was continuously flushed with dried nitrogen.

According to Sperline et al.,[33] the average incidence angle stated by the manufacturer is in most cases not correct because this angle depends on spectrometer characteristics such as the IR beam's intensity profile, the divergence of the beam, and the alignment of the optics. Therefore, the CIRCLE should be calibrated first. Each time the CIRCLE is realigned or the rod is moved in its holder the calibration should be done again. We have used the calibration method described by Sperline et al.[33] This method is based on the comparison of the absorbance of a reference liquid measured by the CIRCLE with that measured by a normal transmission experiment. Both the average incident angle and the number of reflections can be calculated when the solution contact length with the crystal, the diameter of the IRE, and the refractive indices are known. It turned out that in our case $\theta = 38°$ and $N = 13$, whereas the incident angle given by the manufacturer is 30°. For calculating the penetration depth in a solvent at a particular wavenumber, the refractive index of both the silicon rod and the solvent at this wavenumber have to be known. The index of refraction of the silicon rod is fairly constant ($n=3.43$) over the wavenumber range of interest (4000-1500 cm^{-1}).[18] The refractive indices of various solvents as a function of the wavelength are available in the literature.[34-36] For example, carbon tetrachloride has a refractive index of 1.41 for both

wavenumber regions used, i.e., 3045-2770 cm^{-1} and 1761-1691 cm^{-1}.

3.2.4. Sample preparation

The cell must be cleaned before each new experiment. Whether or not the crystal is clean can be simply checked by taking a spectrum of the cell in dried nitrogen. The cleaning procedure was repeated when the spectrum showed bands of contaminating species. The following cleaning protocol gave clean surfaces and reproducible results. Firstly, the cell was filled with a suitable displacer for about 16 hours. The displacer was refreshed several times during this interval. Dioxane turned out to be a good displacer for the polymers used (see results). Secondly, a mixture of hydrogen peroxide, ammonia, and water was placed in the cell for about one hour in order to remove any impurities still left and to obtain a reproducibly oxidized silicon surface. Finally, the cell was rinsed with water and methanol, in that order, and dried in a oven at 120 °C for several hours. An advantage of this cleaning procedure is that it is not necessary to remove the crystal from its holder. There is no need to re-calibrate the cell after cleaning.

The cell was transferred directly from the oven into the sample compartment of the IR spectrometer. The reference spectrum of the empty cell was measured after about one hour, when the cell had cooled down and the water vapour and carbon dioxide coming into the compartment by installing the cell had been removed. In the case of a kinetic experiment, spectra of the sample were collected directly after the cell was filled. The time needed for filling the cell and taking the required number of scans determines the minimum elapsed time for the first data point; this appeared to be a few minutes for 100 scans.

Subtraction of spectra is needed when bands of different species overlap. For instance, when a band of the solvent and one of the polymer overlap, a spectrum of the pure solvent has to be subtracted from the spectrum of the sample in order to separate the absorbances of these two species at this wavelength. The subtraction factor needed for this operation can be determined in a frequency

region where the bands do not overlap. Absorption of any water vapour present in the compartment may also interfere with bands of the adsorbate. In most spectra small absorption peaks of water vapour were still present, despite flushing of the sample compartment with dried nitrogen. The factor needed for subtracting a water vapour spectrum from the spectrum of the sample was determined in the frequency region 4000-3700 cm^{-1} because in this region the substances used in our experiments do not absorb radiation. Integration of peaks was carried out after smoothing of the spectra. This smoothing improves the reproducibility of the integrations but reduces the information about the fine structure of the spectrum. Therefore, smoothing is not recommended for qualitative measurements.

3.3. Results and discussion

3.3.1. Polymer adsorption

Figure 2 shows the absorption dependence of PTHF and PBMA on the polymer concentration in carbon tetrachloride. The parameter S, which gives the absorbance per unit concentration of free polymer, can only be determined separately from A_a when the adsorbed amount does not change with the polymer concentration. This can be achieved in several ways which are described below.

1) The crystal surface can be coated with a more strongly adsorbing polymer. It is characteristic for polymers that adsorption/desorption transitions are very sharp. In a saturated system of two polymers with different adsorption energy, only one polymer will adsorb. Poly(butyl methacrylate) should not adsorb onto a silica surface with pre-adsorbed PTHF because PBMA has a lower adsorption energy on this substrate than PTHF (see the section about polymer desorption). Figure 2 (filled circles) gives the carbonyl (CO) vibration absorbance in the region 1761-1691 cm^{-1} of PBMA as a function of the PBMA concentration for the case that PTHF is pre-adsorbed on the IRE. As can be seen, the intercept which is equal to A_a and is a measure for the adsorbed amount of

PBMA is indeed zero. The increase of absorbance with PBMA concentration is linear over the whole concentration range. The slope of this line is equal to S.
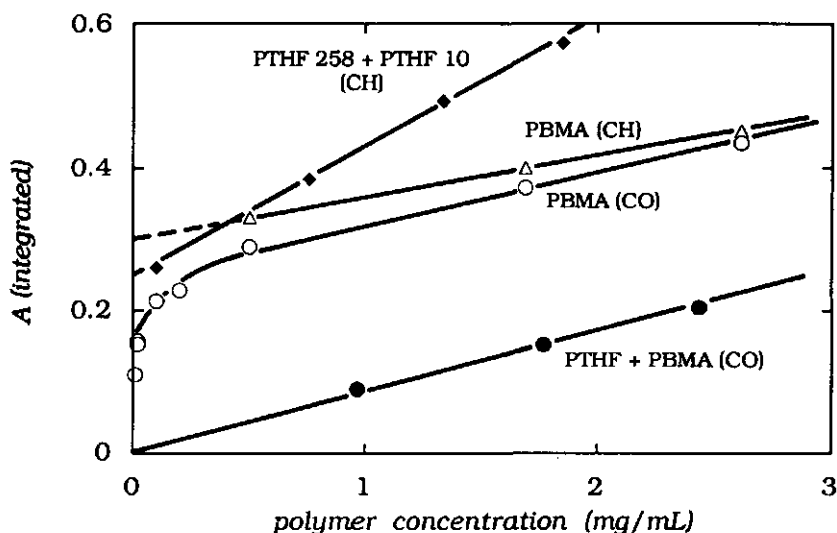

Figure 2. *Absorbance of PBMA and PTHF 10 in carbon tetrachloride as a function of the free polymer concentration without (open symbols) and with (filled symbols) pre-adsorbed polymer on the IRE-crystal. For PBMA the CO-band (1761-1691 cm^{-1}) or CH-band (3045-2840 cm^{-1}) was used, for PTHF the CH-band (3000-2770 cm^{-1}). The pre-adsorbed polymer for PBMA was PTHF 258 (●), that for PTHF 10 was PTHF 38 (◆).*

2) When no pre-adsorbed polymer is used, the absorbance is not proportional to the polymer concentration due to an increase in the adsorbed amount of PBMA (see open circles in Figure 2). However, for high concentrations the slope becomes constant and equal to the one with pre-adsorbed PTHF. For these high concentrations the adsorbed amount does not change any more with concentration because the plateau region of the adsorption isotherm has been reached. The intercept obtained by extrapolation to zero PBMA-concentration corresponds to the adsorbed

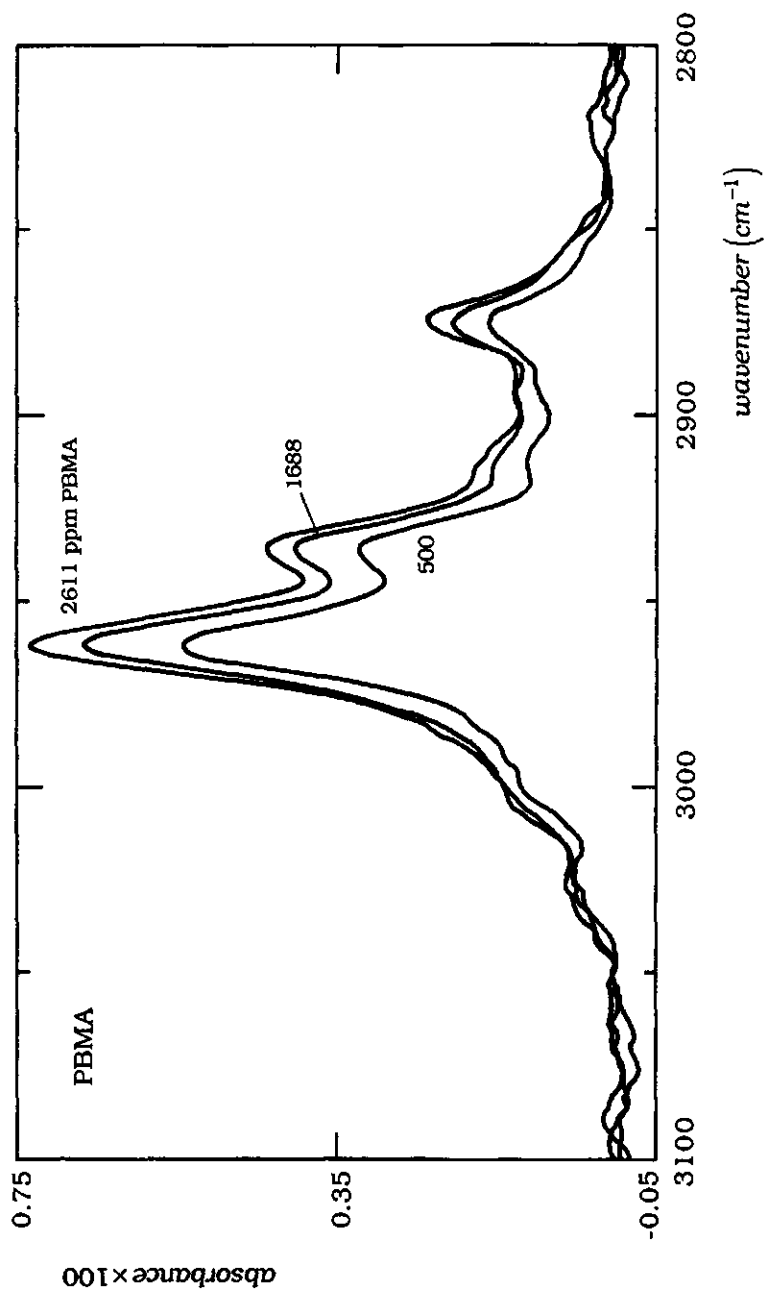48

Figure 3. *Carbon-hydrogen vibration spectra of PBMA in carbon tetrachloride (corresponding to the open triangles in Figure 2). The concentration of PBMA is indicated.*
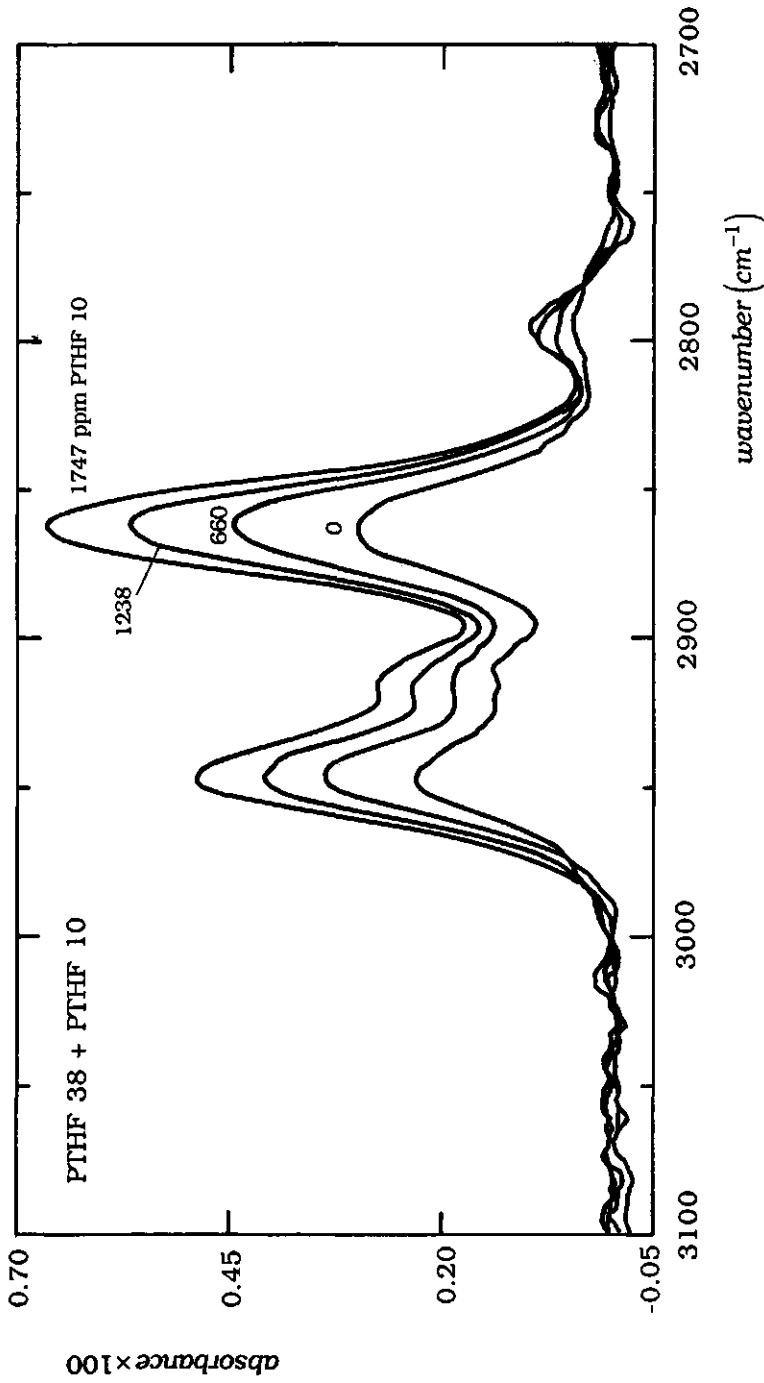
Figure 4. Carbon-hydrogen vibration spectra of PTHF in carbon tetrachloride (corresponding to the filled diamonds in Figure 2). The pre-adsorbed polymer is 100 ppm PTHF 38; the concentrations PTHF 10 are indicated.

amount in the plateau of the isotherm. Besides the CO vibration, we have also used the carbon-hydrogen (CH) vibration of PBMA. The absorbance due to this band (3045-2840 cm^{-1}) is also given in Figure 2 (open triangles). It is clear that A_a for the CH-band is slightly higher than A_a for the CO-band. Spectra of the CH-vibration for PBMA (corresponding to the open triangles in Figure 2) are shown in Figure 3. The peak area (integrated from 3045-2840 cm^{-1}) increases linearly with the PBMA-concentration.

3) The value of S for the CH-vibration of PTHF was determined with two samples of different molecular weight. The low molecular weight sample was added after adsorption of the high molecular weight one in order to increase the free polymer concentration without affecting the adsorbed amount. High molecular weight polymer adsorbs preferentially over low molecular weight for entropical reasons.[37] Hence, no increase in the adsorbed amount is expected when the low molecular weight polymer is added. The results are given in Figure 2 (filled diamonds). The intercept now corresponds to the adsorbed amount for the high molecular weight polymer. For comparison, CH-vibration spectra for PTHF are given in Figure 4. The four curves correspond to the filled diamonds in Figure 2. The lower curve is for an addition of 100 ppm PTHF 38 which is virtually equal to the equilibrium concentration in the cell. The other curves, showing a gradual increase in A, are for successive additions of PTHF 10 to this solution of PTHF 38. Note that the total PTHF-concentration is 100 ppm higher than the added concentration of PTHF 10.

Figure 5 shows the adsorption of monodisperse PTHF 38 from carbon tetrachloride as a function of time, for two polymer concentrations. The adsorbed amount Γ was calculated from Eq. (5), using the values for S and A_a as determined above. Within the time resolution of our apparatus, there is no significant change of Γ as a function of time. After a few minutes, the adsorbed amount was already constant at 0.23 mg/m^2. Similar results were obtained for polystyrene adsorption on silica from cyclohexane by Frantz et al.[38] This observation does, however, not imply that the adsorbed polymer layer is already in the equilibrium state within a few

minutes. There might be still conformation changes going on even though the total adsorbed amount does not seem to change any more. After 16 hours the adsorbed amount had not changed significantly.
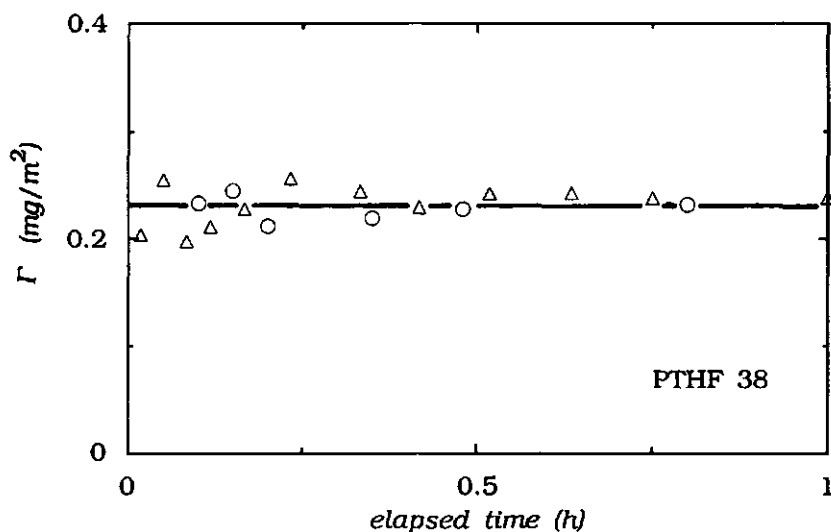
Figure 5. *Adsorbed amount of PTHF 38 in carbon tetrachloride as a function of time for two polymer concentrations.* O, *20 ppm;* Δ, *1000 ppm.*

The scatter in the data at short times can be explained by a lower signal/noise ratio due to shorter sampling times. No significant difference could be measured between the adsorbed amounts from solutions with a polymer concentration of 20 ppm and a concentration of 1000 ppm. This reflects high affinity adsorption as should be expected for monodisperse polymers.

Similar results as given in Figure 5 were obtained for PTHF 4 and PTHF 258. However, the adsorption of PTHF 258 at high concentrations gave an unexpected result which is shown in Figure 6. When the concentration was increased step-wise from 500 ppm to 1688 ppm, the adsorbed amount started to increase with time. We think that this can be attributed to incipient phase separation of
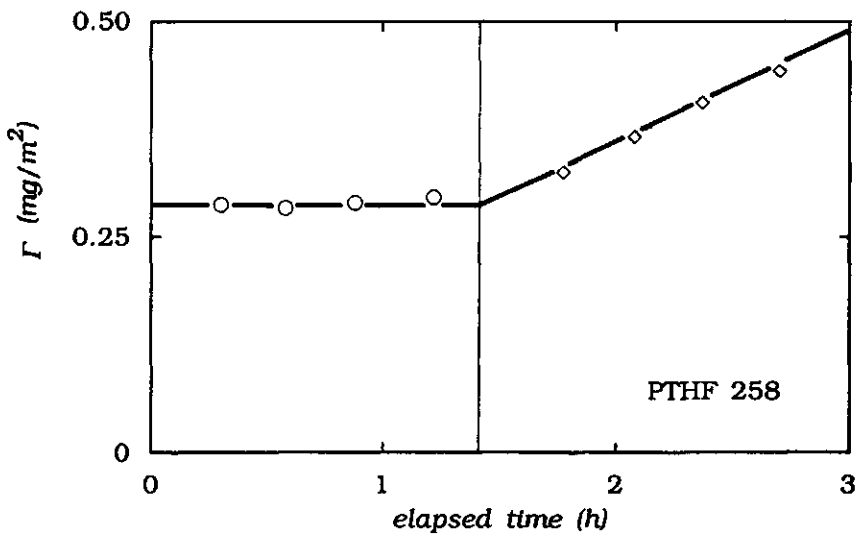
Figure 6. *Adsorption of PTHF 258 from carbon tetrachloride as a function of time. The free polymer concentration was increased from 500 ppm (○) up to 1688 ppm (◇) after 1.4 h (indicated by the vertical line).*
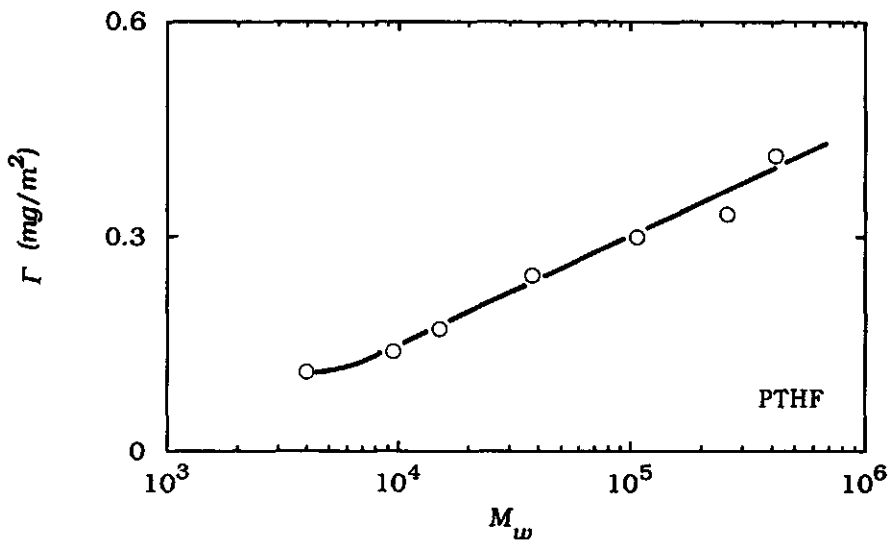
Figure 7. *Adsorption of PTHF from carbon tetrachloride as a function of molecular weight.*

the polymer, which may also show up as an extra adsorbed amount. Phase separation may occur in worse than theta solvents, especially for high molecular weights at high concentrations. We have no independent information about the solvent quality of carbon tetrachloride for PTHF, but the molecular weight dependence of Γ (see Figure 7, below) suggests close-to-theta conditions. Therefore, the measurements with the high molecular weight samples were not carried out at relatively high polymer concentrations.

Figure 7 shows the dependence of the adsorbed amount of PTHF in carbon tetrachloride on the logarithm of the molecular weight. For this polymer/solvent pair, the adsorbed amount increases linearly with the logarithm of the molecular weight. The self-consistent field theory of Scheutjens-Fleer[39] predicts such a dependence for near-to-theta conditions. Hence, this observation provides support to our conclusion that the solvent quality is poor, so that the polymer solution might well phase separate at high polymer concentrations (see Figure 6).

Figure 8. *Adsorbed amount of two PTHF mixtures in carbon tetrachloride as a function of the square root of time.* Δ, *20 ppm PTHF 4 + 5 ppm PTHF 258;* ○, *20 ppm PTHF 4 + 1 ppm PTHF 258.*

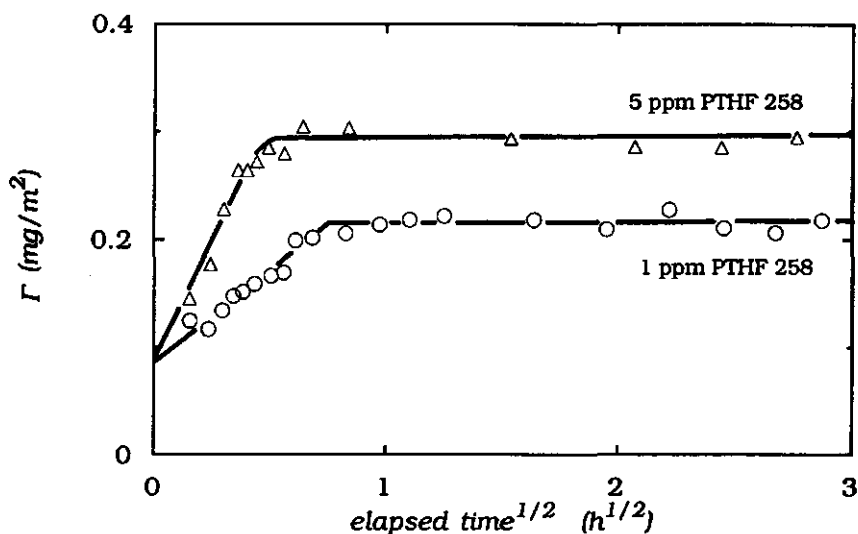The adsorption of a mixture of two PTHF samples in carbon tetrachloride as a function of time is given in Figure 8. The mixtures consist of 20 ppm PTHF 4 and either 5 ppm PTHF 258 or 1 ppm PTHF 258. The concentrations of PTHF 258 in the mixtures are possibly somewhat lower than quoted here due to adsorption onto the walls of the glassware, which might not be insignificant for such low concentrations. Unlike the situation for one-component solutions, there is now a clear time effect. For both mixtures the adsorbed amount initially increases as a function of time and then levels off. The adsorbed amount starts at a value which corresponds to the equilibrium adsorbed amount of PTHF 4. For the mixture with the highest PTHF 258 concentration, the adsorbed amount stops to increase at a value which corresponds to the equilibrium adsorbed amount of PTHF 258. Apparently, the surface is at first mainly covered with the low molecular weight sample, and later on with the high molecular weight polymer. In between, there is a transition from adsorbed PTHF 4 to adsorbed PTHF 258. The short polymer molecules will arrive sooner at the surface than the long ones due to a higher diffusion coefficient and higher concentration. This process is, however, too fast to be measured within the time resolution of our technique. After this process, exchange of small molecules by large ones takes place and this exchange is much slower than the adsorption process on a bare surface. High molecular weight polymer has a higher affinity to adsorb than low molecular weight polymer because the loss of translational entropy is less for large molecules.[37,40] It turns out that the increase of Γ is linear in the square root of time. The mixture with the lowest concentration PTHF 258 shows a final plateau at a lower adsorbed amount than the equilibrium value of PTHF 258. This is probably due to the fact that in this case the PTHF 258 solution becomes exhausted. The rate of exchange is also lower in this case, because of a smaller driving force at smaller dosage.

The next step is to look at adsorption of polydisperse polymers as a function of time. This can be viewed upon as an extension from a bimodal distribution towards a continuous one. Figure 9 shows the adsorption of 20 ppm PBMA in carbon tetrachloride as a function of time. The adsorbed amount was determined from both the CH-
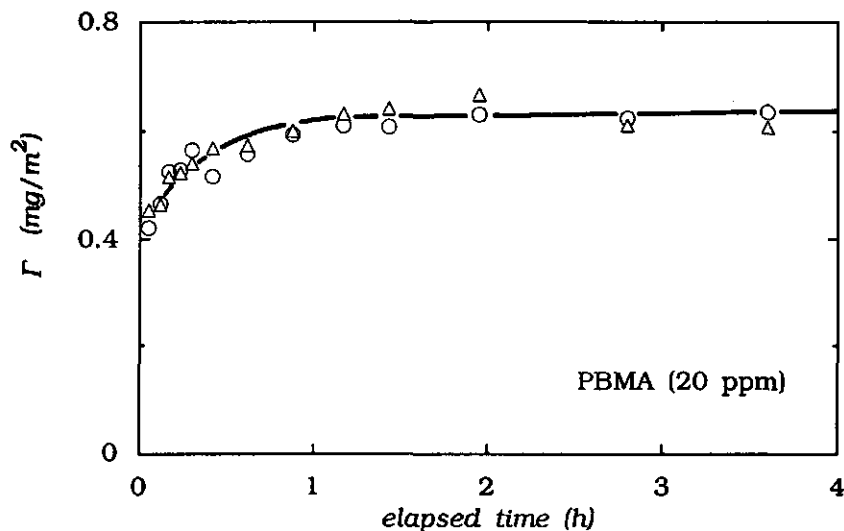
Figure 9. *Adsorption of PBMA from a solution of 20 ppm PBMA in carbon tetrachloride as a function of time, determined from two different absorption bands. O, C-H vibration (integration region 3045-2840 cm^{-1}); Δ, C=O vibration (integration region 1761-1691 cm^{-1}).*

vibration and the CO-vibration band of the polymer. The shape of the carbonyl peak at the low frequency end slightly changes with time, even after several hours. The low frequency end of the spectrum monitors hydrogen bonding between carbonyl groups of the polymer and silanol groups of the surface[13]: the absorbed frequency shifts towards lower values due to this binding. Therefore, small changes in the spectrum in this frequency region indicate (small) orientational rearrangements of carbonyl groups on silanol groups, which still may occur after the adsorbed amount has virtually reached the equilibrium value. Apparently, it takes some time for segments to find the equilibrium (optimal) orientation to active surface sites. The integrated absorbance of the carbonyl peak is, however, not significantly influenced by these small changes: we found within experimental error the same adsorbed amounts for the CO- and the CH-vibrations (Figure 9). Apparently, the error which is made by integrating the entire CO-peak without discriminating the perturbed and unperturbed vibration is very small. The integrated

value will only be significantly affected when both the fraction bound carbonyl groups is high and the molar extinction coefficient of the perturbed carbonyl vibration is very different from that of the unperturbed one.
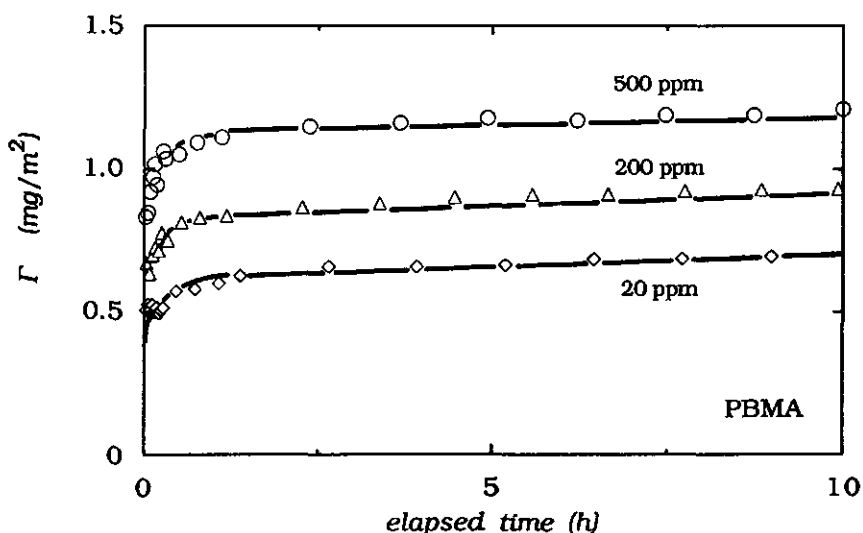
Figure 10. *PBMA adsorption from carbon tetrachloride as a function of time for three polymer concentrations: O, 500 ppm; △, 200 ppm; ◇, 20 ppm.*

Just as for the monodisperse PTHF mixtures, there is an increase in the adsorbed amount as a function of time due to polymer exchange processes. However, as expected this increase is more gradual than for the bimodal mixture (Figure 8); plotting of the data as a function of the square root of time does not produce two linear sections. Similar results for higher concentrations PBMA (and a longer time scale) are given in Figure 10. Two features show up clearly. Firstly, the adsorbed amount increases with concentration. Secondly, polymer is exchanged at a higher rate when the polymer concentration is higher, as can be seen from the initial slopes. These observations can be explained by the fact that at higher dosages the concentrations of all molecular weight fractions in the solution are higher. These increased concentrations are responsible for a faster

exchange. Another observation for all curves is that for longer times the adsorbed amount is still slightly increasing. This may reflect either very slow exchange processes or small changes in the conformation of the adsorbed polymer layer.

An adsorption isotherm of PBMA can be constructed from a cross section of Figure 10. Figure 11 gives such a cross section at long elapsed times; for this figure more polymer concentrations than those indicated in Figure 10 were used. The rounded shape of the isotherm is typical for polydisperse polymers.[37]
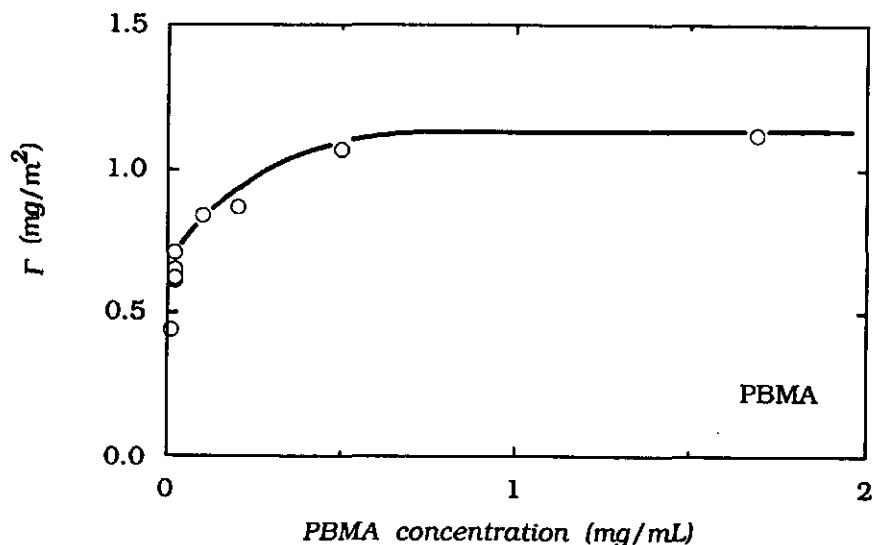
Figure 11. *Adsorption isotherm of PBMA in carbon tetrachloride after 10 hours.*

3.3.2. Polymer desorption

Polymer desorption can be brought about by adding a more strongly adsorbing component, i.e., a displacer. Adding a low molecular weight displacer essentially lowers the effective adsorption energy of the polymer. The amount of displacer which is just needed to entirely displace the adsorbed polymer from the surface is called the critical displacer concentration (critical point).

This concentration is a measure for the adsorption energy of polymer segments. Cohen Stuart *et al.*[27] have developed a model to relate this concentration to the effective adsorption energy of polymer segments.

In Figure 12, we show the desorption of PMMA from silica as a function of the dioxane volume fraction in a dioxane/toluene solvent mixture, measured by IR and by two other techniques. The classical and most laborious technique is the depletion method where the adsorbed amount of polymer is calculated from the free polymer concentration in a dispersion of silica with polymer. This concentration is determined analytically in the supernatant. A very sensitive technique to determine the critical point is Thin-Layer Chromatography (TLC). This method is based on the interfacial residence time of a polymer on a substrate, expressed in the retention factor R_f. For experimental details of both the TLC and the depletion method, the reader is referred to ref 28.

Figure 12. *PMMA desorption from silica by increasing the amount of dioxane in a dioxane/toluene solvent mixture. Three different techniques were used. The curves give the relative absorbance A/A_o (where A_o is the absorbance of PMMA in pure toluene) as measured by FTIR, $1-R_f$ (where R_f is the retention coefficient) from TLC, and the adsorbed amount Γ found from the depletion method.*
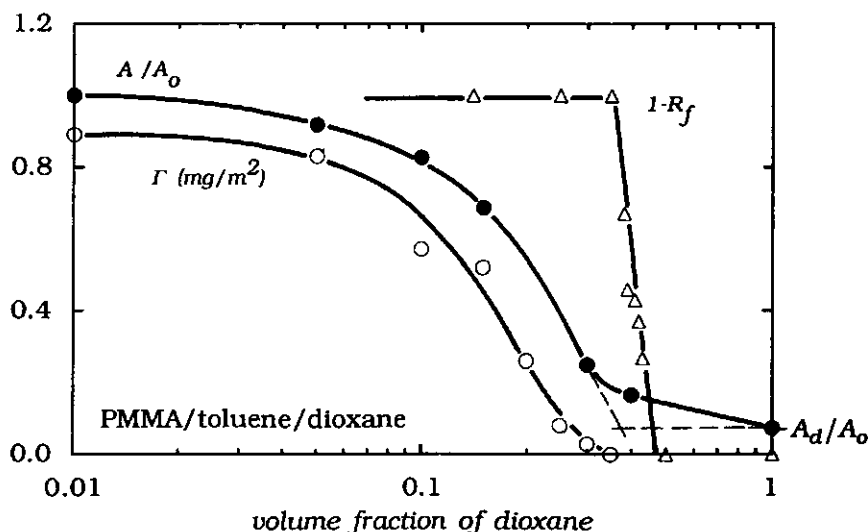
The IR measurements were carried out with solutions of 500 ppm PMMA. These measurements were taken about 16 hours after the cell was filled with the solution. The absorbance A of the carbonyl vibration (1761-1695 cm^{-1}) was used to quantify the adsorbed amount PMMA. The results are plotted as A/A_o, where A_o is the absorbance of PMMA in pure toluene. In order to transform the absorbances into adsorbed amounts, a calibration curve like the one given in Figure 2 would have to be measured for each solvent mixture, because both the molar extinction coefficient and the penetration depth may change with solvent composition. The variation of the penetration depth becomes less important for relatively low free polymer concentrations. However, the effect of these two variations on the absorbance is in most cases small as compared to the effect of the change in the adsorbed amount. Hence, in most instances it is not necessary to do these calibrations if one is only interested in the critical point. The absorbance which remains in the presence of pure dioxane is only due to free polymer. The extrapolation of the curve to the constant level A_d/A_o, where A_d is the absorbance in pure dioxane, may be taken as the critical point. The critical points measured by the three different techniques agree very well. Therefore, also the IR technique is useful for determining critical points. The minor differences between the various methods may be caused by the different types of silica used: aerosil (ox 50 ex Degussa) for the depletion method, kieselgel (silicagel 60 F_{254}, Merck) for TLC, and the oxidized silicon crystal in FTIR. For all these silicas, the PMMA is completely desorbed at a volume fraction dioxane of 0.40 ± 0.06.

Dioxane can also be used to desorb PTHF and PBMA from silica. Figure 13 shows spectra of the carbonyl vibration of PBMA for different volume fractions dioxane in dioxane/carbon tetrachloride solvent mixtures with 20 ppm free polymer. The CO-peak decreases with increasing dioxane concentration. For the dioxane volume fraction of 0.222, only the absorption due to the free polymer is left which is not very significant for such low concentrations. We also tried to study the kinetics of PBMA desorption by dioxane. Three kinetic contributions for a polymer desorption process can be distinguished: the transport of the invading species to the surface,
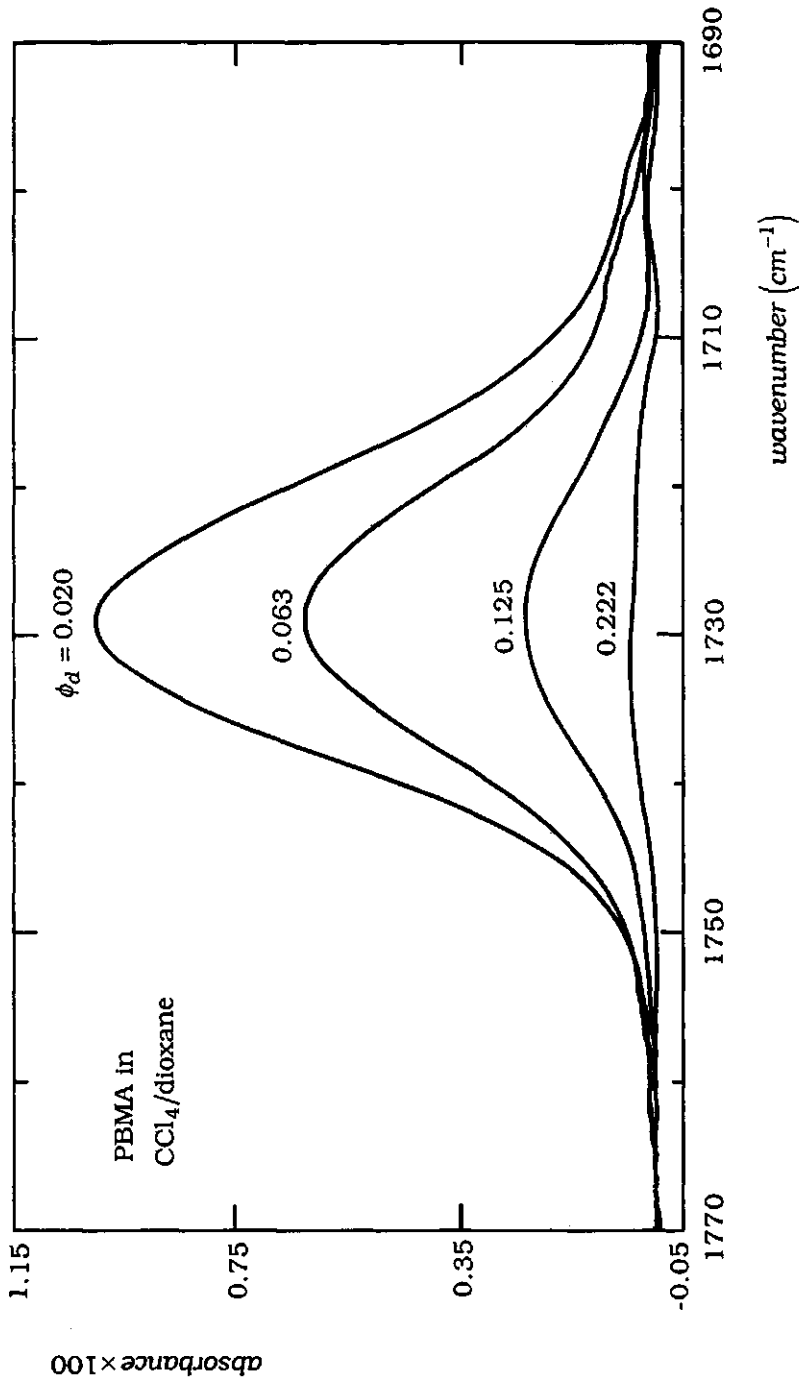
Figure 13. *Carbonyl vibration spectra of adsorbed PBMA in four different dioxane/carbon tetrachloride solvent mixtures. The PBMA concentration is 20 ppm, the volume fraction ϕ_d of dioxane is indicated.*

the displacement of the polymer, and the diffusion of the leaving polymer across the penetration depth. The average time for a polymer molecule to diffuse across the penetration depth is $\tau = d_p^2/4D$. This time is of the order of 10 milliseconds for a typical diffusion coefficient D of $1.0 \times 10^{-7} cm^2/s$[41] and a penetration depth of one micron. At the concentrations used, the first contribution to the desorption process is much more rapid than the last one. So, both the transport contributions are much faster than the time resolution of the experiment. Also the displacement of PBMA by dioxane appeared to be too fast to monitor with our apparatus. Dioxane was added to the cell in which 3.5 hours earlier a solution of PBMA in carbon tetrachloride had been introduced. The final dioxane volume fraction was 0.3 which is higher than the critical displacer concentration (see Figure 14, below). Before we could take our first spectrum, the adsorbed amount had already dropped to zero. Hence, the kinetics of PBMA displacement from a silica surface by a low molecular weight displacer such as dioxane appears to be relatively rapid.

Figure 14 shows equilibrium desorption curves for both PBMA and PTHF as a function of the dioxane volume fraction, measured by IR as well as TLC. The difference between the critical points of the two polymers is small. No significant difference could be measured by the IR technique between PBMA and PTHF. The TLC experiments, however, show that PBMA is more easily desorbed by dioxane than PTHF. When a solution containing both PBMA and PTHF is put into the IR cell, only PTHF will adsorb. This experiment as well as the TLC experiments indicate that PTHF has a higher adsorption energy on silica than PBMA. So, it should be possible to desorb PBMA by PTHF, even if the difference in segmental adsorption energy is small.

One might be surprised that the plateau value of the adsorption isotherm of PBMA in Figure 11 (i.e., 1.1 mg/m^2) is much higher than the adsorbed amounts found for the monodisperse PTHF samples (0.42 mg/m^2 for PTHF 415) whereas the segmental adsorption energy for PTHF in carbon tetrachloride is slightly higher than for PBMA. According to Figure 7, PTHF of the same molecular weight as the largest PBMA molecules of the molecular weight

distribution given in Figure 1 would give a Γ of about 0.54 mg/m^2 which is still much smaller than the adsorbed amount for PBMA. However, when the adsorbed amounts are expressed as the number of monomers per unit of surface area, we obtain for both polymers about the same adsorbed amount, viz. 7.5 $\mu mol/m^2$. Hence, the adsorbed amount expressed in mg/m^2 is larger for PBMA than for PTHF only because of the relatively large PBMA segments.
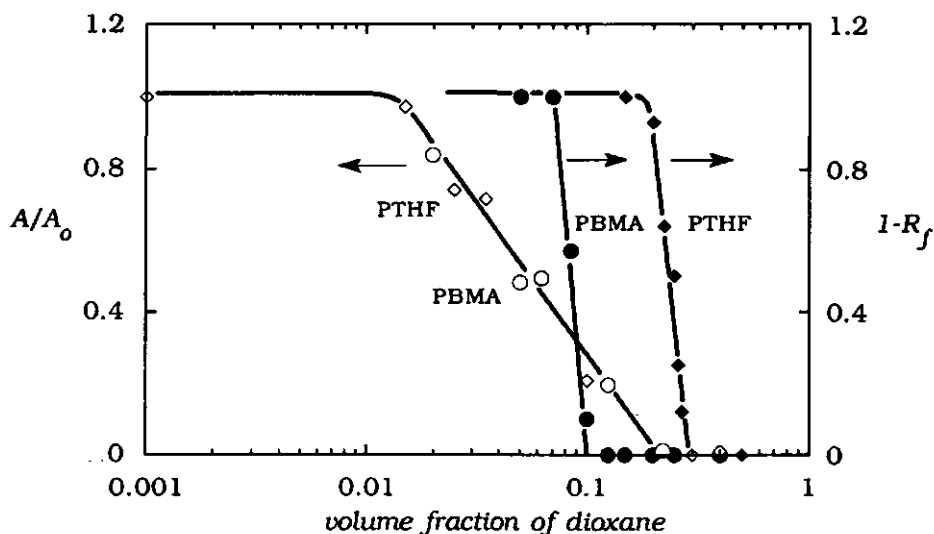
Figure 14. PTHF and PBMA desorption from silica by increasing the amount of dioxane in a dioxane/carbon tetrachloride solvent mixture. Both FTIR and TLC are used to monitor the polymer desorption. The curves give the relative absorbance A/A_o (where A_o is the absorbance of either PBMA or PTHF in pure carbon tetrachloride) and $1-R_f$ (where R_f is the retention coefficient).

Figure 15 shows the competitive adsorption behaviour of PBMA and PTHF on silica from carbon tetrachloride. When a solution of 20 ppm PBMA and 20 ppm PTHF 258 is placed into the cell (solid symbols), PTHF adsorbs rapidly (filled triangles) but after that nothing happens any more. No adsorption of PBMA can be detected (filled circles), while the adsorption of PTHF is the same as for a solution with only PTHF.

The open symbols in this figure represent an experiment where a PTHF 258 solution was added to the cell 3.5 hours after a solution of 20 ppm PBMA. The final free concentrations of both polymers were about the same as in the first experiment. The adsorption of PTHF is again rapid (open triangles). The adsorbed amount is, however, lower than in the case where both polymers are introduced simultaneously. The desorption of PBMA (open circles), on the other hand, is much slower than the concomitant adsorption of PTHF and becomes even slower as time goes by. The total adsorbed amount of polymer (PBMA + PTHF, open diamonds) first increases steeply (this increase cannot be seen in Figure 15) due to the fast adsorption of PTHF and then decreases slowly due to the desorption of PBMA. Hence, desorption of PBMA molecules starts after a certain amount
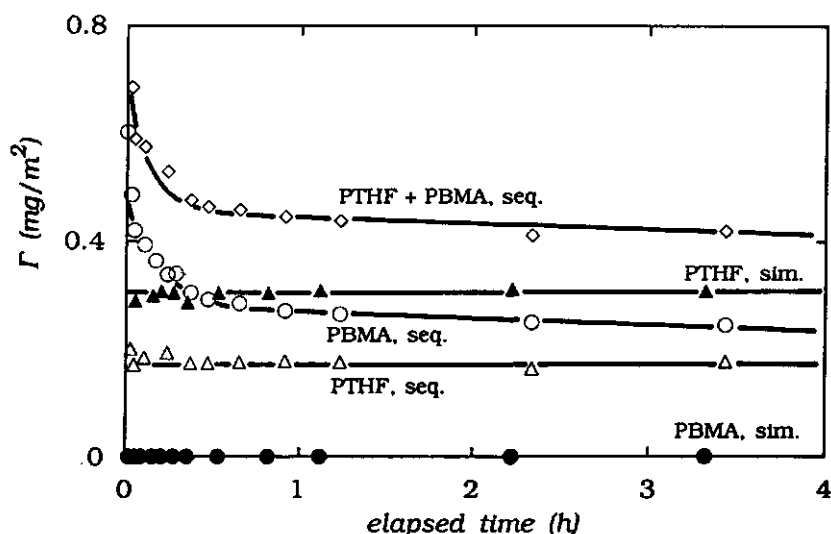
Figure 15. *Two experiments of PBMA displacement by PTHF 258 as a function of time. The final free polymer concentration of both polymers in both experiments was about 20 ppm. In the simultaneous (sim.) experiment (filled symbols), PBMA and PTHF were added at the same time; in the sequential experiment (seq.), PTHF was added 3.5 h after PBMA. The figure gives the adsorbed amount of the individual polymers as a function of time and, in the case of the sequential experiment also the total adsorbed amount.*

of PTHF is adsorbed. These observations lead to the idea that only already anchored PTHF molecules are able to displace PBMA molecules. Probably, desorption of PBMA by PTHF takes place segment-by-segment instead of molecule by molecule. At first, PTHF molecules will adsorb by only one or a few segments, which does not yet cause desorption of whole PBMA molecules. When a PTHF molecule is anchored that way, more PTHF segments will adsorb at the expense of adsorbed PBMA segments. At a given moment, so many PBMA segments are desorbed that a whole PBMA molecule is displaced from the surface. When this happens, a decrease in the adsorbed amount will be observed. It is interesting to note here that also Cosgrove and Fergie-Woods[42] found that in an exchange experiment the attachment of the invading species occurred more rapidly than the desorption of the leaving polymer. Johnson *et al.*[43] measured the fraction of bound segments of the incoming polymer as a function of time. They found that this fraction was still increasing after several hours, which is in line with polymer exchange on a segment-by-segment basis.

Because the final concentrations in both experiments of Figure 15 are the same, the equilibrium adsorbed amounts should also be the same for both cases. As can be seen in Figure 15, there is still a significant difference between the adsorbed amounts of both experiments after four hours. The experiment where both polymers are put together into the cell seems to be in equilibrium within a few minutes: the adsorbed amounts did not change significantly with time. The experiment where the polymers are added sequentially to the cell is still not yet in equilibrium after four hours. Let us focus somewhat more on the desorption kinetics of PBMA. Figure 16a gives the desorption of PBMA by PTHF 258 as a function of time for different concentrations of both polymers. For all cases, PTHF is added 3.5 hours later than PBMA. Remarkably, the PTHF concentration does not significantly affect the desorption rate of PBMA. This means that the desorption is indeed a surface controlled process. When a solution of 350 ppm PBMA is used instead of 20 ppm, the initial adsorbed amount is higher, as expected from the adsorption isotherm (Figure 11). The difference between these
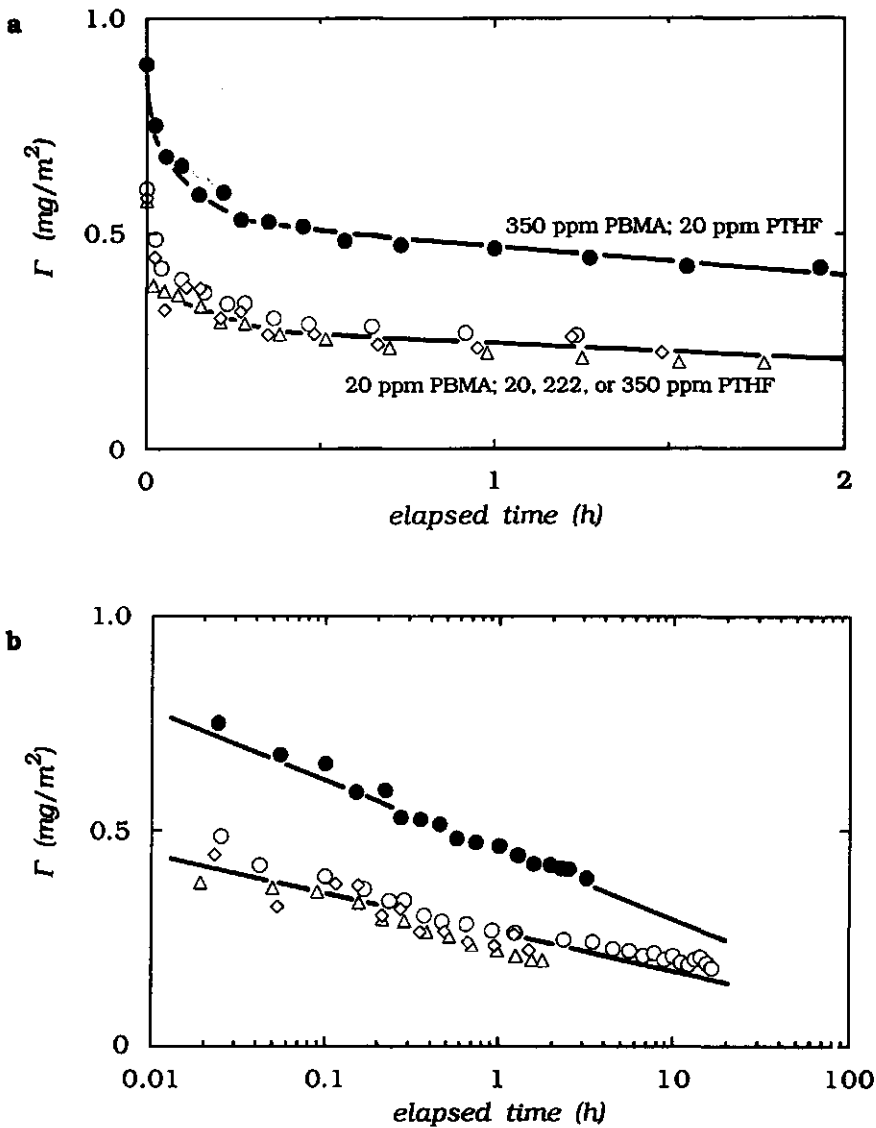
Figure 16. *PBMA desorption by PTHF 258 as a function of time (a) and log(time) (b) for different polymer concentrations. The PTHF was added 3.5 h after the PBMA. The upper curve (●) gives the adsorbed amount of PBMA for 350 ppm PBMA and 20 ppm PTHF. The open symbols represent the adsorbed amount of PBMA for 20 ppm PBMA and 20 (○), 222 (△), or 350 (◇) ppm PTHF, respectively. All concentrations quoted are final concentrations.*

adsorbed amounts becomes slightly smaller as desorption proceeds but it is questionable whether this is significant or not. In order to see how the PBMA desorption proceeds at long times, we have plotted the adsorbed amounts on a logarithmic time scale in Figure 16b. It can be seen again that the results at short times have the largest experimental error. Within this error, the points are well described by straight lines. When we extrapolate these lines to zero adsorbed amount, it turns out that it will take weeks (!) before the systems will be in equilibrium. These extrapolated times are not significantly different for both PBMA concentrations. From the semi-logarithmic plot, it is also clear that the desorption rate for the case of 350 ppm PBMA is somewhat larger than for the lower PBMA concentration.

The observations given above can again be explained in terms of segment-by-segment desorption. In the case of 350 ppm PBMA, more high molecular weight polymer molecules are adsorbed. Larger polymer molecules have higher adsorbed amounts due to longer loops and tails. The amount of train segments is generally the same for molecules of different size. When only the train segments play a role in the desorption process, the time needed for desorption of a certain amount of trains should be the same for different molecular weight samples. But then the desorption rate expressed as the reduction of the adsorbed amount per unit time should be larger for the high molecular weight samples due to a smaller train fraction.

In order to get more insight in the molecular weight dependence of both the invading and leaving polymer on the desorption kinetics one should do displacement experiments with narrow molecular weight fractions of both polymers. Another important question is how polymer desorption proceeds as a function of the time lag between the addition of first and the second polymer (aging experiments). Such experiments will give information about the state of the initial polymer layer. This layer is not yet in the equilibrium state when the desorption kinetics are still changing as a function of the time lag between the polymer additions. Frantz *et al.*[44] have started to do these type of experiments by using protonated and deuterated polystyrene.

3.4. Conclusions

The adsorbed amount of monodisperse PTHF measured as a function of time is already constant within a few minutes. For polydisperse polymers the adsorbed amount increases slowly with time due to the exchange of small polymer molecules by large ones. There are some indications that the adsorbed layer has not yet reached the equilibrium state when the adsorbed amount is already (nearly) constant with time.

The polymers PMMA, PTHF, and PBMA can all be completely displaced from silica by dioxane. The critical points (i.e., the displacer concentration just needed to entirely desorb polymer) can simply be measured by ATR FTIR and agree well with the ones determined by Thin-Layer Chromatography and by the depletion method. PTHF can be used to desorb PBMA because PTHF has a higher adsorption energy than PBMA. Polymer desorption by a more strongly adsorbing polymer is a much slower process than polymer desorption by a low molecular weight displacer. The adsorption of PTHF onto a silica surface with pre-adsorbed PBMA is faster than the concomitant desorption of the PBMA. As a consequence, the total adsorbed amount initially increases steeply and then decreases slowly. Apparently, the desorption starts after a certain amount of PTHF has been adsorbed. All observations support the idea that desorption of one polymer by another occurs segment-by-segment. The time needed to reach equilibrium conditions for these polymer displacer experiments are of the order of weeks.

3.5. References

1. Kobayashi, K; Araki, K.; Imamura, Y. *Bull. Chem. Soc. Jpn.* **1989,** 62, 3421.
2. Kawaguchi, M.; Yamagiwa, S.; Takahashi, A.; Kato, T. *J. Chem. Soc. Faraday Trans.* **1990,** 86, 1383.
3. Schaaf, P.; Déjardin, P.; Schmitt, A. *Langmuir* **1987,** 3, 1131.
4. Dijt, J. C.; Cohen Stuart, M. A.; Hofman, J. E.; Fleer, G. J. *Colloids Surfaces,* **1990,** 51, 141.

5. Leermakers, F. A. M.; Gast, A. P. *Macromolecules* (accepted).

6. Malmsten, M.; Lindman, B. *Langmuir* **1990**, 6, 357.

7. Caucheteux, I.; Hervet, H.; Jerome, R.; Rondelez, F. *J. Chem. Soc. Faraday Trans.* **1990**, 86, 1369.

8. Char, K.; Gast, A. P.; Frank, C. W. *Langmuir* **1988**, 4, 989.

9. Van der Beek, G. P.; Cohen Stuart, M. A. *J. Phys. France* **1988**, 49, 1449.

10. Cosgrove, T.; Heath, T. G.; Ryan, K.; Crowley, T. L. *Macromolecules* **1987**, 20, 2879.

11. Van der Beek, G. P.; Cohen Stuart, M. A.; Cosgrove, T. *Langmuir*, **1991**, 7, 327.

12. Sakai, H.; Imamura, Y. *Bull. Chem. Soc. Jpn.* **1987**, 60, 1261.

13. Fontana, B. J.; Thomas, J. R. *J. Phys. Chem.* **1961**, 65, 480.

14. Iwamoto, R.; Ohta, K. *Appl. Spectrosc.* **1984**, 3, 359.

15. Harrick, N. *Internal Reflection Spectroscopy*; Interscience: New York, 1967; p 30.

16. Peyser, P.; Stromberg, R. R. *J. Phys. Chem.* **1967**, 71, 2066.

17. Chittur, K. K.; Fink, D. J.; Leininger, R. I.; Hutson, T. B. *J. Colloid Interface Sci.* **1986**, 111, 419.

18. Parry, D. B.; Harris, J. M. *Appl. Spectrosc.* **1988**, 42, 997.

19. Simon, A.; Weil, J. M. *Bruker Report* **1989**, 2, 43.

20. Kuzmenka, D. J.; Granick, S. *Colloids and Surfaces* **1988**, 31, 105.

21. Pefferkorn, E.; Carroy, A.; Varoqui, R. *Macromolecules* **1985**, 18, 2252.

22. Pefferkorn, E.; Carroy, A.; Varoqui, R. *J. Polym. Sci., Polym. Phys. Ed.* **1985**, 23, 1997.

23. Cohen Stuart, M. A.; Tamai, H. *Macromolecules* **1988**, 21, 1863.

24. Cohen Stuart, M. A.; Tamai, H. *Langmuir* **1988**, 4, 1184.

25. Pelssers, E. G. M.; Cohen Stuart, M. A.; Fleer, G. J. *J. Chem. Soc. Faraday Trans.* **1990**, 86, 1355.

26. Leonardt, D. C.; Johnson, H. E.; Granick, S. *Macromolecules* **1990**, 23, 685.

27. Cohen Stuart, M. A.; Fleer, G. J.; Scheutjens, J. M. H. M. *J. Colloid Interface Sci.* **1984**, 97, 515.

28. Van der Beek, G. P.; Cohen Stuart, M. A.; Fleer, G. J.; Hofman, J. E. *Langmuir* **1989**, 5, 1180.

29. Müller, G.; Abraham, K.; Schaldach, M. *Appl. Opt.* **1981**, 20, 1182.

30. Caucheteux, I.; Hervet, H.; Rondelez, F.; Auvray, L.; Cotton, J. P. In *New Trends in Physics and Physical Chemistry of Polymers*; Lee, L. H., Ed.; ACS Symposium; Plenum Press: New York, 1989; p 81.

31. Ohta, K.; Iwamoto, R. *Appl. Spectrosc.* **1985**, 39, 418.

32. *Bruker Optics News* **1990**, 1, 10.

33. Sperline, R. P.; Muralidharan, S.; Freiser, H. *Appl. Spectrosc.* **1986**, 40, 1019.

34. Goplen, T. G.; Cameron, D. G.; Jones, R. N. *Appl. Spectrosc.* **1980**, 34, 657.

35. Bertie, J. E.; Eysel, H. H. A. *Appl. Spectrosc.* **1985**, 39, 392.

36. Pinkley, L. W.; Sethna, P. P.; Williams, D. *J. Opt. Soc. Am.* **1977**, 67, 494.

37. Cohen Stuart, M. A.; Scheutjens, J.M.H.M.; Fleer, G. J. *J. Polym. Sci., Polym. Phys. Ed.* **1980**, 18, 559.

38. Frantz, P.; Granick, S *J. Chem. Phys.* **1990**, 92, 6970.

39. Scheutjens, J. M. H. M.; Fleer, G. J. *J. Phys. Chem.* **1979**, 83, 1619.

40. Scheutjens, J. M. H. M.; Fleer, G. In *The effect of polymers on dispersion properties*; Tadros, T. F., Ed.; Academic Press: London, 1981.

41. *Polymer Handbook, 3nd ed.*; Brandrup J., Immergut, E. H., Eds.; Jonn Wiley & Sons: New York, 1989.

42. Cosgrove, T.; Fergie-Woods, J. W. *Colloids and Surfaces* **1987**, 25, 91.

43. Johnson, H. E.; Granick, S. *Macromolecules* **1990**, 23, 3367.

44. Frantz, P.; Granick, S *Phys. Rev. Lett.*, submitted.

Chapter 4

The Hydrodynamic Thickness of Adsorbed Polymer Layers Measured by Dynamic Light Scattering

Abstract

Poly(ethylene oxide) (PEO) adsorption on small silica (Ludox) particles was studied by means of dynamic light scattering, as a function of the segmental binding strength (amount of added displacer). The results show that the hydrodynamic layer thickness δ_h is constant or increases slightly with decreasing adsorption energy up to the *critical point* and then drops sharply to zero. The adsorbed amount decreases much more gradually as a function of the amount of added displacer. The data agree with earlier measurements on different substrates, and are in line with the theoretical result that the segmental adsorption energy has no effect on δ_h until very close to full desorption. The very different results obtained earlier for adsorption on polystyrene latex are therefore explained as due to the heterogeneous structure of the latex surface. Finally, since the silica particles are small, special effects are expected for sufficiently high molecular weight polymers. Some results are indicative of such small particle effects.

4.1. Introduction

Measurement of the hydrodynamic thickness of adsorbed polymer layers has been frequently used to obtain insight into the structure of these layers.[1-3] In order to interpret the experimental data correctly, it is essential to have an understanding of the relation between structure and thickness. Theoretical calculations have shown very convincingly[4] that the thickness is entirely determined by the dilute periphery of the adsorbed layer, and that this periphery is dominated by free chain ends (so-called *tails*).[5] Two effects should be emphasized here:

1) Long tails occur only in saturated adsorption layers, i.e., well into the plateau region of the adsorption isotherm. As a consequence, the hydrodynamic thickness increases very steeply with the adsorbed amount as soon as the layer approaches saturation.[4,6]
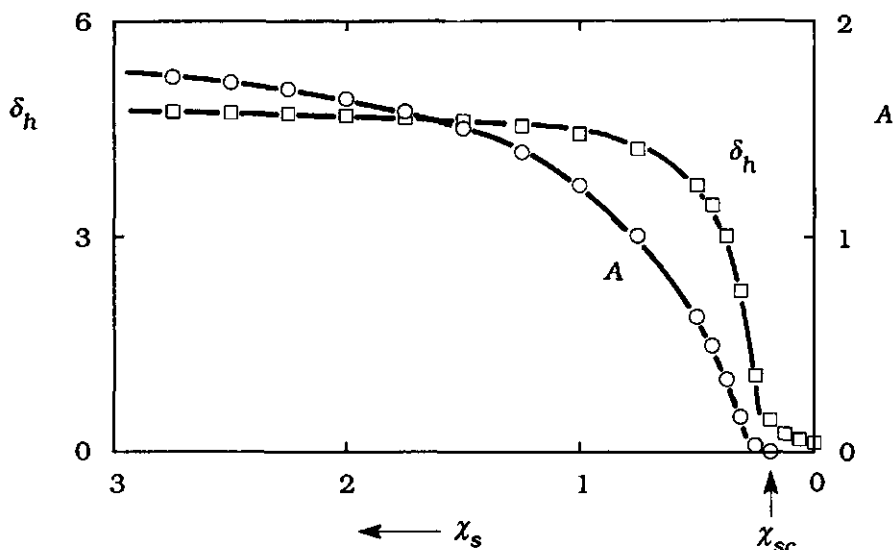
Figure 1. *Theoretical results calculated by the Scheutjens-Fleer theory. Hydrodynamic layer thickness δ_h (expressed in number of layers) and adsorbed amount A (expressed in equivalent monolayers) as a function of the segmental adsorption energy χ_s. The cross-over from the adsorbed to the non-adsorbed regime is located at χ_{sc}. Calculation settings: hexagonal lattice, r (number of segments) = 200, χ (Flory-Huggins parameter) = 0.4, ϕ_b (volume fraction of polymer) = 10^{-3}.*

2) The density profile of tails is almost independent of the segmental adsorption energy, in contrast to the density in loops which varies strongly with this parameter. Calculations by the self-consistent field theory of Scheutjens and Fleer[5] have indeed shown that the hydrodynamic thickness δ_h is almost constant over a very wide range of adsorption energies. Of course, for non-adsorbing polymer $\delta_h = 0$. The transition between these two situations occurs around the critical adsorption energy χ_{sc} and is extremely

sharp, much sharper than the corresponding transition for the adsorbed amount.[5] In Figure 1 we present theoretical curves which substantiate this conclusion. Hydrodynamic thicknesses have been calculated from segment density profiles using a porous layer model. For more details about these calculations the reader is referred to refs 4-7.

Some experimental evidence corroborating the first point mentioned above has been obtained.[9] In this chapter we want to focus on the second aspect. Part of our interest stems from the fact that polymer adsorption/desorption transitions can be used to determine segmental adsorption energies.[10,11] Also, we are motivated by the fact that some authors have invoked differences in segmental adsorption energy to explain differences in δ_h for a given polymer on different substrates.[12] This is clearly at variance with theoretical results and needs to be checked.

In principle, layer thicknesses can be obtained by several techniques. However, methods like optical reflection[13] which yields essentially the first moment of the density distribution are less sensitive to the effects we are interested in and hence we prefer to study δ_h. The technique we use to obtain δ_h is dynamic light scattering on polymer coated colloidal particles. Several authors have studied the hydrodynamic layer thickness of adsorbed polymer layers by this technique.[3,12] Provided particle interactions (structure factors) and effects of free polymer on particle diffusion are properly ruled out, reproducible thicknesses can be obtained.

As the experimental system we choose poly(ethylene oxide) (PEO), adsorbing from aqueous solution onto bare silica particles. Results on a similar system were obtained by Killmann et al.[12] so that a comparison is possible. The effective adsorption energy of PEO on silica can be varied by changing the pH or adding a low molecular weight displacer. The advantage of changing the pH is that the solvent quality remains the same over a wide adsorption energy range. Several studies[14,15] have shown that PEO may completely desorbed at high pH, so that OH⁻ can be regarded as a displacer. In terms of Figure 1, this would mean that the adsorption energy parameter χ_s decreases with increasing pH. Adsorbed amounts as a

function of *pH* have been reported, which show that between *pH* 6 and 10.5 the coverage decreases gradually, at least on non-porous silica.[14,15]

4.2. Experimental section

4.2.1. Materials, apparatus, and sample preparation

For our experiments, we have used Ludox AS_{40} colloidal silica (Du Pont). According to the manufacturer the silica particles have a diameter of 22 *nm* and a specific surface area of 140 m^2/g. Before using the dispersion, it was dialysed against Millipore Super Q deionized water. This water as well as analytical grade chemicals were used throughout.

PCS measurements were done with silica concentrations between 5.0 and 8.2 g/dm^3.

Properties of the PEO samples used in this study are listed in Table 1.

Table 1. *Polymer samples*

sample	manufacturer	$\overline{M}_w$ (kg / mol)	$\overline{M}_w/\overline{M}_n$
PEO 13	(Polymer Laboratories)	12.6	1.04
PEO 23	(Polymer Laboratories)	23.0	1.08
PEO SE-5	(Toyo Soda)	45	1.1
PEO PD	(Aldrich)	60	polydisperse
PEO SE-8	(Toyo Soda)	85	1.1
PEO 246	(Polymer Laboratories)	246	1.09
PEO 325	(Polymer Laboratories)	325	1.06
PEO SE-30	(Toyo Soda)	270	1.1
PEO SE-70	(Toyo Soda)	570	1.1
PEO SE-150	(Toyo Soda)	860	1.2

The aqueous PEO solutions were kept in the dark as much as

possible to prevent photochemical degradation of the polymer. In order to avoid aggregation of the silica particles by adsorbing polymer, the silica dispersion was poured into a polymer solution of the appropriate concentration. Equilibrium between the adsorbed phase and the bulk phase was established by rotating the dispersion end-over-end for about 15 h.

Diffusion coefficient measurements of silica particles with and without PEO were carried out by using either a Malvern 4700 photon correlation spectrometer[1] or an ALV spectrometer with multiple tau digital correlator (ALV-5000). All data were taken at a scattering angle of 90.00° and a temperature of 20.0 °C.

For experiments in which OH⁻ was used as a displacer for PEO, the pH of the samples was adjusted by adding 0.1 M NaOH or 0.1 M HCL (Titrisol, Merck) immediately before the measurement. After the measurement it was checked whether the pH of the samples had not changed. In order to keep the electrolyte concentration as constant as possible we added 2×10^{-3} M NaCl to all samples.

Besides OH⁻, we also used dimethyl sulfoxide (DMSO) and dimethyl formamide (DMF) to displace PEO from silica. Measurements of PEO displacement in binary solvents have the disadvantage that various solvent properties change with solvent composition. For the determination of particle radii by DLS one needs the viscosity and the refractive index of the solvent. Therefore, these solvent properties were measured as a function of the displacer concentration.

We used the depletion method to determine the adsorption isotherms. After equilibrium, the samples were centrifuged at 20,000 r.p.m. during 2 h. The PEO concentration of the supernatant was then measured colorometrically.[17] Absorbance measurements were done with a Beckman 3600 spectrophotometer at 216 nm.

4.2.2. Data analysis

The intensity auto-correlation function $\phi(K,\tau)=\langle I(K,t)I(K,t+\tau)\rangle$ is measured by dynamic light scattering. The parameter τ is the auto-correlation decay time and K represents the scattering vector. According to the Siegert relation,[17] the normalized intensity auto-correlation function, $g^{(2)}(\tau)=\phi(K,\tau)/\langle I(K,t)\rangle^2$, for a monodisperse dispersion can be equated to

$$g^{(2)}(\tau)=1+\beta S(K)\exp\left\{-2K^2 D\tau\right\} \tag{1}$$

where D is the translational diffusion coefficient and β a signal-to-noise factor. The static structure factor is given by $S(K)$. In dilute dispersions, as in our case, $S(K)$ is equal to unity. The diffusion coefficient D can be calculated from the measured correlation function by fitting this function with Eq. (1).

The radius of the spherical particles can be calculated from the diffusion coefficient by the Stokes-Einstein formula

$$D=k_B T/6\pi\eta R \tag{2}$$

where k_B is Boltzmann's constant, T the absolute temperature, η the viscosity of the continuous phase, and R the particle radius. We note that the Stokes-Einstein equation can fail for small spherical particles in polymer solutions because this equation is based on a continuum description of the solvent (i.e., the solvent molecules are much smaller than the particles). Such a description is not valid in the case small particles encounter polymer molecules of its own size. Ullmann et al.[18] investigated experimentally the validity of the Stokes-Einstein relation for particles in PEO/water solutions. The conclusion which can be drawn from that work is that for small particles (as in our case) the Stokes-Einstein relation can be safely used up to a PEO ($M_w=300$ kg/mol) concentration of 500 ppm. This is corroborated by the fact that we did not find a significant difference in the bare hydrodynamic radius between particles in water and in aqueous PEO solutions under desorption conditions (the viscosity of the aqueous PEO solutions was not significantly different

from that of pure water). For polymer concentrations above 500 *ppm* the hydrodynamic radius calculated from the diffusion coefficient by the Stokes-Einstein relation may be significantly different (smaller) from the actual one.

Since our silica is to some extent polydisperse the measured auto-correlation function stems from a distribution of diffusion coefficients. Several methods are available to extract an average particle diffusion coefficient from the measured correlation function. The matter has been reviewed by Stock and Ray.[17] The results obtained by using these various methods are, however, not identical due to the different assumptions which are made in these methods.

We have used for our data analysis the method of cumulants.[17,19] This method is based on an equation which relates $g^{(2)}(\tau)$ to moments of the distribution function of translational diffusion coefficients:

$$\frac{1}{2}\ln\left(g^{(2)}(\tau)-1\right) = \frac{1}{2}\ln\beta - \overline{\Gamma}\tau + \frac{\mu_2}{\overline{\Gamma}^2}\frac{(\overline{\Gamma}\tau)^2}{2!} - \frac{\mu_3}{\overline{\Gamma}^3}\frac{(\overline{\Gamma}\tau)^3}{3!} + \ldots\ldots \tag{3}$$

where $\overline{\Gamma} \equiv D_z K^2$ and D_z is the z-average of the translational diffusion coefficient. The parameter $\mu_2/\overline{\Gamma}^2$ measures the polydispersity of the sample since it is equal to the normalized variance of the distribution function of D. The asymmetry of this distribution is given by $\mu_3/\overline{\Gamma}^3$. In this method it is assumed that the diffusion coefficient distribution is a function with only one maximum.

The Stokes-Einstein relation (Eq. (2)) is used to obtain from D_z an intensity weighted average radius of the particles which can be shown to be

$$\overline{R} = \frac{\sum_i n_i M_i^2}{\sum_i n_i M_i^2 R_i^{-1}} \tag{4}$$

Here n_i is the number of the particles with mass M_i and hydrodynamic radius R_i. Finally, the hydrodynamic thickness δ_h can be determined by subtracting the hydrodynamic radius of bare particles from the radius of particles with adsorbed polymer.

For polydisperse samples, the average diffusion coefficient obtained from the auto-correlation function generally depends on the scattering angle. However, our particles are so small that they may be regarded as Rayleigh scatterers, so that the apparent diffusion coefficient and hence the hydrodynamic radius should be independent of the wave vector. We found indeed that this was the case.

4.3. Results and discussion

The diameter of the bare silica particles was found to be 32 ± 1 nm, at an ionic strength of about 2×10^{-3} M NaCl. Since this particle size is different from that quoted by the manufacturer, the silica sample was also characterized by static and dynamic light scattering as a function of scattering angle in the Van't Hoff laboratory in Utrecht[1]. These results agree nicely with ours. The fact that the manufacturer states a lower particle diameter (22 nm) may be due to a different way of averaging over the polydisperse sample. Because we did not find an angular dependence in the average particle radius it is not very likely that a significant amount of aggregates was present in our Ludox samples. The particle volume fraction was approximately 0.3% so that all structure factor effects may be neglected. Still, we checked by dilution that the assumption of $S(K) = 1$ was justified. Also we observed no dependence of δ_h on pH for the bare particles.

In Figure 2 we give some adsorption data for PEO SE-70 and PEO-PD taken at $pH = 7.5$. It can be seen that a plateau develops at about $A = 0.6$ mg/m^2, a value which is very close to what has been found by Killmann et al.[12,20] and which was also obtained by us on aerosil samples. It is important to note that the average number of polymer molecules per particle, n, calculated as $n = 4\pi \overline{R}^2 A N_{av}/M$ with $\overline{R} = 16$ nm and $M = 570$ kg/mol is of order unity.
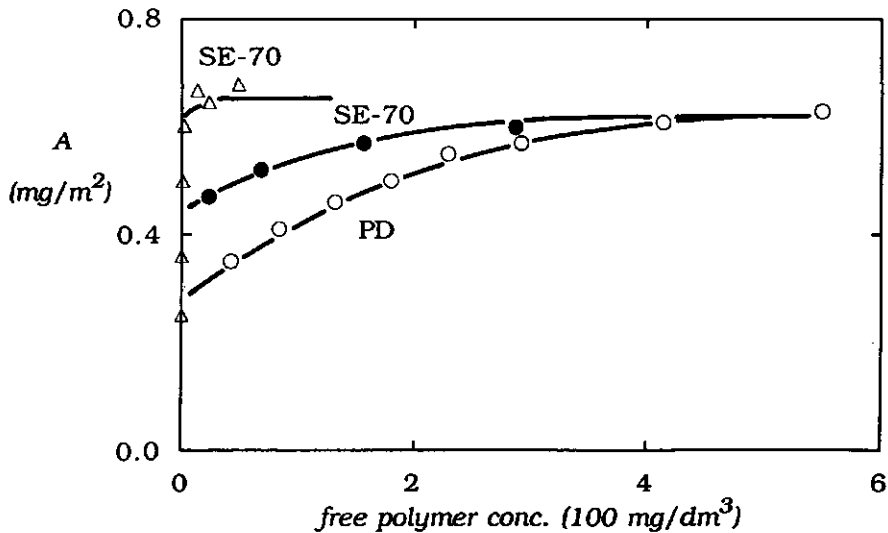
Figure 2. *Adsorption isotherms for monodisperse (SE-70) (●) and polydisperse (PD) (○) PEO on Ludox silica, at pH 7.5. For comparison, an adsorption isotherm for the same polymer on larger particles (△) is shown (taken from ref 12).*

Such a low number raises doubts about the applicability of a flat-plate model, as used to obtain the theoretical results shown in Figure 1. Adsorption of polymers on small colloidal particles was considered by Alexander[21] and Pincus[22]. The latter author pointed out that small spheres can accommodate only a limited amount of polymer, N^* (expressed in number of segments per sphere), which scales for good solvents like $N^* \propto \chi_s R^2$. If N^* corresponds with less than one polymer molecule per particle, part of a polymer chain forms the adsorbed layer and the rest extends far away from the particle as a long free end which may possibly adsorb onto another particle. Pincus[22] shows also that the fraction of train segments per polymer molecule on a highly curved surface (i.e., small spheres) is reduced with respect to a flat surface. For the same train fraction, a polymer molecule on a small particle must deform more (i.e., looses more entropy) than a molecule on a flat surface. Hence, two effects may be expected for adsorption of long molecules on small particles: (i) a decreased diffusion coefficient due to the long free end, which

become more important as $\chi_s \rightarrow \chi_{sc}$, and (ii) a reduced affinity of the adsorption isotherm.

The latter effect clearly shows up in the adsorption isotherms of Figure 2. The isotherm for PEO SE-70 on small silica particles is more rounded than the isotherm for the same polymer on larger particles. We note in passing, that the polydisperse sample has an even more rounded isotherm, which is in line with current understanding of polydispersity effects.[23]

In Figures 3, 4, and 6 adsorbed amounts A and hydrodynamic thicknesses δ_h of adsorbed PEO layers are plotted $vs.$ pH. The curve with the filled circles in Figure 3 is for PEO SE-30. The adsorbed amount is roughly constant up to $pH \approx 8$ and then drops gradually to zero in the pH range 8-11. On the other hand, the thickness δ_h is constant up to pH 10.5 and then drops sharply to zero. These experimental results agree very satisfactorily with the theoretical predictions in Figure 1.

In Figure 4 δ_h $vs.$ pH is given for a higher molecular weight PEO (SE-70). Surprisingly, δ_h is not constant here, but increases substantially over the range pH 9.3-10.5 before it again drops sharply at a pH just above 10.5. At first sight, this result appears very puzzling. However, it should be realized that the theoretical result in Figure 1 is based on a constant solution concentration, whereas in the experiment of Figure 4 the total polymer dose was constant. Since the adsorbed amount decreases with increasing pH, the solution concentration will rise and as we have explained in the introduction, this has an important effect on the layer thickness if the adsorbed layer is *undersaturated*. The effect of increasing polymer concentration on the hydrodynamic layer thickness is shown in somewhat more detail in Figure 5, where the pH was fixed at 7.5. As can be seen, the adsorbed amount does increase slightly whereas the increase in δ_h is much more pronounced. Upon approach of the plateau value of the adsorption isotherm both the adsorbed amount and the layer thickness become constant (*saturation*). Hence, the result of Figure 4 can be explained by an undersaturated adsorbed layer at low pH, i.e., at relatively high adsorption energy. As at higher
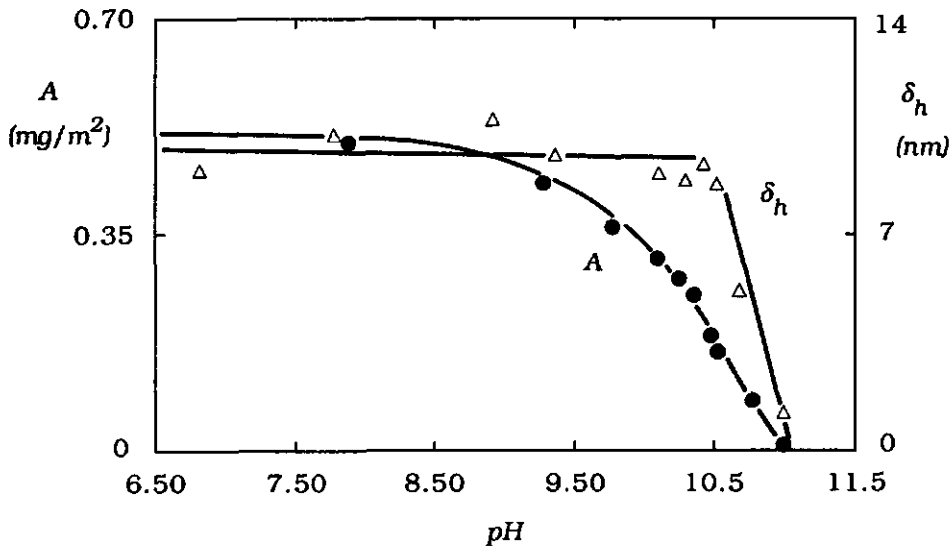
Figure 3. *Hydrodynamic layer thickness δ_h (△) and adsorbed amount A (●) as a function of pH for PEO SE-30 adsorbed on colloidal silica. The free polymer concentration is about 250 mg / dm^3 at pH 7.5.*
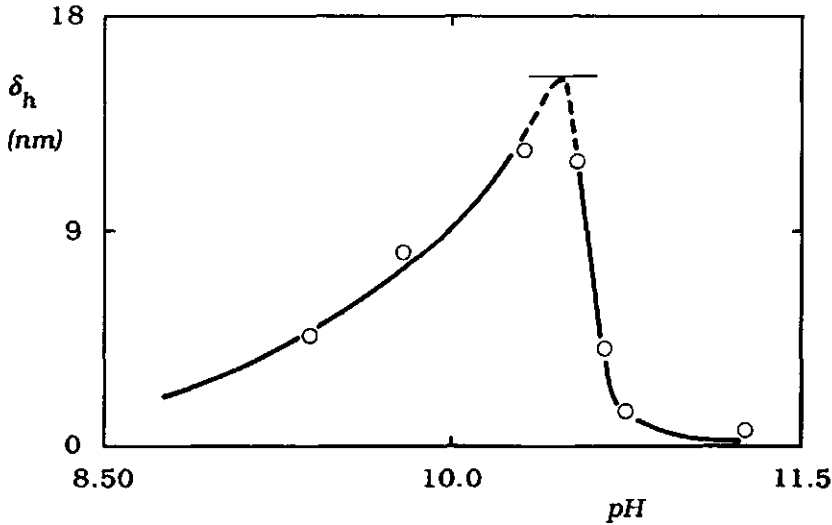
Figure 4. *Hydrodynamic layer thickness δ_h as a function of pH for PEO SE-70 adsorbed on colloidal silica. The maximum corresponds to the (constant) value obtained when more free polymer is present (see also Figure 6). The free polymer concentration is about 70 mg / dm^3 at pH 7.5.*

pH the adsorption energy of the polymer segments becomes lower, the adsorbed layer becomes saturated which shows up as an increase in the hydrodynamic layer thickness. Indeed, it was found that if more polymer is added to the samples these undersaturation effects are reduced, leading to a less pronounced maximum.
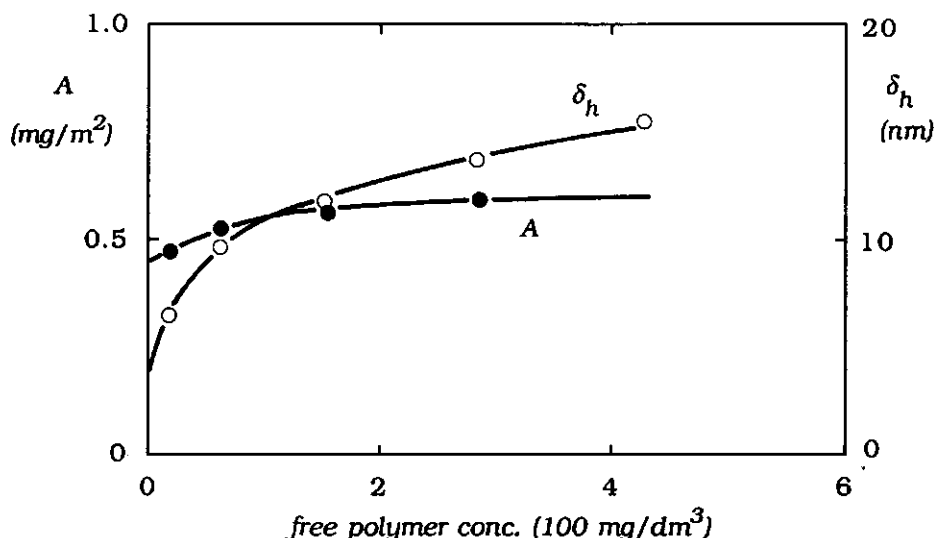
Figure 5. *Hydrodynamic layer thickness δ_h and adsorbed amount A as a function of free polymer concentration for PEO SE-70 on colloidal silica at pH 7.5.*

In Figure 6 we give results for a still higher molecular weight PEO (SE-150), but with much more polymer added. As can be seen, δ_h is now nearly constant over the *pH* range 8-10. There is still a slight increase between *pH* 10-10.2 before the final drop for *pH* > 10.5. This result was reproduced several times. It is tempting to interpret this maximum as due to the finite capacity effect discussed by Alexander[21] and Pincus[22], where a long free end and concomitant reduced diffusion rate is expected when the molecular weight is sufficiently high and χ_s low. Both the position of the maximum and the fact that it is absent for a lower molecular weight PEO (SE-30) agree with this explanation.
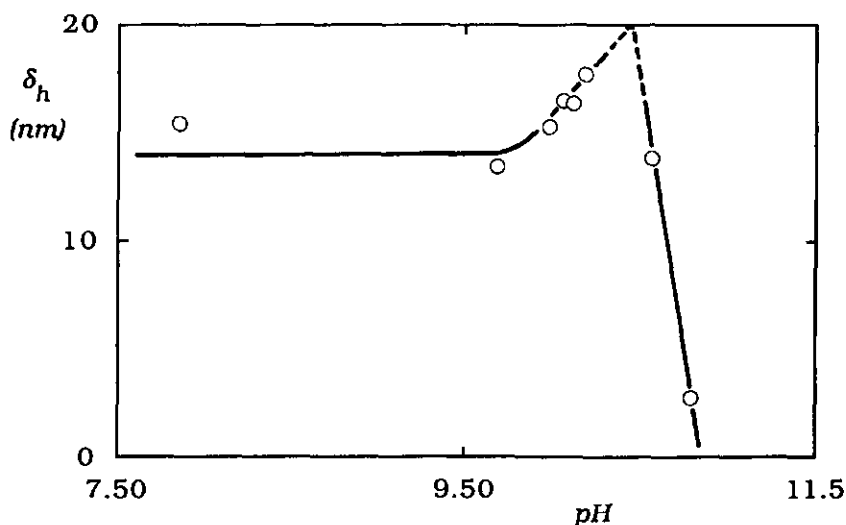
Figure 6. *Hydrodynamic layer thickness* δ_h *as a function of pH for PEO SE-150 on colloidal silica. The free polymer concentration is about 400 mg / dm^3 at pH 7.5.*

However, especially for high molecular weight polymer samples two other effects may also contribute to the observed hump in Figure 6:

- The viscosity of the solution may be significantly enhanced by an increased free polymer concentration as a result of polymer desorption. The diffusion coefficient is inversely proportional to the viscosity. Hence, when the viscosity is not corrected for an increased polymer concentration the calculated layer thickness will be too large. This effect may especially be operative close to and beyond the critical point. Whether or not this effect plays a significant role can be easily checked by comparing the average radius of silica particles determined from dispersions without polymer and with polymer beyond the critical point, where no adsorption occurs. It turned out that the hump is partly due to this effect (at most 40%).

- When the *pH* of the solution is adjusted to a *pH* beyond 10, the electrolyte concentration is increased significantly. Higher electrolyte concentrations reduce the thickness of the diffuse electrical double layer of silica particles. Tails of large polymer molecules may

then extend outside this double layer and cause aggregation due to bridge formation. Lafuma *et al.*[24] have investigated the effect of the polymer concentration, the size of polymers, and the electrolyte concen-tration on particle aggregation. A conclusion from their work is that there is a relation between the range of electrostatic repulsions (controlled by the electrolyte concentration) and the molecular weight of polymers which can bridge particles. For long range electrostatic interactions (low salt concentration) large polymer molecules are needed to establish aggregation. The presence of (small) aggregates in the solution gives an apparently increased average layer thickness. The significance of this effect is, however, rather difficult to check because the formation of small aggregates is a process that strongly depends on small variations in the experimental procedure and mixing conditions, and is therefore in many cases not very reproducible.
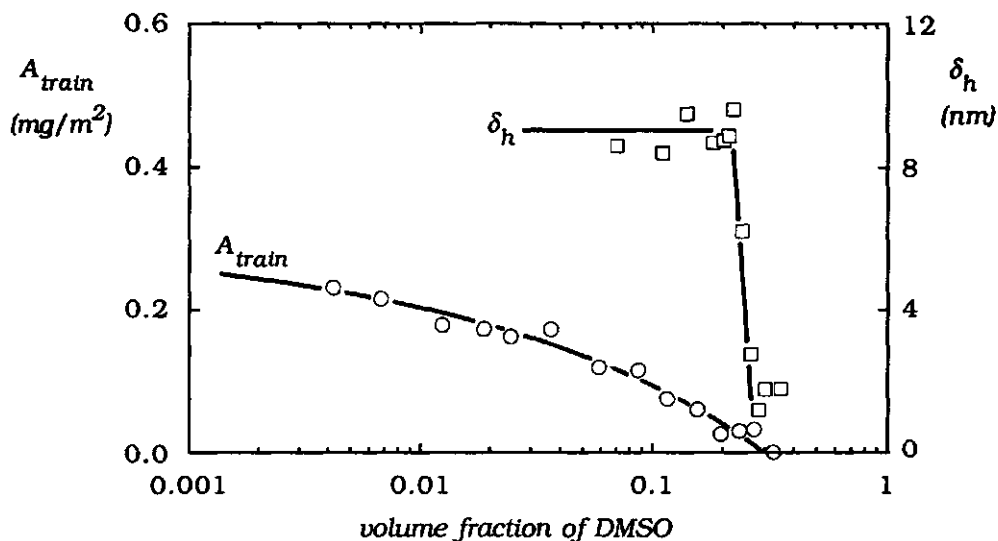
Figure 7. *Adsorbed amount of train segments (taken from ref 25) (○) and hydrodynamic layer thickness (□) of PEO 325 on colloidal silica as a function of the volume fraction of DMSO.*
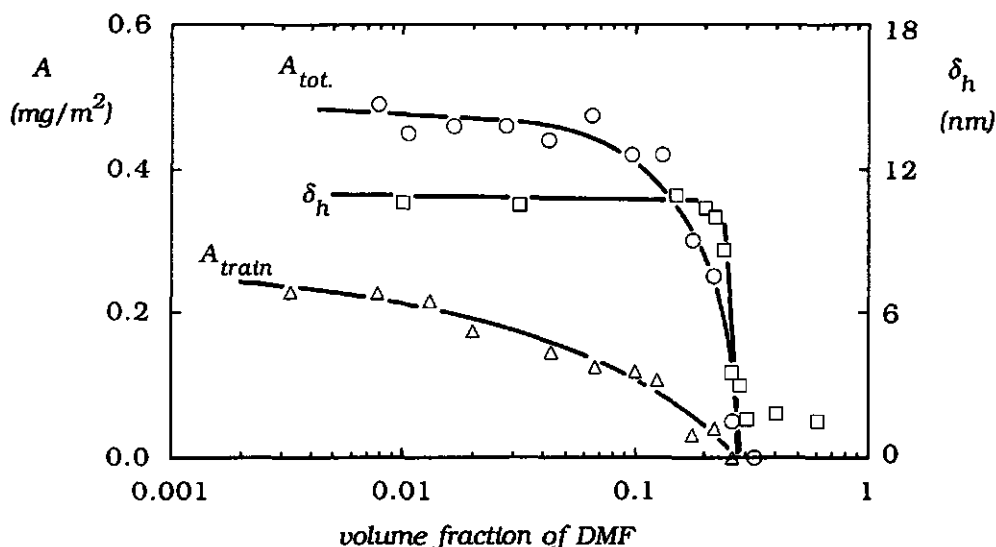
Figure 8. *Total adsorbed amount (○), adsorbed amount of train segments (taken from ref 25) (△), and hydrodynamic layer thickness (□) of PEO 325 on colloidal silica as a function of the volume fraction of DMF.*

Figure 7 shows the dependence of the hydrodynamic layer thickness of adsorbed PEO on the volume fraction of the displacer dimethyl sulfoxide (DMSO). The curves for δ_h as a function of pH (Figure 3) and as a function of DMSO concentration are very similar. The layer thickness remains constant up to very close to the critical point and then drops sharply to zero. Because we used for this figure a lower molecular weight PEO than for Figure 4 no significant increase in the layer thickness is observed before the sharp drop. Varying the concentration of DMSO may change the solvent quality for PEO which affects the adsorbed amount and extension of the adsorbed layer. Probably, this effect is not very significant in this case because we did not observe a change in δ_h before the critical point was reached. For comparison, we also give in Figure 7 the amount of train segments A_{train} as a function of DMSO concentration. This quantity was obtained from magnetic relaxation measurements of silica dispersions with and without polymer (see chapter 5).[25] The critical points obtained by both methods are in excellent agreement.

The amount of train segments decreases gradually with increasing concentration of DMSO. At the displacer concentration just before the critical point almost all train segments have been desorbed whereas the tail density is still constant. Hence, the train density is more affected by the effective segmental adsorption energy than the tail density.

Figure 8 is even more informative about what happens with the structure of the adsorbed layer as the segmental adsorption energy is lowered. In this figure we show three curves for PEO displacement by another displacer, dimethyl formamide (DMF). Besides the hydrodynamic layer thickness and train density[25], also the total adsorbed amount is given as a function of DMF concentration. The curves for A_{train} and δ_h are similar to those found with DMSO. The shape of curve of the adsorbed amount is comparable to that of the train segments. Hence, the decrease in the total adsorbed amount before the critical point is mainly due to a decrease in train segment density.

Having properly understood the effects of segmental adsorption energy and polymer concentration on δ_h we are now in a position to compare our data with those published by Killmann *et al.*[12,20] These authors have determined average particle radii in the same way as we did, but with larger, fairly monodisperse precipitated silica (radius ~100 nm). If we take as our δ_h (at full saturation) the value well before the sharp drop, we obtain the results shown in Figure 9 as the open circles. The agreement between our data and those of Killmann *et al.*[12,20] is very good, which suggests that a $\bar{\delta}_h(M)$ relationship is a good characteristic of a given polymer/solvent/substrate system, provided measurements are taken at saturation. It is somewhat surprising, perhaps, that the size of the bare particles seems to have no effect. Anderson *et al.*[26] made detailed hydrodynamic calculations which suggest that δ_h should decrease with decreasing particle size. Lafuma *et al.*[24] found a significant particle size effect in their measurements, which could be eliminated by means of the geometric correction proposed by Garvey *et al.*[27] Our data, however, would suggest that such corrections are negligible.
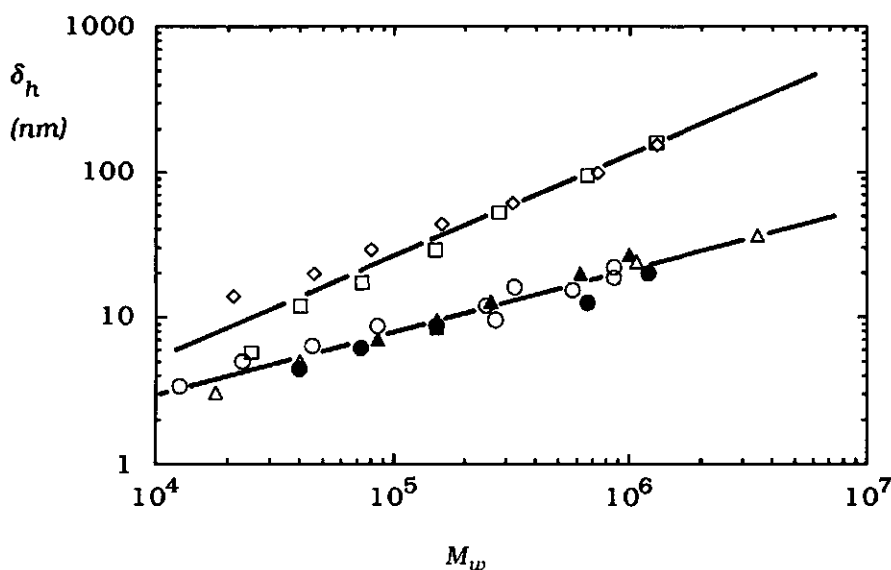
Figure 9. *Double logarithmic plot of δ_h (at saturation) on various substrates as a function of molecular weight for PEO/water.* △, SiO_2[12]; ○, SiO_2 *this work;* ▲, SiO_2[20]; ●, *Millipore*[28]; ◇, *PS-latex*[3]; □, *PS-latex*[4].

We may safely conclude, however, that δ_h at saturation is determined by the periphery of the adsorbed layer (i.e., by the tails) and that, therefore, the adsorption energy per segment plays hardly any role. In other words, given a particular polymer/solvent pair δ_h at saturation will be fixed, whatever the value of the adsorption energy. This is further supported by data from Kawaguchi *et al.*[28] These authors have determined hydrodynamic thicknesses of PEO adsorbed in filter pores (Millipore filters, made from cellulose esters), by measuring the flow rates of water through the filters. As can be seen in Figure 9, their results fall nicely on the same line.

All this is hard to reconcile with the experimental fact that PEO on polystyrene (PS) latex spheres is often found to form layers which are at least four times thicker (some relevant data are given in Figure 9)[3,4].

We suggest that not the segmental adsorption energy, but the difference in surface structure (distribution of adsorption sites) is responsible for this difference. Further research is clearly needed to substantiate this conjecture but the fact that PEO adsorption on PS latex relies on a few (probably acidic) active surface sites [29] seems to corroborate the idea.

There are several experimental indications that the surface of bare latices is hairy.[30,31] This hairiness could also contribute to the deviation between hydrodynamic thicknesses of PEO layers on latices and that on other substrates.

4.4. Conclusions

The hydrodynamic thickness of an adsorbed polymer layer is virtually independent of the segment/surface interaction energy up to very close to the critical adsorption energy. The critical point is characterized by a very sharp drop of δ_h to zero. This conclusion is valid provided the polymer concentration in the solution is constant, or at least high enough to be well into the plateau region of the adsorption isotherm (*saturation*). The dependence of δ_h on the segmental adsorption energy found in this study had been predicted earlier on the basis of theoretical work[5].

For very high molecular weight polymers, we found a small maximum in δ_h just before the sharp drop which is possibly related to a special effect predicted to occur in the case of small particles,[21,22] although particle aggregation and an enhanced viscosity of the solution due to polymer desorption may also contribute to this maximum.

Since the segment/surface interaction strength plays no significant role, δ_h at saturation would be expected to depend only on the properties of the polymer and the solvent. Hence, differences in δ_h between different substrates are due to some other surface properties. We suggest that the structure of the surface (distribution and density of active surface sites and/or geometrical heterogeneity) affects the layer thickness of adsorbed polymer layers.

Critical adsorption conditions can be determined easily and accurately (even without keeping bulk concentrations rigourously constant, or without using monodisperse polymer) because δ_h always drops very sharply to zero in the neighbourhood of the critical point.

4.5. References

1. Doroszkowski, A.; Lambourne, R. *J. Colloid Interface Sci.* **1965**, 26, 914.
2. Varoqui, R.; Dejardin, P. *J. Chem. Phys.* **1977**, 66, 4395.
3. Kato, T.; Nakamura, N.; Kawaguchi, M.; Takahashi, A. *Polym. J.* **1981**, 13, 1037.
4. Cohen Stuart, M. A.; Waajen, F. H. W. H.; Cosgrove, T.; Vincent, B.; Crowley, T. A. *Macromolecules* **1984**, 17, 1825.
5. Scheutjens, J. M. H. M.; Fleer, G. J.; Cohen Stuart, M. A. *Colloids Surf.* **1986**, 21, 285.
6. Scheutjens, J. M. H. M.; Fleer, G. J. *J. Phys. Chem.* **1980**, 84, 178.
7. Scheutjens, J. M. H. M.; Fleer, G. J. *J. Phys. Chem.* **1979**, 83, 1619.
8. Cohen Stuart, M. A.; Mulder, J. W. *Colloids Surf.* **1985**, 15, 49.
9. Cosgrove, T.; Crowley, T. L.; Cohen Stuart, M. A.; Vincent, B. In Polymer *Adsorption and Dispersion Stability*; Vincent, B., Goddard, E. D., Eds.; ACS Symposium Series 240; American Chemical Society: Washington, D. C., 1984; p 147.
10. Cohen Stuart, M. A.; Fleer, G. J.; Scheutjens, J. M. H. M. *J. Colloid Interface Sci.* **1984**, 97, 515.
11. Cohen Stuart, M. A.; Fleer, G. J.; Scheutjens, J. M. H. M. *J. Colloid Interface Sci.* **1984**, 97, 526.
12. Killmann, E.; Maier, H.; Kaniut, P.; Gütling, N. *Colloids Surf.* **1985**, 15, 261.
13. Killmann, E.; Kuzenko, M. *Angew. Makromol. Chem.* **1974**, 35, 39.
14. Rubio, J.; Kitchener, J. A. *J. Colloid Interface Sci.* **1976**, 57, 132.
15. Van den Boomgaard, Th.; Tadros. Th. F.; Lyklema, J. *J. Colloid Interface Sci.* **1987**, 116, 8.

16. Nuysink, J.; Koopal, L. K. *Talanta* **1982**, 29, 495.

17. Stock, R. S.; Ray, W. H. *J. Polym. Sci., Polym. Phys. Ed.* **1985**, 23, 1393.

18. Ullmann, G.; Phillies, G. D. J. *Macromolecules* **1983**, 16, 1947.

19. Koppel, D. E. *J. Chem. Phys.* **1972**, 57, 4814.

20. Killmann, E.; Wild, Th.; Gütling, N.; Maier, H. *Colloids Surf.* **1986**, 18, 241.

21. Alexander, S. *J. Phys. France* **1977**, 38, 977.

22. Pincus, P.; Sandroff, C. J.; Witten, T. A. Jr. *J. Phys. France* **1984**, 45, 725.

23. Cohen Stuart, M. A.; Scheutjens, J. M. H. M.; Fleer, G. J. *J. Polym. Sci., Polym. Phys. Ed.* **1980**, 18, 559.

24. Lafuma, F.; Wong, K.; Cabane, B. *J Colloid Interface Sci.*, submitted.

25. Van der Beek, G. P.; Cohen Stuart, M. A.; Cosgrove, T. *Langmuir*, **1991**, 7, 327.

26. Anderson, J. L.; Kim, J. O. *J. Chem. Phys.* **1987**, 86, 5163.

27. Garvey, M. J.; Tadros, T. F.; Vincent, B. *J Colloid Interface Sci.* **1976**, 55, 440.

28. Kawaguchi, M.; Mikura, M.; Takahashi, A. *Macromolecules* **1984**, 17, 2063.

29. Cosgrove, T.; Heath, T. G.; Ryan, K. *Polym. Commun.* **1987**, 28, 64.

30. Bonekamp, B. C.; Hidalgo Alvarez, R.; De Las Nieves, F. J.; Bijsterbosch, B. H. *J. Colloid Interface Sci.* **1987**, 118, 366.

31. Goossens, J. W. S.; Zembrod, A. *Colloid Polym. Sci.* **1979**, 257, 437.

Chapter 5

Polymer Adsorption and Desorption Studies via ¹H NMR Relaxation of the Solvent

Abstract

Proton NMR relaxation measurements of the solvent in silica dispersions have been carried out as a function of polymer coverage, solution *pH*, and added displacer. We find that the solvent spin-lattice relaxation rate is enhanced as a result of polymer adsorption and that, with proper calibration, this enhancement can be used to obtain the adsorbed amount in trains. The results are consistent with bound fraction estimates obtained from the Scheutjens-Fleer theory of polymer adsorption and also with recent results on the hydrodynamic thickness of adsorbed polymer layers. Besides information about the conformation of adsorbed polymers, the effective polymer adsorption energy can also be determined by this NMR technique.

5.1. Introduction

The conformations of polymers at interfaces have been studied extensively by a number of experimental methods.[1] These include NMR, which has been used to obtain the bound fraction of polymer by direct observation of the spectrum of the polymer,[2] small angle neutron scattering (SANS), which has been used to obtain the volume fraction profile of segments normal to the surface,[3] and hydrodynamic methods (e.g., photon correlation spectroscopy, PCS), which have given data on the maximum extent of the layer.[4,5]

The effective adsorption energy of a polymer segment is one of the parameters that influences the conformation of the polymer at an interface. In 1984 we proposed the use of binary solvents as a method for probing the strength of adsorbed polymer-surface

interactions.[6] The central idea of this method is that a low molecular weight compound can entirely displace an adsorbed polymer, provided its concentration exceeds a certain critical value. This critical concentration, can be straightforwardly measured for a number of systems.[7,8] Thermodynamic analysis shows that the critical displacer concentration is related to the net energy of interaction between the polymer segment and the surface.[6] Several polymer/solvent/substrate systems were studied to extract this interaction energy.[1,8,9] Methods that can be used to determine the critical point include *total adsorbed amount* measurements by the depletion method,[10] measurement of the *adsorbed layer thickness* by means of PCS on dilute dispersions of polymer-coated colloidal particles,[11] and measurement of *interfacial residence time* of polymer on a substrate by means of thin-layer chromatography (TLC).[12] All three quantities show a rapid drop to zero as the critical point is approached. Each method has its limitations as far applicability is concerned: TLC does not work for systems with solvents that have bad developing characteristics for the thin layer (notably water), whereas dynamic light scattering is only possible with stable dispersions that are usually not obtained in organic solvents or with high molecular weight polymers at low adsorbed amounts, and the depletion method can be hampered by analytical problems. Hence, there is a need for techniques to determine critical displacer concentrations, which do not suffer from such limitations. NMR relaxation may be such a method. This potentiality lies in the fact that NMR can discriminate between highly mobile (liquid-like) and immobile (solid-like) protons on the basis of magnetic relaxation times. In earlier work[2], we have made use of this property in order to distinguish between bound (immobile) segments in trains and more mobile segments in loops and/or tails, by virtue of their NMR line width. The surface segments cannot undergo isotropic re-orientations on a fast enough time scale to average out the intermolecular and intramolecular dipole-dipole interactions. The result of this is that the proton spectrum arising from these segments is strongly dipolar broadened and may have a line width in excess of 20 *kHz*. As far as a conventional high-resolution NMR

spectrometer is concerned, these segments are essentially invisible, though they may be observed by solid state methods.[13] These latter techniques are, however, complex, and in particular if high resolution spectra are required, the samples which are dispersions of solids in liquids must be spun at high speeds. In this chapter we propose an alternative NMR approach to study adsorbed polymer whereby the effects of entrained segments at the interface are viewed through the dynamics of the solvent in the system. This method has many advantages, not the least that results can be obtained very rapidly, with good statistics, and with very simple equipment.

As indicated above, NMR relaxation and mobility are directly related. For small molecules undergoing isotropic motion, both the spin-lattice (T_1) and the spin-spin (T_2) relaxation times are inversely proportional to the correlation time. This describes the characteristic lifetime of a particular dynamic process. For a free solvent molecule, nuclear spin relaxation times of the order of several seconds are quite usual. However, when the same molecule is entrained at an interface, and its molecular motion becomes anistropic and also constrained, relaxation becomes very efficient and hence relaxation times become very short. For the case of rapid exchange between molecules at the interface and in the bulk, this results in an effective relaxation rate that is just a weighted sum of the two contributions. Provided enough surface area can be introduced into the detection volume, accurate measurements of this relaxation rate enhancement are possible.[14,15] In as far as polymer segments bound to the surface change the number and mobility of adsorbed solvent molecules, it may be anticipated that an effect proportional to the the amount of surface-bound segments (so-called trains) is found.

In this chapter we explore this hypothesis and discuss whether it can be exploited to determine the adsorption/desorption transition (critical concentration) and obtain information regarding the conformation of adsorbed polymer molecules.

5.2. Theory

The NMR relaxation of water in silica dispersions has been considered by several authors, both experimentally[16,17] and theoretically.[19,20] The essential features of the observed relaxation behaviour can be understood by means of rapid exchange between solvent molecules at the silica surface with a short relaxation time T_{ib} and free molecules in the bulk with a longer relaxation time T_{if}. Although there are solvent molecules with different relaxation times in the system, a single exponential magnetization decay may be observed if the relaxation is dynamically averaged between the different environments. This is the fast exchange limit:

$$1/T_i = (1 - P_b)/T_{if} + P_b/T_{ib} \tag{1}$$

where P_b is the fraction of time a proton spends in the 'bound' environment, which is equal to the fraction of protons in this environment, provided rapid exchange occurs. The index i indicates longitunal ($i=1$) or transverse ($i=2$) relaxation. Fluctuating magnetic dipolar interactions between protons constitute the most important process for proton relaxation in the systems of interest here. These interactions are modulated by the frequency distribution of molecular motions. The relaxation times of bulk water T_{if} can be reasonably estimated, using a diffusion model for rotation and translation.[21] The question of the surface water mobility is rather complex; the dynamics not only are changed by the presence of a phase boundary but also may be modified by specific interactions with the substrate.

A recent view,[20] based on ^2H and ^{17}O quadrupolar relaxation data (whose origin is purely intra-molecular), is that the modified mobility of water molecules in the surface layer is due to anisotropic diffusion. The radial diffusivities of water molecules near the surface are more reduced than the lateral ones. The extension of the surface layer with water molecules of restricted diffusivity is only a few monolayers. Although the contribution of each molecule to the total relaxation rate is presumably dependent on its distance from the

surface, exchanges are always rapid enough that the overall relaxation rate can be treated in terms of a simple two-state model (surface and bulk).

Proton relaxation processes are more complex, as cross-relaxation between protons of hydroxyls on the surface and protons of the solvent (and other intermolecular interactions) also contribute to the observed relaxation. Cross-relaxation leads to magnetization exchange and direct spin relaxation.[22] The observed relaxation times for protons of the substrate and protons of the 'bound' water are then different from the intrinsic values. Besides this magnetization exchange, proton exchange between silanol groups and water molecules may also play a significant role. According to Piculell,[18] this exchange is also very rapid.

We shall discuss our results in terms of the relaxation rate R_i, which is defined as $1/T_i$, and the specific relaxation rate R_{isp}, which describes the relaxation rate with respect to that of pure water, R_i^o:

$$R_{isp} = \frac{R_i}{R_i^o} - 1 \tag{2}$$

The combined relaxation rate for aqueous dispersions can be written as

$$R_{isp} = P_b R_{isp}^b \tag{3}$$

The parameter R_{isp}^b stands for the averaged specific relaxation rate of protons near and at the surface. The fraction of these protons, P_b, is of course proportional to the amount silica per solvent volume.

Finally, we have to note that the relaxation rate may also be enhanced by impurities such as paramagnetic Fe and Ti, which are frequently present in commercial silicas. Because we have evaluated our polymer adsorption experiments in terms of specific relaxation rates with respect to bare silica dispersions instead of pure water, this effect is accounted for. In terms of sensitivity of the technique some trapped paramagnetic material in the particle is an advantage, but if it can be leached out, it would be a serious disadvantage.

5.3. Experimental section

The substrate used in this polymer adsorption/desorption study was Ludox HS_{40} (Du Pont), which is a dispersion of silica particles of about 21 nm diameter (24 nm measured by photon correlation spectroscopy and 18 nm by electron microscopy)[18] with a specific surface area of 230 m^2/g. The Ludox was first purified by dialyzing against Millipore Super Q deionized water. This water and analytical grade chemicals were used for all measurements. The polymers used, were poly(vinylpyrrolidone) (PVP) and poly(ethylene oxide) (PEO) (also denoted as poly(ethylene glycol) (PEG) for lower molecular weights). The sample characteristics are given in Table I. All samples were made up with the same distilled water supply, as variation in oxygen content of water taken from different sources can substantially affect the absolute relaxation times.

Table 1. *Polymer samples*

sample	manufacturer	M_w (kg / mol)
PEG 1000	Fluka AG	1
PEG 2000	Fluka AG	2
PEG	Koch-Light Laboratories	4
PEG	Koch-Light Laboratories	6
PEG 10000	Fluka AG	10
PEG 15000	Fluka AG	15
PEG 20000	Fluka AG	20
PEO	BDH	100
PEO	BDH	300
PVP k15	Fluka AG	10
PVP k25	Fluka AG	24

All silica/polymer dispersions were first rotated end-over-end for at least 12 h before measuring the proton relaxation rate and/or the adsorbed amount, because establishment of equilibrium in polymer adsorption processes can take several hours. Solutions with PEO

were kept in the dark as much as possible in order to prevent photochemical degradation.

Adsorbed amounts of polymer were determined by the depletion method at room temperature. Free polymer was separated from the silica particles with bound polymer by centrifugation. In the case of solvent mixtures, the supernatant was evaporated under reduced pressure at 60 °C. The residue was then dissolved in a known amount of water. Poly(vinylpyrrolidone) concentrations were directly determined spectrophotometrically at a wavelength of 196 nm. Poly(ethylene oxide) concentrations were determined colorometrically by the molybdophosphoric acid method.[23]

A 2.7-MHz NMR spectrometer (Newport Instruments) was used to determine the ^1H spin-lattice relaxation time T_1, by detecting the amplitude of the free induction decay signal after a 90° pulse in a 180°-τ-90° rf pulse sequence. A suitable range of values of τ, the spacing time between the two pulses, was used. The re-establishment of the M_z magnetization, after the 180° pulse, to the equilibrium value of the magnetization, M_z^o, satisfies the equation:

$$M_z(\tau) = M_z^o\left(1 - 2\exp(-\tau / T_1)\right) \tag{4}$$

A non-linear least-squares computer program was used to fit the obtained data with Eq. (4) and to calculate the T_1 value. Care was taken to carry out the measurements at the same temperature.

The ^1H spin-spin relaxation time T_2 was measured on a 100-MHz computer-controlled NMR spectrometer. In principle, T_2 can be obtained directly from the free induction decay following a 90° rf pulse. However, because field inhomogeneities affect the magnetization decay determined in this way, we have determined T_2 from the amplitudes of spin echoes, produced by a CPMG (Carr-Purcell-Meiboom-Gill) pulse sequence[24] with a delay time, τ, between the 180° pulses of 200 μs. Such a delay time is short enough to ensure that diffusion effects are virtually eliminated. The T_2 value is now obtained by fitting the magnetization decay with Eq. (5), where $M_y(0)$ is the transverse magnetization immediately following the 90° pulse (i.e., equal to M_z^o).

$$M_y(t) = M_y(0)\exp(-t / T_2) \qquad (5)$$

5.4. Results and discussion

5.4.1. NMR experiments of silica dispersions without polymer

Figure 1 shows both the longitudinal and transverse relaxation rate observed with a dispersion of silica at different solid concentrations. As expected, in the fast exchange limit, there is a linear relation between available surface area (assuming there is no flocculation/aggregation) and the relaxation rate. The slopes of the lines
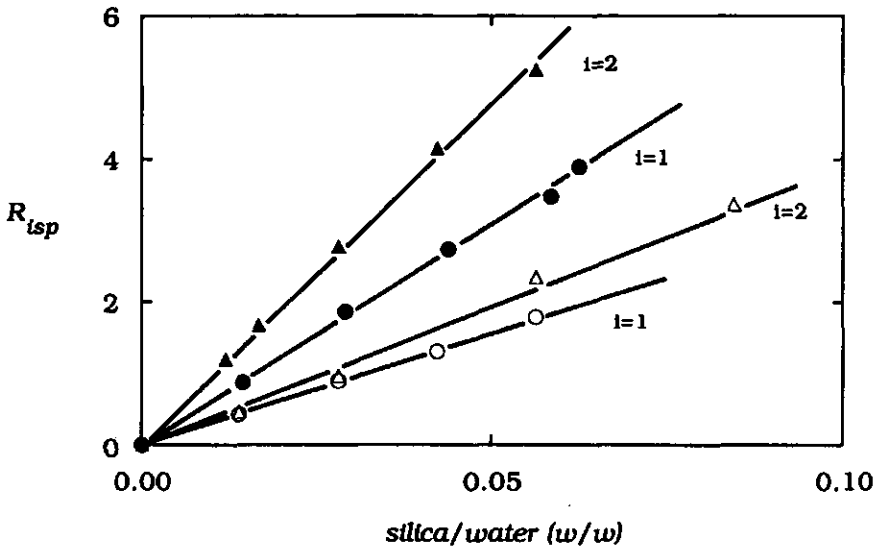
Figure 1. *Specific longitunal relaxation rate (R_{1sp}) and transverse relaxation rate (R_{2sp}) of silica dispersions without polymer and with adsorbed PVP, as a function of the silica concentration: ○, R_{1sp} of samples without polymer; ●, R_{1sp} of samples with adsorbed PVP k15; △, R_{2sp} of samples without polymer; ▲, R_{2sp} of samples with adsorbed PVP k15.*

presented are proportional to R_{isp}^b (Eq. (3)). For water bound to silica without polymer, the transverse relaxation rate (R_{2sp}^b) is somewhat

higher than the longitunal one (R_{1sp}^b). This can be interpreted as low frequency molecular motions occurring at the interface. Very slow motions lead to static non-averaged dipolar interactions which increase R_{2sp}^b but have no influence on R_{1sp}^b, provided the magnetic field is sufficiently high. The difference between the two relaxation rates becomes possibly larger if both measurements had been carried out at 100 *MHz*.
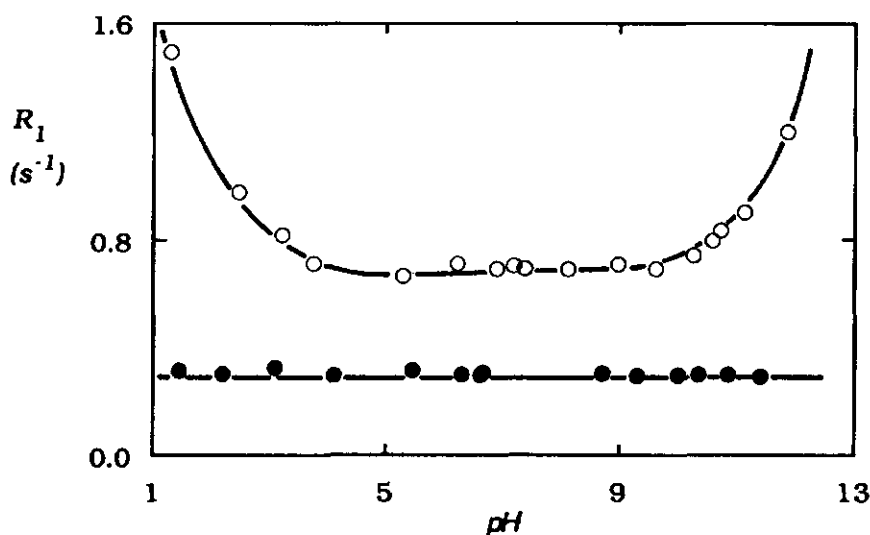
Figure 2. *Relaxation rate R_1 of pure water (●) and a silica dispersion with a silica/water mass ratio of 0.0515 (○) as a function of the pH.*

Figure 2 shows a rather interesting *pH* effect on T_1. The relaxation rate for 'bound' water is rather dramatically enhanced for high and low *pH* values though the effect of changing *pH* on bulk water can be seen to be negligible. According to Belton *et al.*,[25] this may be explained by the following proton exchange reactions:

$$\equiv SiOH + {}^\bullet HOH \;\rightleftharpoons\; \equiv SiOH^\bullet + HOH \qquad \text{(a)}$$

$$\equiv SiOH + H_3O^+ \;\rightleftharpoons\; \equiv SiOH_2^- + H_2O \qquad \text{(b)}$$

$$\equiv SiOH + OH^- \;\rightleftharpoons\; \equiv SiO^- + H_2O \qquad \text{(c)}$$
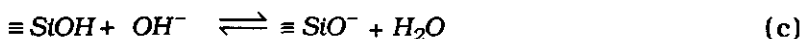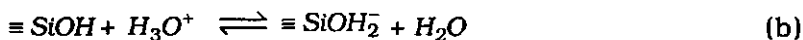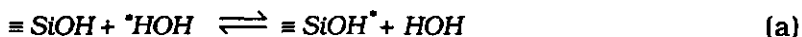
The rate constants for reactions (b) and (c) are on the order of 10^6 times higher than the rate constant for reaction (a). This means that when the OH^- or H_3O^+ concentration becomes sufficiently high (i.e., $\geq 10^{-5}$), the proton exchange rate will be enhanced. Between pH 4 and 10 the relaxation rate is constant, although the number of bound protons varies. At high and low pH the relaxation rate is further enhanced, indicating that it is indeed the lifetime of the chemically bound protons that is the determining factor. Thus, the relaxation of the chemically bound protons can only be observed, albeit indirectly, at high and low pH when the exchange rate with water molecules is sufficiently high.

Above pH 12 dissolution of silica may also occur. This should reduce the observed relaxation rate due to a reduction of the total surface area but enhance the relaxation rate if paramagnetic ions are released (Ludox HS_{40} contains 0.02 wt % Ti and 0.01 wt % Fe).[18] However neither of these effects occurred over the pH range used in this study as the variation of the relaxation rate with pH was completely reversible. For the majority of the present work we shall be interested in the pH range 4-10 where the relaxation rate enhancement of the silica is pH independent and where there is negligible dissolution of the silica.

5.4.2. Polymer adsorption

The adsorption isotherms for PEO (PEG 15000) and PVP (k25) on silica particles dispersed in water of $pH=7.5$ are shown in Figure 3. The surface to volume ratios used for these isotherms are 13.5 and 12.4 m^2/mL for PEO and PVP, respectively. Although the molecular weights for both polymer samples are rather similar, the adsorbed amount of PVP is much larger than that of PEO.

Figure 4 shows the specific ^1H longitunal relaxation rate R_{1sp} of water as a function of the silica to water ratio for dispersions without polymer, with PEO, and with two different molecular weight PVP samples. The polymer concentrations used correspond to adsorbed amounts in the plateau of the adsorption isotherm. As for bare silica, the relaxation rate for coated silica is proportional to the silica concentration but the R_{1sp} values are larger. The enhancement of the

relaxation rate due to PVP adsorption is much larger than that for PEO adsorption. No significant difference in R_{1sp} was found between the two PVP samples.
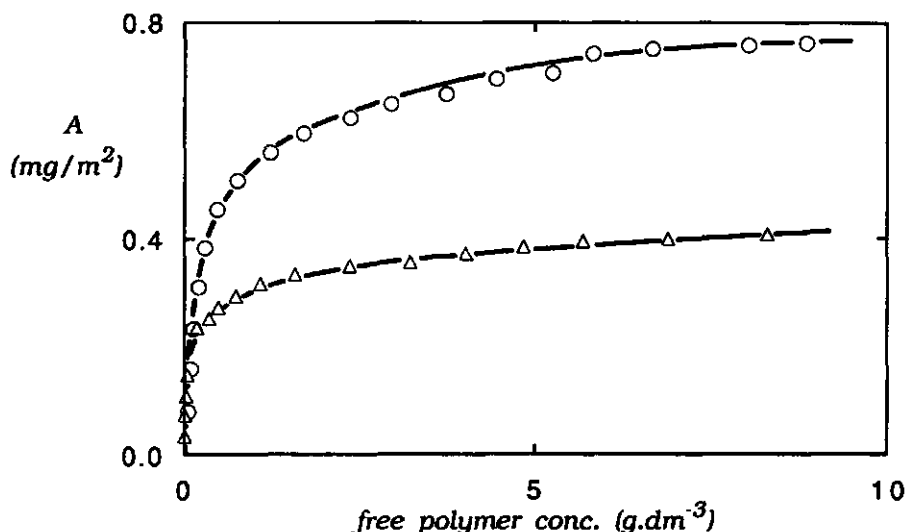
Figure 3. *Adsorption isotherms of PEG 15000 (△) and PVP k25 (○) on Ludox HS$_{40}$ particles at a pH of 7.5 and with surface to volume ratios of 13.5 and 12.4 m^2/mL, respectively.*

Figure 1 shows the effect of PVP adsorption on R_2. The same trend is found as for the R_1 measurements. The increase in this relaxation rate by polymer adsorption is, however, more pronounced. Hence, both R_1 and R_2 are indicative of either an increased number of immobilized water molecules or an increased residence time. This is so because free polymer concentrations up to 10,000 *ppm* do not significantly affect relaxation rates.

The conformation of an adsorbed polymer on a solid surface can be described in terms of trains (segments directly bound to the surface), loops, and tails (free chain ends). For higher molecular weights, the adsorbed amount increases due to the formation of longer tails and loops. Hence, if all the segments in the adsorbed polymer contribute equally to the relaxation rate, R_{1sp} should vary with molecular weight.
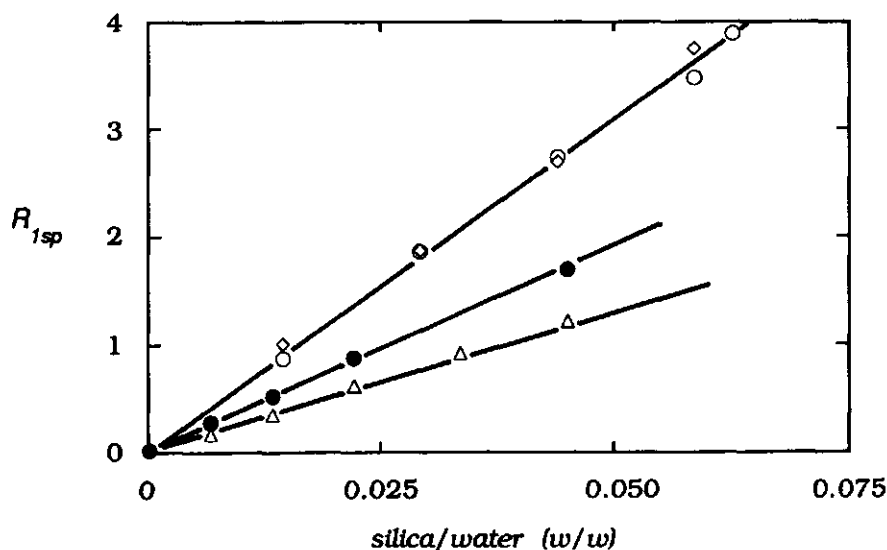
Figure 4. *The specific longitunal relaxation rate R_{1sp} of Ludox HS_{40} without polymer ($\triangle$) and with adsorbed PVP k15 ($\bigcirc$), PVP k25 ($\diamond$), and PEG 15000 ($\bullet$), as a function of the silica concentration.*
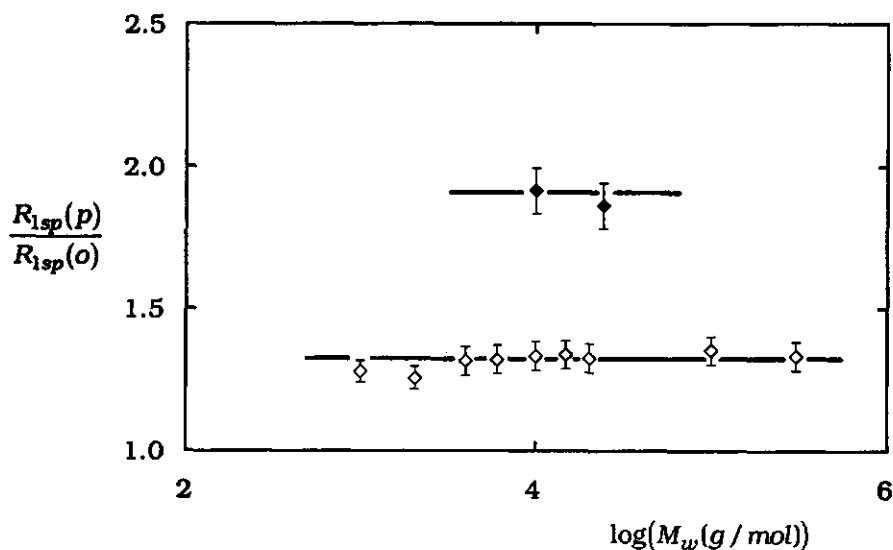
Figure 5. *Relaxation rate enhancement $R_{1sp}(p)/R_{1sp}(o)$ (where p refers to silica with polymer and o to bare silica) for PEO ($\diamond$) and PVP ($\blacklozenge$) adsorption on silica as a function of the molecular weight.*

Figure 5 shows the relative enhancement of the specific relaxation rate (i.e., R_{1sp}(silica with polymer)/R_{1sp}(bare silica)) by PEO and PVP adsorption onto silica as a function of molecular weight (M_w). For PEO, this enhancement is constant over a M_w range of 3 decades. This is remarkable, given that for the higher molecular weights, less than one polymer molecule per silica particle is adsorbed, yet the same relaxation rate enhancement is found. Similarly, no dependence of R_{1sp} on molecular weight for PVP was seen in Figure 4. Enhancement factors for PEO and PVP adsorption onto silica from water are thus on average 1.3 and 1.9, respectively. Apparently, part of the adsorbed polymer is still sufficiently mobile to produce no effect (viz. free polymer in solution). As the number of train segments is only very weakly dependent on molecular weight, we attribute the relaxation enhancement to trains rather than loops/tails. Further support of this conclusion comes from Figures 6-8.
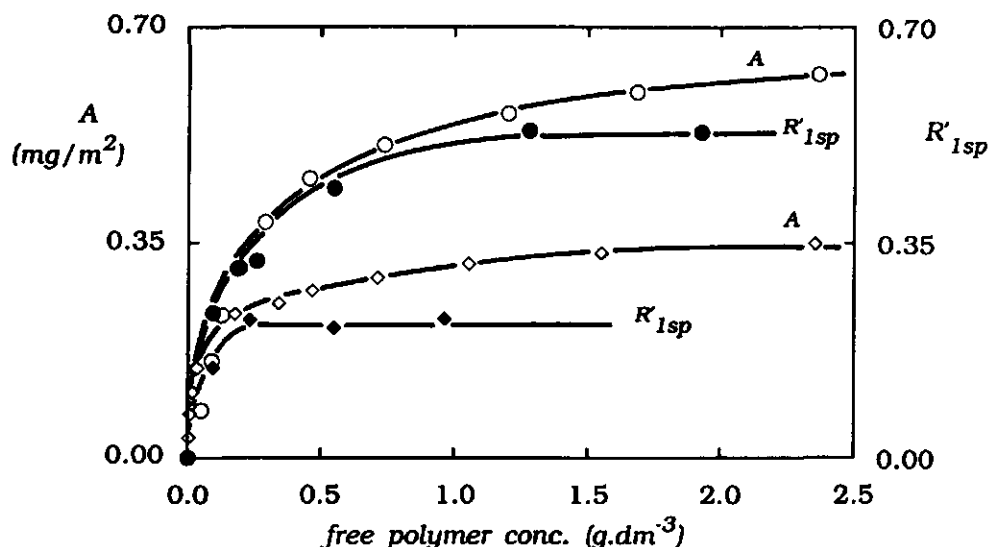
Figure 6. Adsorbed amount A and specific relaxation rate R'_{1sp} as a function of the equilibrium polymer concentration: ◇, A for PEG 15000; ◆, R'_{1sp} for adsorbed PEG 15000; ○, A for PVP k15; ●, R'_{1sp} for adsorbed PVP k15.

In Figure 6, both the adsorbed amount and R'_{1sp} are plotted as a function of the equilibrium polymer concentration. The specific relaxation rate R'_{1sp} is now defined with respect to silica dispersions without polymer. At low polymer concentrations (undersaturation), the adsorbed molecules lay flat on the surface. The train fraction then approaches unity. When more polymer is adsorbed, competition of segments to form the train layer will lead to the formation of loops and tails. For both PEO and PVP the increase in the relaxation rate is already at its plateau level, long before the adsorbed amount reaches saturation. This suggests strongly that R'_{1sp} essentially detects trains. This is seen more clearly by plotting the R'_{1sp} values of Figure 6 against the total adsorbed amount of the same equilibrium polymer concentration (Figure 7). The specific relaxation rate appears to be proportional to the adsorbed amount and then suddenly levels off when the train segment density is saturated. The adsorbed amount however, continues to increase.
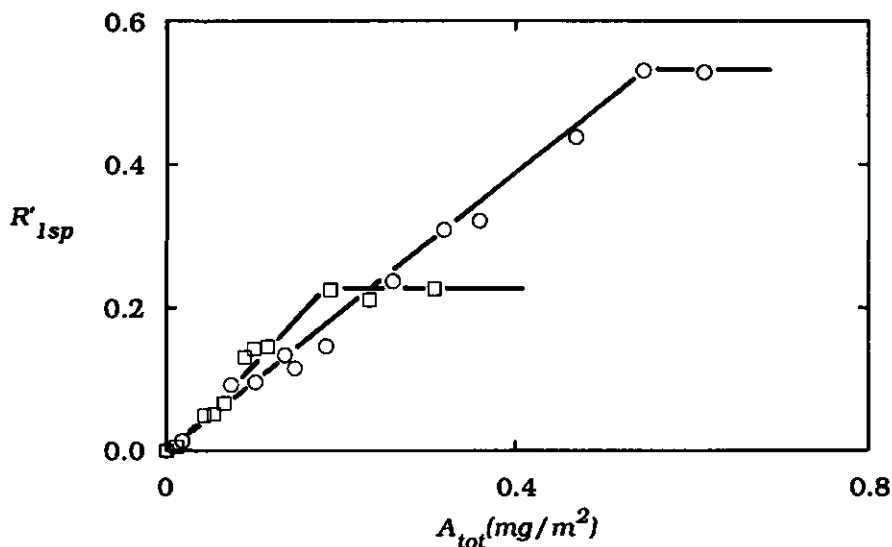
Figure 7. *Specific relaxation rate R'_{1sp} as a function of the total adsorbed amount of polymer: □, PEG 15000; ○, PVP k15.*

Figure 8 shows theoretically calculated adsorbed amounts of train segments as a function of the total adsorbed amount using the self-

consistent field theory of Scheutjens and Fleer[26,27] for two different polymer chain lengths. The initial slopes of the curves however are independent of molecular weight as the chains lie virtually flat at the interface. The similarity between this theoretical plot and Figure 7 supports our conclusion that the measured relaxation rate is proportional to the number of bound segments.
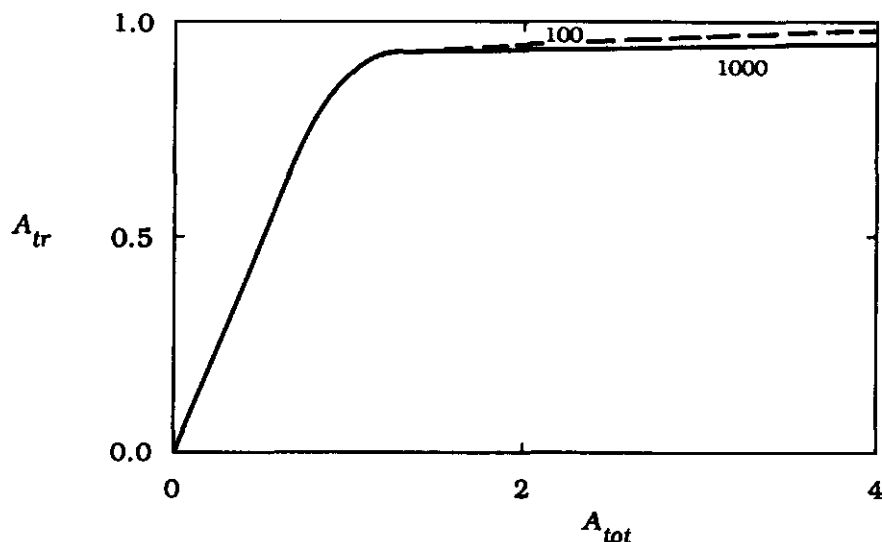
Figure 8. *Theoretical plot calculated by the Scheutjens-Fleer theory. The fraction occupied train layer A_{tr} is given as a function of the total adsorbed amount A_{tot}, expressed in equivalent number of monolayers, for an athermal solvent. The lattice used was hexagonal and χ_s^{po} equal to 3. The chain length r, expressed in the number of monomers, is indicated.*

Also of note in Figure 7 is that although the total relaxation enhancement (i.e., the 'plateau' value) for PVP is larger than for PEO, the enhancement per adsorbed amount (i.e., the slope of the line) is lower. The initial parts of the curves in Figure 7, which have slopes k of 1.32 and 0.96 m^2/mg for PEO and PVP, respectively, can be used to transform determined values of R'_{1sp} into adsorbed amounts of train segments, A_{tr}:

$$A_{tr} = k^{-1}R'_{1sp} \tag{6}$$

It should be noted that A_{tr} as measured by this method is not defined precisely, but phenomenologically. Trains are distinguished from other parts of the polymer on a mobility criterion, and the train fraction is assumed to be unity at low coverage. There is a vast amount of evidence that adsorbed layers at low coverage are very thin, indicating a flat 'all train' conformation. In the following discussion A_{tr} will be used instead of R'_{1sp}. When A_{tr} is divided by the corresponding A_{tot}, the train fraction is obtained. At saturation, these fractions are 0.46 and 0.68 for PEG 15000 and PVP k25, respectively. Although in these two cases the molecular weight of PVP is somewhat higher than that of PEO, PVP has the highest bound fraction.

5.4.3. Interpretation of relaxation rate enhancement by polymer adsorption

The addition of polymer (Figure 1) leads to an enhancement in the surface relaxation. At first sight, this is somewhat unexpected as it might be presumed that an adsorbing polymer segment will effectively *reduce* the number of available surface sites for the solvent. Polymer hydration seems to be excluded since the effect of polymer in solution on the relaxation rate is negligible.

It is useful to consider dynamic coupling between the motion of water in the surface layer of a particle and the motion of the particle itself. With respect to a fixed point, the motion of surface water is a superposition of the motion of the particle and the motion of this surface water relative to the particle. When the motion of the particle is very slow (i.e., for particles with radii $ca. > 10$ nm),[20] the motion of the surface water relative to a fixed point is the same as relative to the motion of the particle. So, for particles that are not too small, it is not necessary to consider the motional behaviour of the particle itself in describing the proton relaxation of the surface water.

The mobility of water interacting with a flexible polymer in solution is more complex, because the mobility of this water is now a

superposition of the mobility of the whole polymer, the individual polymer segments, and the 'hydrated' water itself. For the molecular weight under consideration here, the motion of the whole polymer is slow compared to the mobility of the individual polymer segments. Apparently, the mobility of the polymer segments is still high enough, and the lifetime of water in the hydration shell small enough, such that there is no observed increased proton relaxation rate of the water. This is not so for proteins. 'Segments' in proteins are less mobile because of many intra-molecular bonds and the lifetime of the 'bound' water layer is such that the proton relaxation rate is enhanced.[28]

For an adsorbed polymer, the mobility of segments, especially for ones attached to the silica surface, is reduced drastically[2] and hence the mobility of 'bound' water. This will lead to an enhanced relaxation rate of the water. Protons of the adsorbed polymer segments may also contribute to the observed relaxation rate. This is probably less important, because the lifetime of these segments is considerably larger than for water molecules at the surface. Assuming that only the extra immobilized water causes the relaxation rate enhancement, then the enhancement factors from Figure 5 for PEO and PVP adsorption directly indicate the amount of bound water. Not only the number but also the mobility of the 'bound' water molecules affect the relaxation rate. So, relaxation rate enhancement by polymer adsorption is a reflection of the extent of monomer hydration and surface proximity. The situation is obviously complex and the residence time of the polymer segment at the interface is also important. Given the greater mass and stronger surface affinity of the PVP, the greater enhancement is almost certainly due to the increased polymer segment/surface residence time and the number of water molecules coordinated to each polymer segment.

Hence, the relaxation rate enhancement gives a measure of the number of surface bound polymer segments. This effect should therefore, to a first approximation, be molecular-weight independent in the plateau region of the adsorption isotherm and also independent of the polymer concentration. This is confirmed rather well by the data shown in Figures 5 and 6 for both systems. It should be noted that the relaxation rate enhancement is dependent on the

polymer of interest, for example, the chain stiffness and the degree of hydration. The A_{tr} values obtained from the relaxation rate enhancement do not depend on the degree of hydration because this effect is accounted for by using calibration curves, *viz.* Figure 7. The chain stiffness however affects A_{tr} for polymer adsorption under saturated conditions because the calibration curves are based on adsorbed polymers in which almost all segments are bound to the surface (undersaturation). When loops and tails are present, the chain stiffness determines how many segments near the interface contribute to the relaxation enhancement. It is possible therefore, that the train fraction is somewhat over-estimated by the NMR technique in a way determined by the specific characteristics of the polymer under investigation.

5.4.4. Polymer desorption

Polymer desorption can occur by adding a more strongly adsorbing component (displacer). This displacer essentially lowers the effective adsorption energy of the polymer. Poly(ethylene oxide) and poly(vinylpyrrolidone) can be desorbed from silica at high *pH*, and so OH^- can be regarded as a displacer. In Figure 9, we show PVP desorption from Ludox HS_{40} particles by increasing the *pH*. Both the decrease in A_{tot}, determined by the depletion method, and A_{tr}, which is obtained from R'_{1sp} (Eq. (6), assuming k does not change with *pH*), are given. As was seen in Figure 4, the relaxation rate of silica dispersions beyond *pH* 10 increases with *pH* and so, for these high *pH* values, the relaxation rate of silica dispersions of the same *pH* were used as reference samples when calculating R'_{1sp} and A_{tr} values. The curves for A_{tot} and A_{tr} have almost the same shape and end at the same point, i.e., the critical point. The *train fraction* (A_{tr}/A_{tot}) at *pH* 7.5 is in excellent agreement with the one found earlier from Figure 7. This fraction becomes smaller, when polymer is desorbed. In other words, the amount of segments in trains is more sensitive to adsorption energy than the amount in loops and tails.
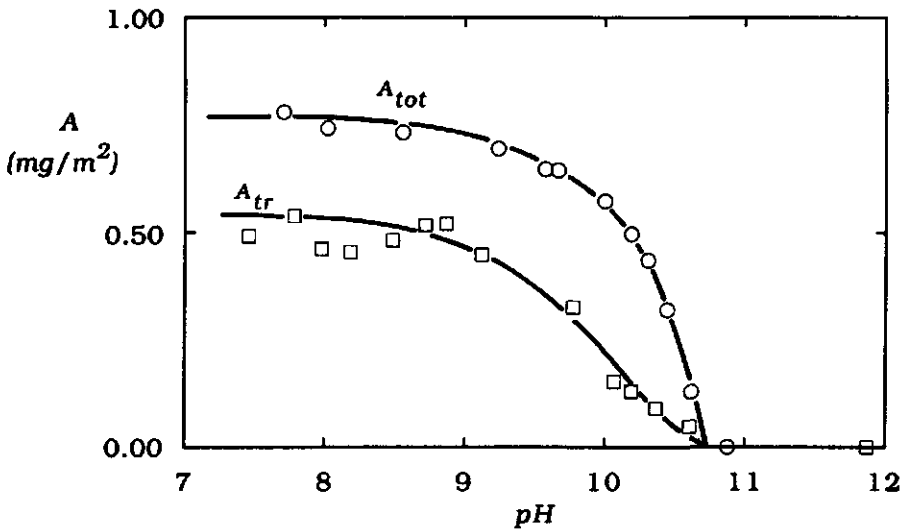
Figure 9. *PVP (k25) desorption from silica by increasing pH:* □, *adsorbed amount of train segments;* ○, *total adsorbed amount.*

This conclusion is supported by the data for PEO, presented in Figures 10-12. Figure 10 shows PEO desorption with increasing *pH*, determined by the two techniques described above and by dynamic light scattering. This last technique yields the hydrodynamic thickness δ_h of the adsorbed layer, which is entirely determined by the tails of the adsorbed polymer. The curves for A_{tot} and δ_h are taken from ref 5. In this study monodisperse PEO of a molecular weight of 270 *kg/mol* and Ludox particles of 32 *nm* diameter were used. The data in Figure 10 directly compare the relative changes in tail and train densities as the net adsorption energy is reduced. This picture is rather informative and shows that the tail density (as seen by the hydrodynamic thickness) remains constant up to *pH* 10.5 whereas the loss in the adsorbed amount is primarily due to a reduction in trains. The effect is not surprising given that only one segment of a polymer needs to be adsorbed for the whole chain to be held at the surface. Beyond *pH* 10.5 there is a dramatic loss in the adsorbed amount and in the tail density whereas the train fraction is almost totally depleted at *pH* 10.5.
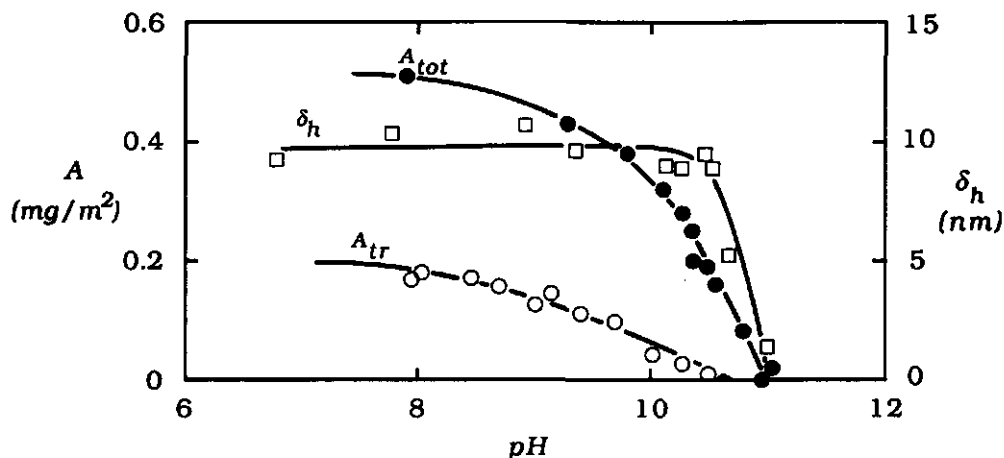
Figure 10. *PEO ($M_w = 270$ kg/mol) displacement from silica by increasing pH: ○, adsorbed amount of train segments; ●, total adsorbed amount[5]; □, hydrodynamic layer thickness[5].*

The advantage of studying polymer desorption by varying the *pH* is that most of the solvent properties do not change when more displacer is added. Thus, OH^- can act as a displacer but is not a solvent component of the system. The model of Cohen Stuart *et al.* [6] used to extract adsorption energies from polymer displacement studies, is based on polymer desorption in binary solvent mixtures as a function of the solvent composition. This model is not suitable for polymer desorption by ions. We therefore extended this study to two organic displacers. Poly(ethylene oxide) can be displaced from silica by dimethyl sulfoxide (DMSO) and dimethyl formamide (DMF). These two solvents cannot be used for displacement of PVP from silica, because PVP still adsorbs onto silica in pure DMSO and DMF. A conclusion that can be drawn directly from this is that PVP adsorbs more strongly on silica from water than PEO.

A complication of the NMR measurement in a binary solvent mixture is that, in general, the relaxation rate of the solvent itself will change when more displacer is added to the system. Two effects may play a role:

- Proton relaxation of the displacer (second solvent component) may affect the measured relaxation rate. This effect is, however, negligible for low displacer concentrations but may need corrections at high concentrations. If necessary, this relaxation component can be totally eliminated by using deuterated displacers or using high-resolution NMR techniques.
- The presence of a second solvent component can affect the molecular dynamics of the first component. Increasing solvent-displacer contacts may change the amount of specific bonds (e.g., hydrogen-bond) per molecule and hence the spectral density of the solvent molecules. This may lead to changes in relaxation rates (especially R_1). The use of deuterated displacers does not eliminate this effect.

In the case of DMF and DMSO, the second effect is more important than the first one. The relaxation time of the solvent mixtures diminishes with increasing displacer concentration, while neither the relaxation rate of pure DMSO nor that of DMF are very different from that of pure water.

Figure 11 shows the effect of 16.7 vol% DMF and 16.7 vol% DMSO on R_{1sp} of silica dispersions. As a reference for calculating these relaxation rates, we used R_1 of the corresponding solvent mixtures without silica, so the effect of the displacer on the relaxation of the bulk is accounted for. A concentration of 16.7 vol% DMSO or DMF corresponds to the plateau value of the adsorption isotherms for these two components on silica.[9] Hence, the concentration near the surface is maximized. As can be seen in Figure 11, there is still a linear relationship between R_{1sp} and the silica concentration. The line for dispersions with DMSO is not significantly different from the one for silica dispersions without a displacer. The slope of the line for DMF, as the extra component in the system, is, however, slightly larger. As can be seen from the comparison between Figure 11 and Figure 4, the effect of DMSO and DMF adsorption on the relaxation rate of aqueous silica dispersions is much less than that of polymer adsorption. These displacers can therefore be used to study PEO desorption by the NMR technique.
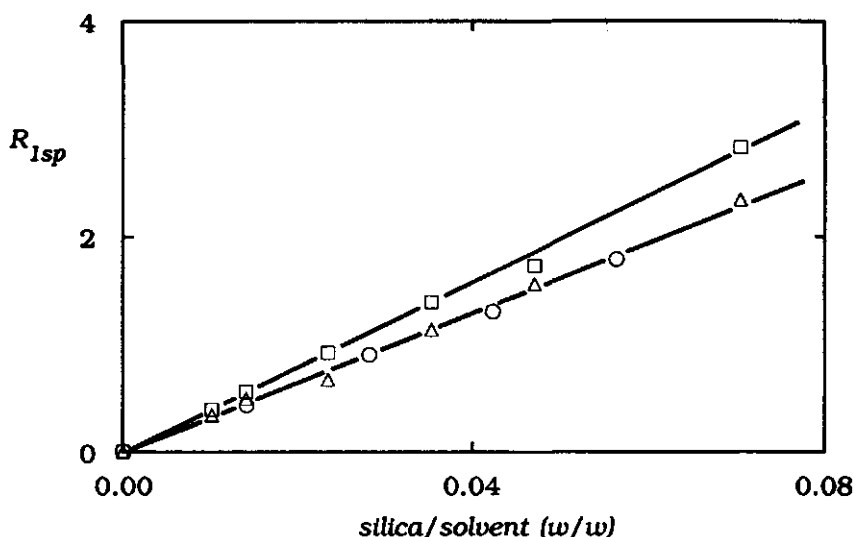
Figure 11. *Specific relaxation rate R_{1sp} of silica dispersions with and without displacers as a function of the silica water ratio:* ○, *without displacer;* △, *with 16.7 vol% DMSO;* □, *with 16.7 vol% DMF.*

The change in the relaxation rate of a silica dispersion when more displacer is added can (over-)compensate the reduction in relaxation rate due to polymer desorption. It is therefore imperative to measure the relaxation times of silica dispersions with different concentrations of displacer, in order to extract the effect caused by polymer desorption. Specific longitudinal relaxation rates as a function of the volume fraction displacer, $R'_{1sp}(\phi^d)$ are now defined with respect to R_1 values of silica dispersions with the same volume fraction displacer but without polymer. Furthermore, it is assumed that the displacer concentration does not affect the proportionality between R'_{1sp} and A_{tr}, which was found for the single solvent (Eq. (6)). Figure 12 shows the desorption of PEO from silica by DMSO and by DMF, respectively. Remarkably, the desorption curves for train segments are the same for both displacers, within experimental error. Apparently, the adsorption energies for DMSO and DMF are not very different. The total adsorbed amount as a function of the displacer concentration is only given for displacement by DMF.

The critical points, determined with both techniques are in excellent agreement. The volume fractions at the critical point are equal to 0.26, both for DMF and DMSO.
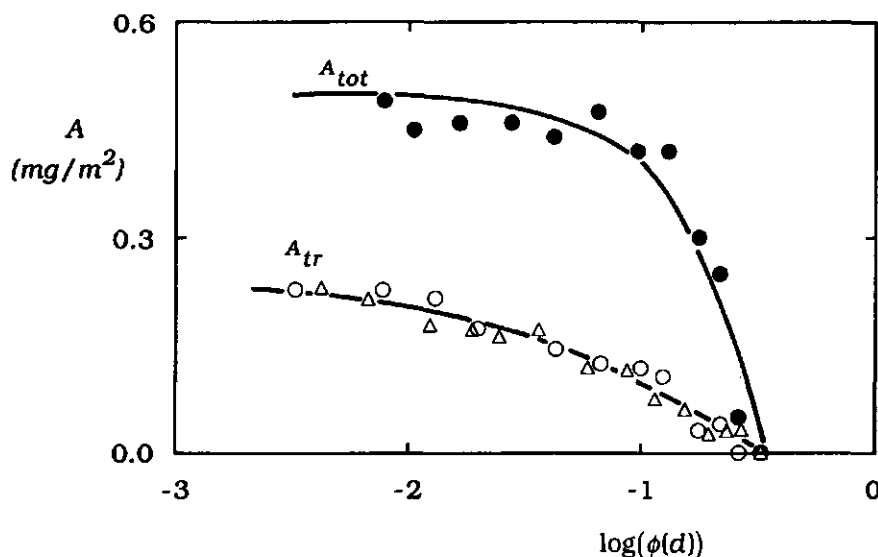
Figure 12. *PEO (PEG 20,000) desorption from silica by increasing the volume fraction $\phi(d)$ of displacer: O, adsorbed amount of train segments for DMF as displacer; ●, total adsorbed amount for DMF as displacer; △, adsorbed amount of train segments for DMSO as displacer.*

5.4.5. Calculated polymer desorption curves

Figure 13 shows examples of theoretical polymer desorption curves obtained from the Scheutjens-Fleer theory. Both A_{tot}, expressed in equivalent number of monolayers, and A_{tr}, expressed in the fraction occupied train layer, are shown. The desorption curves have the same shape and relative position as found experimentally. Figure 13a shows the effect of the solvent-polymer interaction on the desorption curves for trains, loops, and tails and for the train segments only. The calculations were all carried out for one value of the polymer adsorption energy. (For this adsorption energy, we use
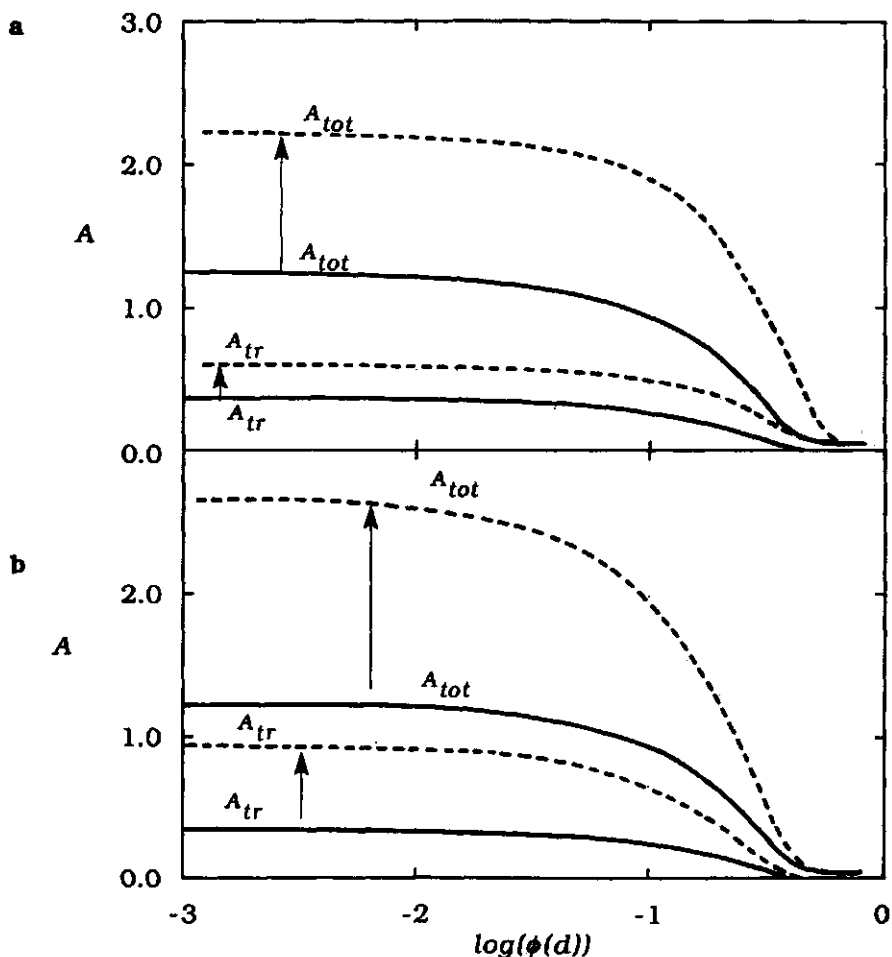
Figure 13. *Theoretical displacement isotherms (calculated by the Scheutjens-Fleer theory) based on a hexagonal lattice, a polymer volume fraction of 10^{-3}, and r (number of polymer segments) = 100. The adsorbed amounts are expressed in equivalent numbers of monolayers.* **a.** *Effect of the solvent quality on the displacement curves for $\chi_s^{po} = 1$, $\chi_s^{do} = 1.1$: solid lines, A_{tr} and A_{tot} for an athermal solution; broken lines, A_{tr} and A_{tot} for $\chi^{po} = \chi^{pd} = 0.4$ and $\chi^{do} = 0$.* **b.** *Effect of the adsorption energy on the displacement curves for athermal solutions: solid lines, A_{tr} and A_{tot} for $\chi_s^{po} = 1$ and $\chi_s^{do} = 1.1$; broken lines, A_{tr} and A_{tot} for $\chi_s^{po} = 3.5$ and $\chi_s^{do} = 4$.*

the parameter χ_s^{po}, which is defined as the adsorption energy difference between a polymer segment (p) and a solvent molecule (o) in units kT. The parameter χ_s is defined in such a way that χ_s^{po} is counted positive if the polymer adsorbs preferentially from the solvent. The adsorption energy of the displacer (d), χ_s^{do}, is defined in the same way. The solvent quality is expressed in the well-known Flory-Huggins parameter, χ.) In Figure 13a, polymer desorption in an athermal solution (i.e., all χ parameters are zero) and in a solution where $\chi^{po} = \chi^{pd} = 0.4$ and $\chi^{do} = 0$ are shown for $\chi_s^{po} = 1$. The solvent quality in both systems has been fixed when the solvent composition is changed. In the case of a poor solvent, this leads to more adsorbed polymer, and this affects A_{tot} more than A_{tr}. At high adsorption energies, in particular, the solvent quality becomes unimportant for A_{tr} because solvent-polymer interactions play then a minor role in the surface layer.

The effect of the adsorption energy on both A_{tot} and A_{tr}, is shown in Figure 13b. The total adsorbed amount and train segment density for an athermal solution both show a large increase when the χ_s^{po} value is increased from 1 to 3.5. The occupied fraction of the train layer, however, reaches a maximum for high adsorption energies, i.e., $\chi_s^{po} > 3.5$; the train layer is virtually completely full.

Given that A_{tr} is independent of the molecular weight of the polymer, it can be concluded that in contrast to A_{tot}, A_{tr} is a good indicator of the polymer adsorption energy. This implies that, for a given polymer-solvent pair, R'_{1sp} depends on the adsorption energy (i.e., on the substrate). The result that A_{tr} (R'_{1sp}) values for PVP adsorption are larger than for PEO agrees with the fact that PVP has the higher adsorption energy. It should be noted that one cannot compare train segment densities for different polymeric species without further specific corrections to the NMR data.

5.5. Conclusions

By comparing theoretical results for adsorbed homopolymers with measured ^1H spin-lattice relaxation rates of the solvent in dispersions of silica with adsorbed polymer, we have obtained strong

evidence that the increase in relaxation rate which is found can be ascribed to the enhanced immobilization of solvent by surface-bound polymer segments (so-called trains). Making use of this finding, we are able to obtain information regarding the conformation of adsorbed polymers by comparing the total adsorbed amount with the amount adsorbed as train segments. The train density as a function of the concentration of a low molecular displacer has also been obtained. This displacement experiment yields a critical displacer concentration that is in good agreement with those obtained by other methods. The shape of the displacement isotherm measured by NMR agrees very well with that of theoretically calculated train segment densities as a function of the solvent/displacer composition.

5.6. References

1. Cohen Stuart, M. A.; Vincent, B.; Cosgrove, T. *Adv. Colloid Interface Sci.* **1986**, 24, 143.
2. Barnett, K. G.; Cosgrove, T.; Vincent, B.; Sissons, D. S. *Macromolecules* **1981**, 14, 1018.
3. Cosgrove, T.; Heath, T. G.; Ryan, K.; Crowley, T. L. *Macromolecules* **1987**, 20, 2879.
4. Cohen Stuart, M. A.; Waajen, F. H. W. H.; Cosgrove, T.; Vincent, B. *Macromolecules* **1984**, 17, 1825.
5. Van der Beek, G. P.; Cohen Stuart, M. A. *J. Phys. (Paris)* **1988**, 49, 1449.
6. Cohen Stuart, M. A.; Fleer, G. J.; Scheutjens, J. M. H. M. *J. Colloid Interface Sci.* **1984**, 97, 515.
7. Cohen Stuart, M. A.; Scheutjens, J. M. H. M.; Fleer, G. J. In *Polymer Adsorption and Dispersion Stability*; Vincent, B., Goddard, E. D., Eds.; ACS Symposium Series 240; American Chemical Society: Washington, DC, 1984; p 53.
8. Van der Beek, G. P.; Cohen Stuart, M. A.; Fleer, G. J.; Hofman, J. E. *Langmuir* **1989**, 5, 1180.
9. Kawachuchi, M.; Hada, T.; Takahashi, A. *Macromolecules* **1989**, 22, 4045.

10. Cohen Stuart, M. A.; Fleer, G. J.; Scheutjens, J. M. H. M. *J. Colloid Interface Sci.* **1984**, 97, 526.
11. Garvey, M. J.; Tadros, Th. F.; Vincent, B. *J. Colloid Interface Sci.* **1976**, 55, 440.
12. Belenkii, B. G.; Gankina, E. S. *J. Chromatogr.* **1977**, 141, 13.
13. Cosgrove, T.; Barnett, K. G. *J. Magn. Reson.* **1981**, 43, 15.
14. Woessner, D. E. *J. Magn. Reson.* **1980**, 39, 297.
15. Walmsley, R. H.; Shporer, M. *J. Chem. Phys.* **1978**, 68, 2584.
16. Hanus, F.; Gillis, P. *J. Magn. Reson.* **1984**, 59, 437.
17. Zimmerman, J. R.; Brittin, W. E. *J. Phys. Chem.* **1957**, 61, 1328.
18. Piculell, L. *J. Chem. Soc., Faraday Trans. I* **1986**, 82, 387.
19. Halle, B. *Mol. Phys.* **1985**, 56, 209.
20. Halle, B.; Piculell, L. *J. Chem. Soc., Faraday Trans. I* **1986**, 82, 415.
21. Carrington, A.; McLachlan, A. D. *Introduction to Magnetic Resonance*; Chapman and Hall: London, 1979; p 183.
22. Lynch, L. J. In *Magnetic Resonance in Biology*; Cohen, J. S., Ed.; John Wiley & Sons, Inc.: New York, 1983.
23. Nuysink, J.; Koopal, L. K. *Talanta* **1982**, 29, 495.
24. Meiboom, S.; Gill, D. *Rev. Sci. Instrum.* **1958**, 29, 688.
25. Belton, P. S.; Hills, B. P.; Raimbaud, E. R. *Mol. Phys.* **1988**, 63, 825.
26. Scheutjens, J. M. H. M.; Fleer, G. J. *J. Phys. Chem.* **1980**, 84, 178.
27. Scheutjens, J. M. H. M.; Fleer, G. J. *J. Phys. Chem.* **1979**, 83, 1619.
28. Hallenga, K.; Koenig, S. H. *Biochemistry* **1976**, 15, 4255.

Chapter 6

Segmental Adsorption Energies for Polymers on Silica and Alumina

Abstract

Segmental adsorption energies for polymers on inorganic solids can be determined from adsorption/desorption transitions in binary solvent mixtures. These transitions were measured for various polymer/solvent/substrate systems by thin-layer chromatography.

Polymers with either phenyl, ether, or ester groups were classified according to their adsorption strength on both silica and alumina. A consistent trend with respect to the adsorption energy for the different polymers was observed for both substrates. Polymer chains with larger alkyl side groups or more -CH$_2$- groups between ether groups in the backbone have a lower adsorption energy. The adsorption energy for each individual polymer is higher on the silica than on the alumina surface.

For the polymers studied, the main contribution to the work of adhesion on silica with respect to vacuum is due to dispersive interactions.

6.1. Introduction

During the last few decades the interest in polymers at interfaces has continuously been growing. Polymers may be considered as tools to manipulate the properties of interfaces, and such modified interfaces are very important in many industrial products and technological processes. The strength of polymer/interface bonds may be of great relevance for the efficiency of processes and the quality of products. For instance, in the case of polymer composites, the adhesion strength between the matrix polymer and the reinforcing filler affects the toughness and flexibility of the composites.[1]

Generally, the adhesion strength of polymers on a substrate can be determined in two ways. The first method involves mechanical removal of polymer from a substrate. This macroscopic disruption process is always irreversible. For such processes the measured adhesion strength (work of adhesion) depends on experimental conditions, such as crack speed and temperature. The reversible (intrinsic) adhesion strength is always smaller because of energy dissipation in the irreversible process. During the detachment of a polymer film from a substrate, energy may be absorbed by the deformation of the polymer film. This viscoelastic component may even be (much) larger than the reversible adhesion strength.

The second way to determine the adhesion strength of polymers is microscopic and reversible. Now, chemical energy instead of mechanical work is used to displace polymers from a substrate. Chemical energy is added to the system in the form of a certain chemical compound, a so-called *displacer*. The method gives the segmental adsorption energy which can be related to the thermodynamic work of adhesion. In principle, the thermodynamic work does not depend on experimental conditions and is therefore an intrinsic quantity for the particular system.

The latter method has been proposed and developed by Cohen Stuart *et al.*[2,3] The experiments are carried out in solution. The amount of displacer which has to be added to the solution for complete desorption of the polymer is called the *critical displacer concentration* or, shortly, the *critical point.* This critical concentration can be related to the segmental adsorption energy of the polymer. The thermodynamic work of adhesion can be calculated from this energy provided the number of segments bound per unit surface area is known.

In this study we measured critical points by thin-layer chromatography. In a previous paper[4] (chapter 2) we showed that this technique is sensitive and works very well for polystyrene on silica. The adsorption energies of polystyrene on silica calculated from critical points using different displacers agree very satisfactorily.

In this chapter, the determination of the segmental adsorption energies of five different polymers with basic (proton accepting)

functional groups (phenyl, ester, ether) on both alumina and silica is described. Besides the effect of a particular functional group, the influence of the chain structure on the adsorption energy is studied. The polymers are classified according to their adsorption energy. Not only adsorption energies of polymers can be obtained from critical points but also the adsorption energies of displacers. Energies for adsorption of displacers on silica and alumina are also given.

The last part of this chapter deals with the work of adhesion of various polymers on silica and involves an attempt for a molecular interpretation. Discrimination is made between the contributions of dispersive interactions and of specific interactions to the work of adhesion of the polymers on the substrate.

6.2. Methods

6.2.1. Adsorption energy

Two interaction parameters play a role for polymer adsorption from solution onto an adsorbent, one for polymer-surface contacts, and one for polymer-solvent contacts.

For the interaction free energy of polymer-surface contacts we use Silberberg's[5] χ_s parameter which is defined as the adsorption energy (in units of kT) of a polymer segment with respect to that of a solvent molecule. The χ_s parameter is by definition counted positive if the polymer adsorbs preferentially from the solvent. It is well known that polymers adsorb only if χ_s exceeds a critical value χ_{sc} which corresponds to the adsorption/desorption transition. The χ_{sc} parameter is related to the conformational entropy loss per segment upon adsorption.

Contact (free) energies between polymer segments and solvent molecules are usually represented by the familiar Flory-Huggins χ parameter.

Values for the χ parameter can be obtained from various observable properties, such as intrinsic viscosity, light scattering, and osmotic pressure. The χ_s parameter can only be determined by

a method proposed by Cohen Stuart *et al.*[2,3] This method is based upon polymer desorption in binary solvent mixtures. Polymers which are adsorbed from solution on an adsorbent may be desorbed by increasing the concentration of a more strongly adsorbing solvent component (displacer). The displacer concentration needed to entirely desorb the polymer is the *critical point* referred to in the introduction.

In a three-component system (polymer, solvent, displacer), two χ_s and three χ parameters are needed to describe all the interactions. The different χ parameters in such a system are indicated by the superscripts *po*, *pd*, and *do*, which correspond to polymer-solvent, polymer-displacer, and displacer-solvent contacts, respectively. The same superscripts can be used for the χ_s parameters. Now, the superscripts indicate the adsorption of polymer from solvent, polymer from displacer, and displacer from solvent, respectively. These three χ_s parameters are interrelated because of their exchange character: $\chi_s^{po} = \chi_s^{pd} + \chi_s^{do}$. Therefore, only two independent χ_s parameters occur.

Cohen Stuart *et al.*[2] have derived an equation which relates the volume fraction ϕ_{cr} of displacer at the critical point to the segmental adsorption energy parameters χ_s^{po} and χ_s^{do}:

$$\phi_{cr} = \frac{\exp\left(\chi_s^{po} - \chi_{sc} + \left\{(1-\lambda_1)(1-\phi_{cr})\left(\chi^{po} + \chi^{do} - \chi^{pd}\right) - \lambda_1\left(\chi^{do} - \chi^{pd}\right)\right\}\right) - 1}{\exp\left(\chi_s^{do} + \left\{2(1-\lambda_1)(1-\phi_{cr})\chi^{do} - \lambda_1\chi^{do}\right\}\right) - 1}$$

$$(1)$$

The parameter λ_1 comes from the lattice which is used to describe the solution and represents the fraction of contacts that a site has with sites in one of the adjacent lattice layers. For a hexagonal lattice λ_1 is equal to $3/12 = 0.25$. In this model, it is assumed that one lattice site is occupied by either one solvent molecule, one displacer molecule, or one polymer segment.

The terms -1 in Eq. (1) may be ignored if the exponentials are much larger than unity, i.e., for strong anchoring of the polymer segments. In this case, Eq. (1) simplifies to

$$\chi_s^{po} = \chi_s^{do} + \ln \phi_{cr} + \chi_{sc} - \left\{ \lambda_1 \chi^{pd} - (1 - \phi_{cr})(1 - \lambda_1) \Delta \chi^{dop} \right\} \qquad (2)$$

showing that in this limit ϕ_{cr} depends exponentially on $\chi_s^{po} - \chi_s^{do}$. All terms of Eqs. (1) and (2) within braces refer to solute/solvent interactions. For athermal behaviour of the solution these terms are equal to zero. The parameter $\Delta \chi^{dop}$ is an abbreviation for $\chi^{pd} + \chi^{do} - \chi^{po}$.

The critical adsorption energy parameter χ_{sc} can, in principle, be determined from desorption experiments with the monomer unit of the polymer as the displacer. For such displacers χ_s^{do} may be taken equal to χ_s^{po}. The χ_{sc} value can then be calculated directly from ϕ_{cr} by using Eq. (2) if the χ_s parameter for monomer adsorption from solvent is not too small (i.e., > 2). For small values of this parameter, χ_{sc} has to be calculated from ϕ_{cr} using the full Eq. (1) with $\chi_s^{po} = \chi_s^{do}$. However, in that case the value of χ_s^{do} is needed explicitly.

When a polymer is desorbed by its monomeric equivalent, the critical displacer volume fraction is usually found to be close to unity. For such systems, the solute/solvent interaction term with the pre-factor $(1 - \lambda_1)(1 - \phi_{cr})$ is very small and can therefore be ignored. The terms $\lambda_1 \chi^{pd}$ (in Eqs. (1) and (2)) and $\lambda_1 \chi^{do}$ (in Eq. (1)) may both be significant and have to be taken into account. However, just as in the case of high adsorption energies, the $\lambda_1 \chi^{do}$ terms of Eq. (1) also cancel if ϕ_{cr} is close to unity.

The critical energy parameter can also be estimated theoretically from the reduction of possible orientations of a segment upon adsorption. Within the restriction of a lattice and ignoring rotational entropy, χ_{sc} calculated in this way equals $-\ln(1 - \lambda_1)$, which, for a hexagonal lattice, is 0.288.

In chapter 2, we showed that the chromatographic solvent strength concept of Snyder[6] may be interpreted according to the model of Cohen Stuart et al.[2] However, Snyder considers only athermal solution behaviour. Tabulated solvent strengths of various solvents (eluotropic series) in the literature[6,7] serve as an useful source of information for determining adsorption energies. We derived[4] the following relations between our χ_s parameters and Snyder's solvent strengths ε:

$$\chi_s^{do} = \alpha'A(\varepsilon_d - \varepsilon_o) \tag{3}$$

$$\chi_s^{po} = \alpha'A(\varepsilon_{cr} - \varepsilon_o) + \chi_{sc} \tag{4}$$

Here, the parameters ε_o and ε_d are the solvent strengths of pure solvent and pure displacer, respectively, and ε_{cr} is the solvent strength of the solvent mixture at the critical point. The former two parameters are tabulated by Snyder, the latter can be calculated by Snyder's equation for the solvent strength of binary solvent mixtures[6]:

$$\varepsilon_{cr} = \varepsilon_o + \frac{\ln\{\phi_{cr}\exp[\alpha'A(\varepsilon_d - \varepsilon_o)] + 1 - \phi_{cr}\}}{\alpha'A} \tag{5}$$

The parameter A is the surface area occupied per adsorbate molecule (in nm^2) and α' (which has a dimension of nm^{-2}) is the activity of the adsorbent. We should note here that Snyder originally expressed A in units of $0.085\ nm^2$, which corresponds to a (dimensionless) surface area of 6 for benzene. In order to equate $\alpha'A\varepsilon$ to the molecular adsorption energy in units of kT, we defined[4] an activity α' which is a factor $(\ln 10)/0.085 = 27.1$ greater than Snyder's α. The value of α' depends on such quantities as the amount of physisorbed water, the surface porosity, and the distribution of active sites on the surface.[6] For the determination of α', which is essentially a calibration of the adsorbent, we used the method described by Snyder[6]. This method involves retention factor measurements of several standard (aromatic) compounds on the thin layer, with pentane as the eluent.

The combination of Eqs. (3)-(5) can be written as $\phi_{cr}(\exp\chi_s^{do} - 1) = \exp(\chi_s^{po} - \chi_{sc}) - 1$, which is the athermal equivalent of Eq. (1). Extending Eq. (4) with the solute/solvent interaction term of Eq. (2) gives

$$\chi_s^{po} = \alpha'A(\varepsilon_{cr} - \varepsilon_o) + \chi_{sc} - \{\lambda_1\chi^{pd} - (1 - \phi_{cr})(1 - \lambda_1)\Delta\chi^{dop}\} \tag{6}$$

We have to note that the solvent/solute interaction term in Eq. (6) is only valid for the case of high adsorption energies. This means that Eq. (6) is not suitable for systems that have low adsorption energies and strong solvent/solute interactions at the same time. The advantage of Eq. (6) for the determination of χ_s^{po} is that tabulated solvent strength data can be used instead of χ_s^{do} parameters which have to be measured separately. In ref 4 (chapter 2) we showed that this method works very well for polystyrene (PS) on silica. However, for strongly adsorbing polymers which can only be displaced by very strong displacers another complication arises, namely that the solvent strength of strong displacers is no longer a constant but depends on the displacer concentration. Snyder explains this phenomenon by *solvent localization*.[7,8] At low displacer concentrations the adsorbed monolayer is undersaturated with displacer. In such cases, all displacer molecules may be *localized* on the surface, i.e., have an optimal orientation with respect to surface sites. The tendency for localization of adsorbate molecules on the substrate increases as the interaction between these molecules with surface sites becomes stronger. At high surface concentrations, molecules become *delocalized* due to sterical hindrance between molecules in the surface layer. The adsorption energy of localized adsorbed molecules is usually more negative than that of delocalized ones.

Instead of using solvent strength data or measuring the adsorption energy of the displacer, one can also use the adsorption energy of a second polymer to determine the χ_s^{po} value for a particular polymer/solvent combination. The difference in adsorption energy for a polymer a and polymer b on the same type of surface sites is by definition:

$$\chi_s^{ab} = \chi_s^{ao} - \chi_s^{bo} \tag{7}$$

This difference may be found from the critical points by applying Eq. (1) for both polymer a and b and the same displacer/solvent/substrate combination. For athermal solution behaviour Eq. (1) may be written as $\exp\left(\chi_s^{po} - \chi_{sc}\right) = \phi_{cr}\left(\exp\chi_s^{do} - 1\right) + 1 \cong \phi_{cr}\exp\chi_s^{do} + 1$,

where the last approximation is valid for strong displacers (high χ_s^{do}). Hence,

$$\chi_s^{ab} = \ln\left(\phi_{cr}^a \exp(\chi_s^{do}) + 1\right) - \ln\left(\phi_{cr}^b \exp(\chi_s^{do}) + 1\right) + \chi_{sc}^a - \chi_{sc}^b \tag{8}$$

Two more simplifications are possible. Firstly, in terms of a lattice model (where the rotational entropy is disregarded), χ_{sc} depends only on lattice coordination numbers. Hence, χ_{sc} parameters of different polymers can be taken equal so that the critical adsorption energy terms in Eq. (8) cancel. (In reality differences between the χ_{sc} values for various polymers may arise due to variations in chain stiffness. The lattice model does not account for such an effect.)

Secondly, for not too small χ_s^{ao} and χ_s^{bo} values the terms $\phi_{cr}^a \exp\left(\chi_s^{do}\right)$ and $\phi_{cr}^b \exp\left(\chi_s^{do}\right)$, respectively, are much larger than unity. In such cases, the terms $+1$ in the logarithmic terms of Eq. (8) may be omitted. As a result, the expression for χ_s^{ab} becomes very simple:

$$\chi_s^{ab} = \ln\left(\phi_{cr}^a / \phi_{cr}^b\right) \tag{9}$$

Hence, χ_s^{ab} may be found from the ratio between critical points, regardless of the displacer used, provided that the individual χ_s values with respect to the solvent are large enough. The effect of the omission of solute/solvent interactions on the determination of χ_s is usually relatively small. We have already shown this for PS on silica.[4] The above assumptions of athermal solvent behaviour and $\chi_{sc}^a = \chi_{sc}^b$ lead probably to less significant errors than the description of the solution by a lattice in which sites are occupied by either one solvent molecule, one displacer molecule, or one polymer segment. The parameter χ_s^{ab} as given by Eq. (9) is equal to the difference between the chemical potential of the displacer in the critical solvent mixture for polymer a and for polymer b, under ideal conditions. Hence, for a polymer which is more strongly adsorbed more chemical energy, substantiated by the amount of displacer, has to be added to the system for complete displacement of the polymer.

For PS we have determined the effective segmental adsorption energy χ_s^{po} using the solvent strength concept.[4] The value obtained

can be used to transform polymer adsorption energies relative to PS into adsorption energies relative to the solvent, using Eqs. (7)-(9).

In the same way as adsorption energies for one polymer can serve as a standard for another, polymer adsorption energies can also be used to determine displacer adsorption energies χ_s^{do}. Adsorption energies of displacers (notably those for which no solvent strength is tabulated) can be calculated from critical points with the help of either Eq. (1) or (2) provided the χ_s^{po} value for the polymer in question is known. Hence, both polymers and displacers can be classified according to their adsorption strength by the method given above.

6.2.2. Thermodynamic work of adhesion

So far, we expressed the adhesion strength of polymers as the segmental adsorption energy relative to that of a solvent molecule, i.e., the interaction energy difference between a polymer/surface and a solvent/surface contact. The segmental adsorption energy is a *reversible* measure for the adhesion strength.

In macroscopic adhesion strength experiments the interaction energy is found as the *work* per unit of surface area needed to disrupt a polymer/substrate joint, i.e., to replace a polymer/substrate interface by an air/substrate plus a polymer/air interface. This work of adhesion is determined in an *irreversible* way because energy dissipation takes place during the disruption process.

In this section we want to convert molecular adsorption energies (χ_s) into the *reversible* work of adhesion with respect to vacuum rather than solvent. The work of adhesion obtained from segmental adsorption energies is a *thermodynamic* (intrinsic) quantity.

Intermolecular surface forces may be decomposed into two categories: dispersive (D) interactions and specific (SP) interactions. Dispersive interactions are always present and may be split up into a long range term (DL) and a short range term (DS). The short range interactions extend only to the first monolayer, the long range term accounts for forces acting over more than one layer.

The specific interactions, such as hydrogen bonding and polar forces, occur only if the interacting species contain specific groups. This type of interactions may be regarded as short range.

Assuming a simple additivity rule, the intrinsic work of adhesion W_{so} of a liquid (o) on a solid (s) in terms of the interaction types discussed above is given by

$$W_{so} = W_{so}^{DL} + W_{so}^{DS} + W_{so}^{SP} \tag{10}$$

The dispersion contribution W_{so}^{D} ($= W_{so}^{DS} + W_{so}^{DL}$) may be approximated as twice the geometric mean of the dispersion force components of the surface tensions γ^{D} of each of the participating species[9]:

$$W_{so}^{D} = 2\left(\gamma_s^{D} \gamma_o^{D}\right)^{\frac{1}{2}} \tag{11}$$

Fowkes[1,10] claims that the specific contribution W_{so}^{SP} can be described entirely by acid-base (AB) interactions. Acid-base interaction energies may be predicted by several semi-empirical models. Fowkes uses the model of Drago et al.[11] These authors have correlated the enthalpy of acid-base interactions ΔH^{AB} to two constants (C_B, E_B) for the base and two constants (C_A, E_A) for the acid: $-\Delta H^{AB} = C_A C_B + E_A E_B$. This formula is known as the Drago equation. The products $C_A C_B$ and $E_A E_B$ represent the covalent (C) and electrostatic (E) character of the acid-base interaction, respectively. For various compounds the constants E and C are tabulated in the literature.[12] Molar enthalpies of many acid-base pair interactions can then be estimated from the Drago equation.

The analogon of Eq. (10) for the reversible work of adhesion between a polymer (p) and a solid (s) is

$$W_{sp} = W_{sp}^{DL} + W_{sp}^{DS} + W_{sp}^{SP} \tag{12}$$

Subtracting Eq. (10) from Eq. (12) gives

$$W_{sp} - W_{so} = W_{sp}^{DL} - W_{so}^{DL} + \left(W_{sp}^{DS} + W_{sp}^{SP}\right) - \left(W_{so}^{DS} + W_{so}^{SP}\right) \tag{13}$$

The short range interaction energy of a polymer with a substrate minus that of a solvent with the same substrate (i.e., the terms in between the brackets in Eq. (13)) can directly be related to χ_s^{po} because this parameter accounts precisely for the short range interactions with the substrate. The value of χ_s^{po} divided by the surface area A of one monomer unit gives the difference in the free energy of interaction per unit of surface area. Hence, the last four terms in the right-hand side of Eq. (13) may be replaced by $\chi_s^{po}kT/A$.

Assuming the long range dispersive interaction energy difference between a polymer/surface and a solvent/surface contact is not significant, the term $W_{sp}^{DL} - W_{so}^{DL}$ in Eq. (13) may be neglected.

For solvents with no specific groups, the term W_{so} in the left-hand side of Eq. (13) is equal to W_{so}^{D} and may then be substituted by $2\left(\gamma_s^D \gamma_o^D\right)^{1/2}$ (Eq. (11)). Equation (13) can now be rewritten as

$$W_{sp} = 2\left(\gamma_s^D \gamma_o^D\right)^{1/2} + \chi_s^{po}kT/A \qquad (14)$$

Hence, the reversible work of adhesion of a polymer on a substrate may be estimated if an apolar solvent ($\gamma_o \approx \gamma_o^D$) is used which does not have specific interactions with the surface ($W_{so} \approx W_{so}^{D}$). This work is then obtained from χ_s^{po} as measured by displacement, the solvent surface tension γ_o, and the dispersion contribution γ_s^D of the surface free energy of the substrate.

In solution, the dispersive interaction energy (long range plus short range) difference between polymer segments with the substrate and solvent molecules with the substrate is in most cases very small. Hence, the energy difference between a polymer/surface and a solvent/surface contact, represented by χ_s^{po}, is mainly determined by the difference in specific interaction energy. For solvents with no specific interactions, χ_s^{po} may be approximated as the specific interaction energy of a polymer segment with the surface.
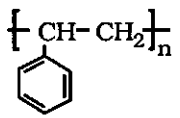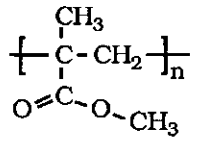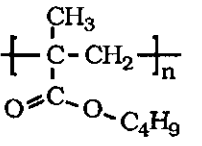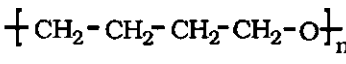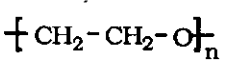
The procedure given above is of course somewhat rough. For instance, all functional groups which have contact with the surface

are assumed to have the same adsorption energy. In practice, there may be different types of surface sites. Moreover, it is likely that on a fully covered surface not all segments can assume an optimal orientation towards the surface sites.

6.3. Experimental

The polymers used in this study were polystyrene (PS), poly(methyl methacrylate) (PMMA), poly(butyl methacrylate) (PBMA), poly(tetrahydrofuran) (PTHF), and poly(ethylene oxide). Three different functional groups occur in these polymers, i.e., a phenyl (PS), an ester (PBMA, PMMA), and an ether group (PTHF, PEO). The particular samples and the chemical structure of the polymers are given in Table 1. We have chosen polymers with a molecular weight of about 100 kg/mol for the following reasons. The retention behaviour of polymers with $M_w > 10 kg/mol$ on thin layer plates is known to depend little on the molecular weight.[13] However, for very high molecular weight polymers ($M_w > 1000$ kg/mol) the kinetics for polymer exchange between the stationary and the mobile phase may become too slow. The obtained retention factor is then not only a function of thermodynamic quantities. Another consequence of slow exchange kinetics between the different phases is that in the case of desorption the size of the final spot becomes larger. As an illustration, Figure 1 shows final spots of different molecular weight PS samples eluted on alumina with pure toluene (which is a displacer for PS). The elution time for all samples was about half an hour. As can be seen in this figure, the polymer moves with the eluent front. The final spot size for the samples with a molecular weight of 9 and 120 kg/mol is relatively small, whereas the size of the spot for $M_w = 3000$ kg/mol is rather big. For the highest molecular weight sample the exchange kinetics of polymer between the mobile and stationary phase becomes too slow, so that part of the polymer lags behind. The polymer is then distributed over a considerable area.

Table 1. *Polymer samples*

sample	structure	M_w (kg / mol)	$\dfrac{M_w}{M_n}$
Polystyrene (Polymer Laboratories)	$\left[\text{CH}-\text{CH}_2\right]_n$ with phenyl group	120	1.03
Poly(methyl-methacrylate) (Aldrich)	$\left[\overset{\text{CH}_3}{\underset{\underset{\text{O}=\text{C}-\text{O}-\text{CH}_3}{|}}{\text{C}}}-\text{CH}_2\right]_n$	90	2.0
Poly(butyl-methacrylate) (Aldrich)	$\left[\overset{\text{CH}_3}{\underset{\underset{\text{O}=\text{C}-\text{O}-\text{C}_4\text{H}_9}{|}}{\text{C}}}-\text{CH}_2\right]_n$	240	2.5
Poly(tetrahydrofuran) (Polymer Laboratories)	$\left[\text{CH}_2-\text{CH}_2-\text{CH}_2-\text{CH}_2-\text{O}\right]_n$	258	1.13
Poly(ethylene oxide) (Polymer Laboratories)	$\left[\text{CH}_2-\text{CH}_2-\text{O}\right]_n$	246	1.09

The retention behaviour of different polymers on a thin layer plate was recorded as a function of binary eluent (*displacer/solvent*) composition. For all experiments we used carbon tetrachloride as the *solvent*. The displacers have to be chosen carefully because the polymer in question must be soluble in each of the eluent mixtures and the displacer has to be strong enough to desorb this polymer. In total we used 16 displacers with different displacement strengths. All displacers and the solvent carbon tetrachloride were of analytical grade. Some displacers contain stabilizing agents. Such additives have to removed if the displacer is weak and the additive adsorbs strongly (e.g., ethanol in chloroform). Although the concentration of

such an additive is usually very low, it may be responsible for polymer desorption instead of the displacer itself.[4]
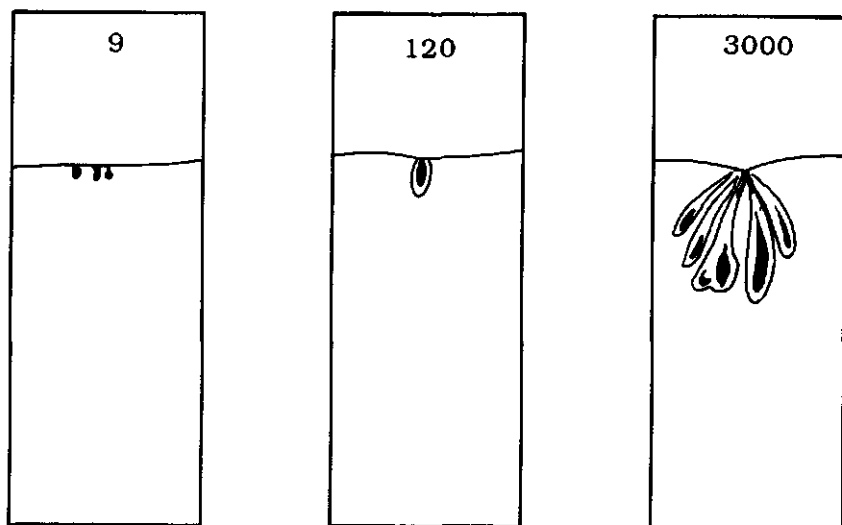
Figure 1. *Final spots of monodisperse polystyrene on an alumina thin layer developed by the displacer toluene, for polymer samples of three different molecular weights. The molecular weights (kg / mol) a r e indicated in the chromatograms.*

The thin layer chromatoplates used were plastic sheets with either a silica layer (Kieselgel 60 F_{254}, Merck) or an aluminium oxide layer (type 60 F_{254}, Merck) of 0.2 *mm* thickness. Before use, the plates were dried in a oven at 120 °C for about 16 *h*. Spots of polymer were brought upon the thin layer, about 2 *cm* from the bottom line of the plate, by evaporating a few droplets of polymer solution with a concentration of 4000 ppm. The size of the spot depends on the solvent used for this deposition. When the solvent has a weaker interaction with the substrate than the polymer, the distribution of polymer within the circular spot has a Gaussian form.[14] When the solvent is a *displacer*, the deposited polymer will mostly be found at the periphery of the spot. Because a Gaussian distribution of the polymer is the most favourable one for determining the retention factor we used solvents from which the
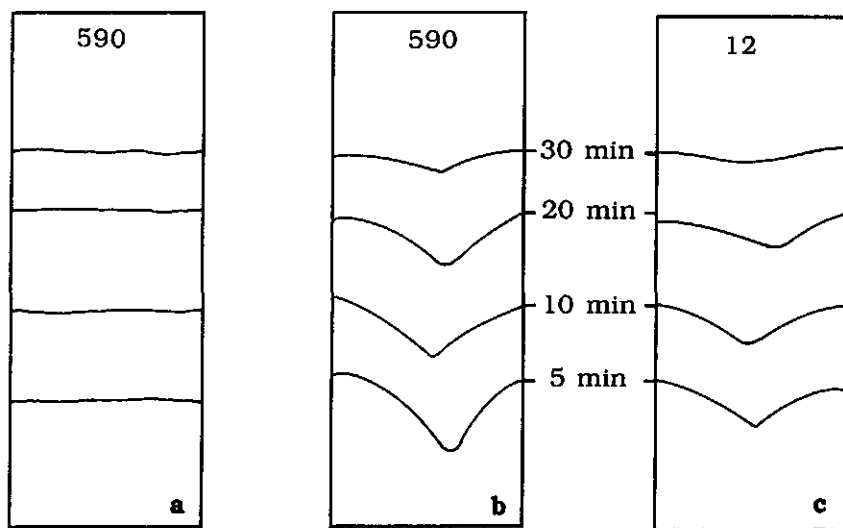
Figure 2. *Shapes of eluent fronts on alumina thin layers with monodisperse PMMA for different elution times, eluents, and molecular weights of PMMA. The molecular weights (kg / mol) and elution times are indicated in the figure. The eluents used are toluene, in which PMMA on the thin layer is immobile (a) and dioxane (where it is mobile) (b, c).*

polymer adsorbs on the thin layer. Prior to development, the plate was suspended just above the eluent with the appropriate composition in a closed thermostatted cylindrical vessel for 45 minutes. This ensures equilibrium between the liquid phase, the vapour phase, and the adsorbed phase, and prevents solvent demixing on the thin layer during the development. The upward elution is then started by lowering the plate just into the eluent. All experiments were carried out at 35 °C. After elution the eluent front on the thin layer was marked before the plate was dried. The shape of this front gives already an indication whether the polymer is displaced or not. Figure 2 shows examples of eluent fronts for PMMA eluted on alumina with either pure dioxane (displacer, middle and right) or toluene (solvent, left). For toluene, in which the polymer is immobile, the boundary is a straight line. In the case of dioxane, this

front shows a dip at the position of the polymer spot. This dip becomes smaller for lower molecular weight polymers and longer elution times. The appearance of this dip signals a reduction of the elution rate and can be explained by an increase in viscosity due to polymer dissolved in the mobile phase. Besides this direct indication for complete polymer desorption we used the following methods to visualize polymer spots: fluorescence quenching, iodine vapour, and wetting.

The fluorescence quenching method is especially suitable for localizing polystyrene spots. This method can only be used for polymers which absorb ultraviolet light.

Exposure of thin layer plates to iodine vapour is a more general staining method. Almost all polymers except those which have a very low polarity form complexes with iodine, giving dark brown spots.

The wetting method can be applied to hydrophobic polymers on hydrophylic thin layers like silica and alumina. Spraying the thin layer plate with water wets the whole plate except the polymer spot, which then shows up as a bright patch because it scatters more light than the wet parts.

6.4. Adsorption mechanisms

6.4.1. Silica surface

The silica surface has an acidic character $(pH^0 = 2-3)$.[15] This character may vary somewhat due to variations in the number of silanol groups on the surface, the surface regularity, and crystallinity. Basic functional groups adsorb onto the hydroxyl groups of silica by acid-base interaction. The π-electrons of aromatic molecules and the lone electron pairs of basic molecules interact with the protons of the silanol groups (hydrogen bonding). Infrared studies show that the frequency of silanol vibrations changes upon adsorption of basic molecules on silica.[16] Kawaguchi et al.[17] and several other investigators[18-20] were able to determine the fraction of occupied silanol groups by PS or other polymer chains from the intensity ratio of perturbed and unperturbed OH-vibrations.

The *activity* of silica surfaces shows a maximum as a function of the activation temperature (from 25 to 1000 °C), which also proves that the hydroxyls are the active surface sites.[6] The adsorbent activity is first increased due to a reduction of physically adsorbed water, which liberates hydroxyl groups on the surface. For high temperatures the activity decreases because the number of surface hydroxyl groups reduces due to condensation reactions.

We have to note that there are different types of silanol groups present on a silica surface (isolated, vicinal, and geminal hydroxyls) with different adsorption strengths. Not only the total amount of silanol groups diminishes upon heating but also the relative proportions of the different groups change.[21,22]

6.4.2. Alumina surface

Alumina exists in many different crystal forms. The alumina surface has both acidic and basic groups. We consider only the acidic sites because the polymers we used have basic functional groups. The hydroxyls on the alumina surface are not the only active sites for the adsorption of basic molecules as in the case of silica. Aluminium ions, which act as Lewis acid sites, may also bind basic molecules. The aluminium ions are not found in the top layer but may be exposed by vacancies in the surface layer consisting of oxygen and hydroxyl ions.[23,24] There are different Lewis acid sites with varying acidity due to the existence of different kinds of vacancies. Vacancies may differ with respect to size and nearest neighbour configuration. Vacancies in the top layer are formed as the temperature is increased due to surface dehydroxylation. Hence, the amount of hydroxyl groups decreases and the number of Lewis acid sites increases with increasing activation temperature. Not only the number but also the strength of the Lewis acid sites may be increased by heating. Snyder[6] has measured the activity of alumina as a function of temperature with aromatic probe molecules. The activity appears to increase continuously with increasing temperature, indicating that the Lewis acid sites are the most active binding sites for basic molecules. The relative binding strength and concentration of different adsorption sites on solids are usually

probed by Infrared Spectroscopy.[25,26] Acidic surface sites are frequently characterized by pyridine adsorption because this substance is a very strong base.[24,27,28] Infrared spectra of adsorbed pyridine give a clear distinction between molecules bound on hydroxyls and on Lewis acid sites. Healy *et al.*[29] have studied the adsorption of pyridine and other strong bases on different kinds of alumina. The following results of this study indicate that the Lewis acid sites are indeed the most strongly binding sites for basic molecules:

- The shift of a particular absorption band of pyridine upon adsorption on Lewis acid sites is larger than on hydroxyls.
- The adsorption of pyridine on Lewis acid sites have a more pronounced high affinity character than of pyridine which binds only via hydrogen bonding.
- The ratio of Lewis acid coordination to hydrogen-bonded complexes increases with decreasing pyridine vapour pressure.
- The percentage of pyridine molecules left on the surface upon increasing temperature is much larger for molecules adsorbed on aluminium ions than on hydroxyls.

6.4.3. Adsorption of phenyl groups on inorganic solids

Aromatic molecules tend to adsorb in a flat conformation on active surface sites of inorganic solids.[30] The solvent strength concept of Snyder predicts retention values of many aromatic compounds on alumina and silica only correctly if a value for the surface area of the adsorbate is used which corresponds to flat adsorption.[6,31] Aromatic molecules with strongly adsorbing substituents, such as phenols, may, however, adsorb in a vertical orientation.[32-34]

Nagao *et al.*[35] have studied the adsorption of benzene, toluene, and chlorobenzene on hydroxylated and dehydroxylated titanium oxide (rutile). From IR measurements they concluded that on a dehydroxylated surface these aromatic molecules were adsorbed as Lewis acid-base complexes with the titanium ions, whereas on a hydroxylated surface adsorption was due to interaction with hydroxyl groups. The occupied area for a benzene molecule on a dehydroxylated surface obtained from the monolayer capacity was

0.55 nm^2. This value is somewhat higher than the cross sectional area of benzene (0.43 nm^2) which supports the idea that the molecules have a flat orientation on the surface. The fraction of covered surface area as calculated from the adsorbed amount and the cross sectional area per molecule is about 0.78. For a fully hydroxylated surface this fraction appears to be about 0.95. Hence, benzene covers a hydroxylated rutile surface more effectively than a dehydroxylated one. The same conclusion can be drawn for the adsorbates toluene and chlorobenzene.

The observed difference in adsorption onto hydroxylated and dehydroxylated rutile surfaces can be explained by different active site densities. However, also the fact that Lewis acid sites have more rigidly fixed positions on the surface than protons taking part in hydrogen bonding may explain this observation. Steric hindrance between adsorbate molecules in the surface layer becomes more important as the adsorbed amount increases. This increased hindrance will lead to less optimal orientations for adsorbate molecules on Lewis acid sites, which reduces the affinity for adsorption. Hydroxyl groups, however, have the ability to rotate, and may therefore adjust their direction to the adsorbing groups for optimal interactions. Hence, the adsorption energy is less affected by steric hindrance between adsorbate molecules than in the case of adsorption onto Lewis acid sites. The surface layer can now be packed more densely without loosing much adsorption energy per molecule. Phenyl groups may even adsorb in a moderately tilted orientation on hydroxyls and still have efficient interaction. Several orientations of adsorbed benzene molecules on hydroxyl groups with equal interaction energy are schematically shown in Figure 3a. Figure 3b shows the only favourable conformation of a benzene molecule on a Lewis acid site. Figures 3a and 3b also show that for a same distribution of active sites more benzene molecules may be adsorbed on the hydroxylated than on the dehydroxylated titanium oxide surface.

Adsorption of basic functional groups on silica only takes place onto hydroxyl groups. Hence, the silica surface may, in this respect, be compared to a hydroxylated titanium oxide surface.

3a

3b
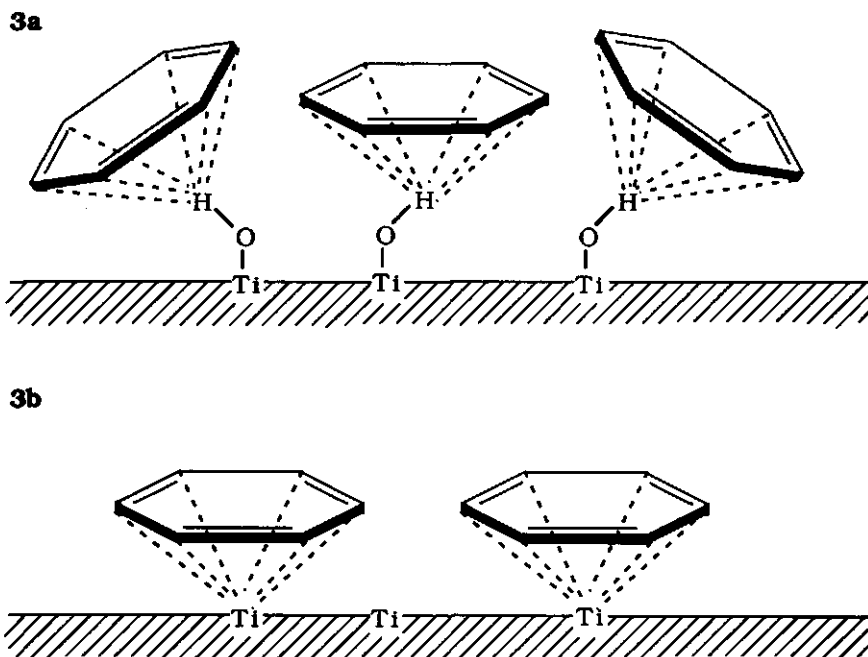
Figure 3. *Possible conformations of benzene molecules adsorbed on hydroxyl groups (a) and on a Lewis acid sites (b) of titanium oxide.*

For an alumina surface with both alanol groups and exposed aluminium ions on the surface, adsorption of basic functional groups takes place on both types of active sites. In this case, the surface takes an intermediate position between a fully hydroxylated and dehydroxylated rutile surface.

6.5. Results and discussion

6.5.1. Segmental adsorption energy for PS

In chapter 2 we already discussed the adsorption energy of PS on silica relative to cyclohexane and carbon tetrachloride, respectively, measured at a temperature of 25 °C. The data for PS in carbon tetrachloride from this study are included in Table 2. This table

gives critical points for the displacement of PS from both silica and alumina in carbon tetrachloride by various displacers. We checked that a temperature difference of 10 °C did not affect the critical displacer concentration. By way of example, retention curves of PS on alumina and silica are shown in Figure 4, for the aromatic
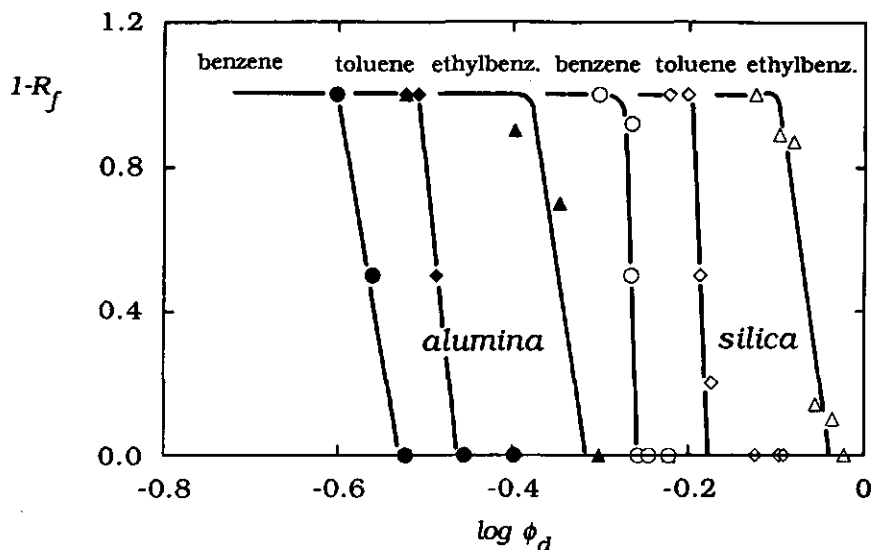
Figure 4. *Retention* $(1 - R_f)$ *of PS on silica (open symbols) and alumina (filled symbols) in carbon tetrachloride/displacer mixtures as a function of the logarithm of the volume fraction of three displacers: ethyl benzene (triangles), toluene (squares), and benzene (circles).*

displacers benzene, toluene, and ethyl benzene. The transition between complete retention $(1 - R_f = 1)$ and no retention $(1 - R_f = 0)$ of the polymer on the thin layer is in all cases very sharp. Small changes in the molecular structure of the displacer give a distinctly different retention curve. Hence, TLC is a very sensitive method to determine critical points.

Table 2 and Figure 4 show that PS is displaced easier from alumina than from silica by nearly all displacers used in this study. Only ethyl ether and isopropyl ether have about the same critical points on both substrates. The order of displacement strengths (as

measured by the critical volume fraction) is the same on both substrates, for all displacers used.

Table 2. *Critical points ϕ_{cr} for PS on silica and alumina in carbon tetrachloride*

displacer	silica	alumina
ethyl benzene	0.92	0.48
toluene	0.68	0.33
chloroform	0.68	0.22
benzene	0.55	0.28
methylene chloride	0.35	0.18
1,2-dichloroethane	0.33	0.13
isopropyl ether	0.026	0.027
ethyl ether	0.019	0.021
dioxane	0.028	0.014
isopropyl acetate	0.027	0.012
tetrahydrofuran	0.015	0.011
ethyl acetate	0.017	0.009
acetonitrile	0.012	0.008
acetone	0.008	0.005

Ethyl benzene, which is the weakest displacer, may be considered as the monomer unit of PS. In this case we may, as a first approximation, assume $\chi_s^{do} = \chi_s^{po}$. Then Eq. (2), which applies only if χ_s^{do} is high enough, could be used to estimate χ_{sc}; the precise value of χ_s^{do} is then irrelevant. If χ_s^{do} is small, the full Eq. (1) has to be used, for which the value for χ_s^{do} is needed.

An estimate for χ_s^{do} can be obtained by using Eq. (3). Solvent strengths and areas per molecule of various displacers and carbon tetrachloride on both silica and alumina are given in Table 3. Because of the assumption made in the model of Cohen Stuart *et al.*[2] that the size of a displacer molecule, a solvent molecule, and a polymer segment are equal we use a value for A which is the average of A_o, A_d, and A_p for the calculation of χ_s^{po}, χ_s^{pd}, and χ_s^{do}. The contact area A_p of a PS segment is, according to Glöckner,[36] equal

to 0.57 nm^2. The activity α' of the adsorbent, which is also needed for the calculation of the adsorption energy, was determined according to Snyder's method. This quantity appeared to be 11.1 nm^{-2} for the alumina we used. For silica we already determined this parameter in our previous work,[4] and found 17.6 nm^{-2}. Average A values and the calculated χ_s^{do} for various displacers in PS/carbon tetrachloride systems are given in Table 4.

Table 3. *Solvent strengths ε and molecular areas A of solvents and displacers*[7]

solvent (o)/displacer (d)	$\varepsilon_o, \varepsilon_d$		A_o, A_d
	silica	alumina	(nm^2)
carbon tetrachloride (o)	0.11	0.17	0.43
toluene (d)	0.22	0.30	0.58
benzene (d)	0.25	0.32	0.51
chloroform (d)	0.26	0.36	0.43
methylene chloride (d)	0.30	0.40	0.35

The value of χ_s^{do} for ethyl benzene with respect to carbon tetrachloride on silica and alumina can not be calculated directly from Eq. (3) because Snyder does not give solvent strengths of ethyl benzene. However, the χ_s^{do} values of ethyl benzene are certainly not higher than those of toluene, which are 1.0 and 0.76 on silica and alumina, respectively. Hence, χ_s^{do} for ethyl benzene is too small to justify the use of Eq. (2).

The χ_s^{do} parameters for ethyl benzene may be estimated from χ_s^{do} as found for toluene and benzene. This estimate is based on the assumption that each additional methylene group gives the same increment to χ_s^{do}. Using χ_s^{do} for toluene and benzene as given in Table 4, we find values of χ_s^{do} for ethyl benzene of 0.8 and 0.7 on silica and alumina, respectively.

In order to calculate χ_{sc} from the full Eq. (1), we need the solvency parameters χ^{pd}, χ^{po}, and χ^{do}. The χ values for PS-ethyl benzene and PS-carbon tetrachloride interactions are given in Table

5. For the interaction between ethyl benzene and carbon tetrachloride we have taken the same χ^{do} as for toluene and carbon tetrachloride (i.e., -0.05). This last assumption does certainly not lead to serious errors because a change of less than 0.2 in χ^{do} has no significant effect on the calculated χ_{sc}. The term $\lambda_1 \chi^{pd}$ constitutes the most important correction. The critical adsorption energies are found as 0.2 and 0.4 for silica and alumina, respectively. Note that the athermal version of Eq. (1), neglecting all solvency effects, would have given χ_{sc} as 0.05 for silica and 0.3 for alumina. Apparently, the solvency correction increases χ_{sc} by about 0.1.

Table 4. *Average molecular areas* $\overline{A}$ *and* χ_s^{do} *values of various displacers in PS/carbon tetrachloride systems with either silica or alumina*

displacer	$\overline{A} / nm^2$	χ_s^{do}	
		silica	alumina
methylene chloride	0.45	1.50	1.15
benzene	0.50	1.23	0.83
toluene	0.53	1.03	0.76
chloroform	0.47	1.24	0.99

The obtained χ_{sc} values for PS are comparable to the theoretical prediction of 0.288 for a hexagonal lattice. It is remarkable that χ_{sc} for PS on alumina is somewhat different from that on silica. Theoretically, χ_{sc} does not depend on the type of substrate, because rotational entropy effects are neglected in the lattice model. The reason for the difference in the experimental χ_{sc} may perhaps be found in the adsorption mechanism. Polystyrene adsorbs on alumina by interaction of the phenyl groups with both hydroxyl groups and Lewis acid sites. The phenyl groups attached to the polymer chain may have less possibilities for optimal orientation towards the Lewis acid sites than adsorbed ethyl benzene molecules. Polystyrene segments may therefore have a lower adsorption energy on these sites than the detached monomers. Hence, the assumption $\chi_s^{po} = \chi_s^{do}$ which was made for the determination of χ_{sc} is perhaps not valid in

this case. When χ_s^{po} is smaller than χ_s^{do} the value for χ_{sc} calculated in the way described above is too high. For PS adsorption on hydroxyls of an alumina or silica surface the effect of the internal sterical hindrance of the polymer chain is partly compensated by the rotational mobility of the active hydroxyl groups. Because the silanols are the only active sites on a silica surface the determination of χ_{sc} based on the assumption that $\chi_s^{po} = \chi_s^{do}$ is still tenable for this substrate, and $\chi_{sc} = 0.2$ is a reasonable estimate for this case.

Since the value 0.4 obtained for alumina is less reliable, we assume $\chi_{sc} = 0.2$ also for PS on alumina. Anyhow, in the determination of χ_s^{po} the χ_{sc}-term usually constitutes only a small correction.

Table 5. *Flory-Huggins interaction parameters*

component a	component b	χ^{ab}	ref
carbon tetrachloride	toluene	-0.05	37
	benzene	0.19	38
	PS	0.396	39
polystyrene	toluene	0.432	39
	benzene	0.438	39
	ethyl benzene	0.45	40, 41

We are now in the position to calculate χ_s^{po} from critical points. To that end, we used Eqs. (5) and (6) and the solvent strengths given in Table 3, for the displacers methylene chloride, benzene, toluene, and chloroform. Chloroform is a relatively acidic displacer which can have specific interactions with PS. This means that desorption of polymer may also occur due "inactivation" of the polymer, i.e., the specific interaction between polymer and displacer could be stronger than that between polymer and substrate. This desorption mechanism may affect or even determine polymer displacement. However, this displacer gave the same χ_s^{po} for PS on silica as the other displacers, indicating that specific interactions between chloroform and PS do not significantly affect the results.

For each displacer we calculated ε_{cr} from Eq. (5) and the athermal χ_s^{po} from Eq. (4), for PS adsorbing from carbon tetrachloride on alumina. Results are given in Table 6. For benzene and toluene, for which the solvency parameters are known, we calculated also the non-athermal χ_s^{po} value from Eq. (6). The Flory-Huggins parameters needed for this calculation are given in Table 5. For comparison, we also inserted in Table 6 the energy parameters for polystyrene adsorption on silica from our previous work.[4]

Table 6. *Critical solvent strengths ε_{cr} and χ_s^{po} values for PS on silica and alumina*

	silica			alumina		
displacer	ε_{cr}	χ_s^{po}		ε_{cr}	χ_s^{po}	
		(1)	(2)		(1)	(2)
methylene chl.	0.23	-	1.1	0.23	-	0.49
benzene	0.21	1.0	1.1	0.23	0.53	0.51
toluene	0.20	0.9	1.0	0.23	0.41	0.53
chloroform	0.23	-	1.2	0.23	-	0.51

(1) calculated by Eq. (6), χ values taken into account.
(2) calculated by Eq. (4), athermal solvent behaviour assumed.

The χ_s^{po} values for PS on silica and alumina, determined with the different displacers, agree very well with each other, which supports the consistency of the procedure. For alumina, the average non-athermal and athermal χ_s^{po} values for PS from carbon tetrachloride are 0.47 and 0.51, respectively. The difference is small and not very significant, just as in the case of silica. Apparently, the solvency correction is relatively unimportant in these cases. Comparison between the data for silica and alumina leads to the conclusion that the segmental adsorption energy of PS on silica is higher by an amount of about 0.5 kT.

In Table 4 it can be seen that the (athermal) adsorption energies of small molecules with a phenyl ring are also higher on silica than on alumina. For benzene and toluene we find differences of 0.40 and 0.27 kT, respectively, between silica and alumina. These differences

are, however, smaller than those obtained for PS. The adsorption energy for PS on alumina is lower than on silica for two reasons: a smaller interaction energy with the active surface sites and a less effective contact between the phenyl groups and the surface due to their restricted orientational freedom. For the small molecules, only the former effect plays a role.

Kawaguchi et al.[42,43] have also published data for PS displacement from silica into carbon tetrachloride. The critical adsorption energy for PS obtained by these authors is 0.5 which differs significantly from our value. We note that the value for χ_{sc} from Kawaguchi et al. is questionable for several reasons. Firstly, they assumed benzene to behave as the monomer unit of PS. As can be seen from our results, the critical points of benzene and ethyl benzene, which we take as the monomer unit of PS, differ significantly. Secondly, they used Eq. (2) for the calculation of χ_{sc}. As discussed above, this equation is not valid for low χ_s^{po} and χ_s^{do} values and can therefore not be used for PS/carbon tetrachloride systems. Finally, their solvency correction term $\lambda_1 \chi^{pd}$ has the wrong sign. Apart from this erroneous χ_{sc}, Kawaguchi et al.[42,43] report several χ_s values which are also incorrect because of their using Eq. (2) where this is not allowed.

6.5.2. Adsorption energies for other polymers and displacers

Figure 5 shows the displacement of PS, PBMA, PTHF, PMMA, and PEO from alumina by dioxane in a carbon tetrachloride/dioxane solvent mixture. This figure gives already an indication of the adsorption energies of the different polymers. For instance, PBMA can be entirely displaced at a much lower dioxane concentration than needed for PEO. Hence, PBMA on alumina has a smaller adsorption energy than PEO. Table 7 gives the critical points of the given polymers on both silica and alumina for various displacers. The dashes in the table represent systems where either the polymer cannot be desorbed by the particular displacer or the polymer does not dissolve in the displacer/solvent mixture with the critical composition. The descending order of the displacers in this table corresponds to an increasing displacement strength for most polymers. This order agrees very well for the different substrates.
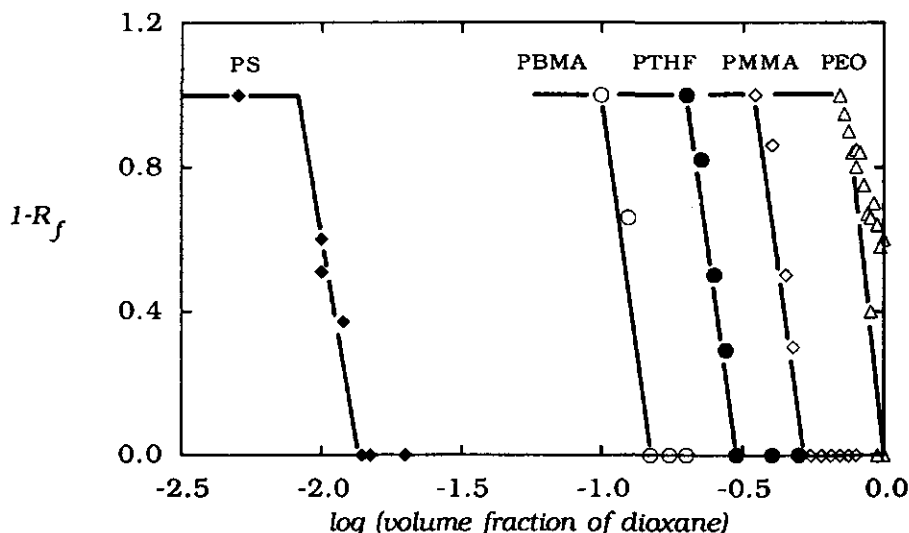
Figure 5. *Retention* $(1 - R_f)$ *of five polymers on an alumina thin layer in carbon tetrachloride/dioxane mixtures, as a function of the logarithm of the volume fraction of dioxane.*

A remarkable finding is that we were not able to displace PTHF from silica by acetonitrile whereas this could be done at low volume fractions of acetonitrile from alumina. Acetonitrile is a non-solvent for PTHF. Higher concentrations of acetonitrile reduce the solubility of this polymer in the solvent mixture. Poly(tetrahydrofuran) does not dissolve any more in the solvent mixture with an acetonitrile concentration which would be needed for total displacement of PTHF from silica. This is the reason why PTHF is easily displaced by acetonitrile from alumina but not at all from silica. The critical points for the other displacers in Table 7 are smaller for PTHF on silica than for PTHF on alumina.

Most of the displacers given in Table 7 have only basic characteristics just as the polymers. Only acetone and acetonitrile are exceptions. According to Fowkes[10] these displacers have also some acidic properties. Acetonitrile is, however, much more acidic than acetone. For displacers which are both acidic and basic care has to be taken in the interpretation of the results for the following reasons.

Table 7. *Critical points ϕ_{cr} for several polymer/displacer combinations on silica and alumina in carbon tetrachloride*

displacer	silica					alumina				
	PS	PBMA	PTHF	PMMA	PEO	PS	PBMA	PTHF	PMMA	PEO
ethyl ether	0.019	0.35	-	-	-	0.021	-	-	-	-
isopropyl acetate	0.027	0.24	-	-	-	0.012	0.34	0.57	-	-
ethyl acetate	0.017	0.18	-	0.85	-	0.009	0.22	0.37	-	-
tetrahydrofuran	0.015	0.11	0.35	0.53	-	0.011	0.19	0.38	0.75	-
acetone	0.008	0.10	0.28	0.39	-	0.005	0.12	0.33	0.58	-
dioxane	0.028	0.11	0.28	0.39	-	0.014	0.14	0.29	0.49	1.0
acetonitrile	0.012	0.12	-	0.32	-	0.008	0.09	0.12	0.34	-
pyridine		0.06	0.14	0.26	0.52		0.08	0.20	0.35	0.50

- Displacers with both acidic and basic groups can display significant self-association which may affect their displacement strength. This effect may have a greater influence on the critical point for one polymer than for another because self-association is concentration dependent. A measure for self-association is the acid-base contribution to the surface tension of a liquid. For acetonitrile 28% of the surface tension is considered to be due to acid-base interactions. In the case of acetone the acid-base contribution is only 4%.[10]
- Displacers with acidic characteristics may also change the desorption mechanism. Desorption caused by strong specific interactions of the displacer with the basic groups of the polymer may significantly contribute to the displacement of the polymer. The model used in this study does not apply for displacement due to specific interactions between polymer and displacer, since, at best, average interactions in solution are taken into account through the χ parameters.
- In the case of alumina and displacers with acidic properties, strong interaction between the basic surface sites and the acidic group of the displacer may be possible. Because of steric hindrance, displacer molecules on basic surface sites may reduce the accessibility of basic polymer groups to the acidic sites of the substrate.

Adsorption energy differences between polymers can be calculated from the critical points given in Table 7 by using either Eq. (8) or (9). The results are collected in Table 8. All the χ_s^{ab} values were calculated relative to PBMA adsorption. For the strongly adsorbing polymers PTHF, PMMA, and PEO the simple Eq. (9) could be used. The adsorption energy of PS relative to PBMA has to be calculated from Eq. (8) because the χ_s^{po} values for PS on both silica and alumina are too low to use Eq. (9). This implies that for this calculation χ_s^{do} values of the relevant displacers have to be known. Adsorption energies of displacers can be obtained from the critical points for PS and the adsorption energy of PS (Table 6) using the athermal version of Eq. (1). We did not correct for solvency effects because

Table 8. *Values for χ_s^{ab} of several polymers relative to PBMA, on both silica and alumina*

displacer	silica				alumina			
	PS	PTHF	PMMA	PEO	PS	PTHF	PMMA	PEO
ethyl ether	-2.4	-	-	-	-	-	-	-
isopropyl acetate	-1.7	-	-	-	-2.1	0.6	-	-
ethyl acetate	-1.9	-	1.6	-	-2.0	0.5	-	-
tetrahydrofuran	-1.6	1.2	1.6	-	-1.7	0.7	1.4	-
acetone	-2.1	1.0	1.4	-	-2.0	1.0	1.6	-
dioxane	-1.0	0.9	1.3	-	-1.3	0.7	1.3	2.0
acetonitrile	-1.8	-	1.0	-	-1.3	0.3	1.3	-
pyridine		0.9	1.5	2.2		0.9	1.5	1.8
average	**-1.8**	**1.0**	**1.4**	**2.2**	**-1.7**	**0.7**	**1.4**	**1.9**

not all relevant χ values are known and the corrections are usually small. The χ_s^{do} values calculated in this way are given in the columns designated "PS" in Table 10. The remainder of Table 10 will be discussed below.

Table 8 gives the χ_s^{ab} values calculated as described above for various polymer/displacer combinations on both silica and alumina. The variation in the values for the adsorption energy of a particular polymer calculated for the different displacers is very reasonable, in view of the assumptions made in the model applied here. The largest scatter is obtained for PS, which is because of the very small critical concentrations and the dependence of the results on the adsorption energy of displacers. In the last line of Table 8 we give the average adsorption energy determined for each polymer. These average values and χ_s^{po} for PS (see Table 6) were used to construct Figure 6, which is a diagram of the adsorption energies relative to carbon tetrachloride for the various polymers on both silica and alumina. Differences between polymer adsorption energies on silica and alumina can be clearly seen in this diagram.

The difference in adsorption energies for polymers with the same functional group but with different chain structure can be relatively large. The ether groups in the main chain of PEO and PTHF are separated by two and four methylene groups, respectively. Due to this difference in the chain, the χ_s^{po} value for PEO is 1.2 higher than for PTHF on both silica and alumina. The adsorption energy difference between the polymers with ester groups (PBMA and PMMA) is for both substrates equal to 1.4 kT. In the latter case, the backbone of the polymer chains is the same but the side groups are different. The butyl group linked to the ester group of PBMA is for PMMA replaced by a methyl group.

Hence, the functional (active) group of a polymer is not the only property to determine the adsorption energy, but the rest of the chain is also important in this respect. The results of Inagaki et al.[14,44] confirm this conclusion. These authors studied the separation and fractionation of polymeric substances and report the chromatographic behaviour of 10 different polymers, including five polymers with an ester group, on a silica thin layer using binary developers of 2-butanone and carbon tetrachloride with different
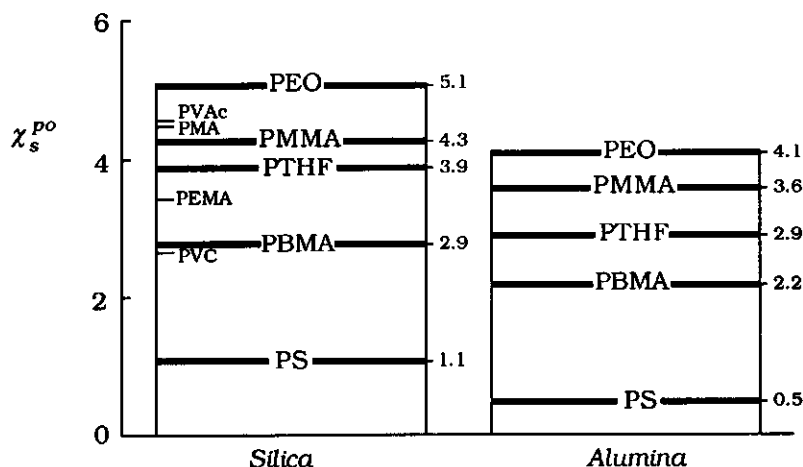
Figure 6. *Adsorption energies (χ_s^{po}) of polymers relative to carbon tetrachloride on both silica and alumina. The χ_s^{po} values of polymers indicated in small print were calculated from results reported by Inagaki et al.[14,44] The adsorption energies indicated by bold lines were determined in this work.*

compositions. In the study of Inagaki *et al.*, not critical volume fractions of 2-butanone but volume fractions at which polymer samples just start to migrate are given. The latter volume fractions are probably not much different from the critical points because transitions between complete polymer retention and no retention are very sharp (see Figures 4 and 5). The volume fraction data of Inagaki *et al.*[14,44] and the adsorption energies calculated from these values (using Eq. (9)) are given in Table 9. We could not give χ_s^{ab} for polybutene, poly(α-methylstyrene), and poly(p-chlorostyrene) because the χ_s^{po} values for these polymers are too low to use Eq. (9). Calculation of χ_s^{ab} by Eq. (8) is hampered by the fact that we do not know χ_s^{do} for 2-butanone on the silica sample used by Inagaki *et al.* For comparison, we have also determined the critical volume fraction of 2-butanone for PBMA and PMMA on our silica sample. These volume fractions and our average adsorption energy are given within brackets in Table 9. Qualitatively, the results of Inagaki agree

with our data, i.e., polyesters with larger alifatic groups have lower adsorption energies.

Table 9. *Critical 2-butanone volume fractions, taken from Inagaki,[14] for several polymers, and χ_s^{ab} values relative to PBMA*

polymer	ϕ_{cr}' [1]	χ_s^{ab} [2]
polybutene (PB)	0.00	-
poly(α-methylstyrene) (PMS)	0.02	-
poly(p-chlorostyrene) (PCS)	0.03	-
polystyrene (PS)	0.07	-
poly(vinyl chloride) (PVC)	0.19	-0.1
poly(butyl methacrylate) (PBMA)	0.21 (0.14)	0.0
poly(ethyl methacrylate) (PEMA)	0.38	0.6
poly(methyl methacrylate) (PMMA)	0.62 (0.58)	1.1 (1.4)
poly(methyl acrylate) (PMA)	0.77	1.3
poly(vinyl acetate) (PVAc)	0.86	1.4

[1] Volume fraction of displacer where polymer starts to migrate.
[2] Calculated from the first column with the help of Eq. (9).

The segmental adsorption energies for the polymers poly(vinyl chloride) (PVC), poly(ethyl methacrylate) (PEMA), poly (methyl acrylate) (PMA), and poly(vinyl acetate) (PVAc) on silica, which were calculated from Inagaki's results (Table 9) with the help of Eq. (7), are incorporated in Figure 6 (indicated in small print). The χ_s^{po} value of PMA and PVAc, as given in this figure, are not based on the segmental adsorption energy of PBMA, but on that of PMMA. PMA and PVAc have adsorption energies quite different from that of PBMA, but close to that of PMMA. Using χ_s^{po} of PMMA for the calculation of the adsorption energy for PMA and PVAc reduces the absolute error in the calculated values.

We have to note that the experimental conditions, such as temperature, molecular weights of the polymers, type of silica, and pre-treatment of the thin layer before development are not mentioned by Inagaki *et al.*[14,44] and were probably different from ours. Because Inagaki *et al.* carried out their displacement

experiments with only one displacer under unknown experimental conditions the polymer adsorption energies calculated from these data are only indicative.

In Figure 6 it can be seen that the polymer adsorption energies on silica are all larger than on alumina. The order of increasing adsorption strength is the same for both substrates. The adsorption energies of the polyesters (PBMA, PMMA) is $0.7kT$ larger on silica than on alumina. For the polyethers (PTHF, PEO) this energy difference is equal to $1kT$ which is the largest energy difference between adsorption on silica and alumina we have found. This relatively large interaction energy difference of ethers is confirmed by the displacement experiments of PS. The critical points for isopropyl ether and ethyl ether, respectively, were about the same for both substrates while we found for the other displacers a much lower critical volume fraction on alumina than on silica. The weaker a displacer is, the more of it has to be added to obtain the same displacement strength.

The large energy difference between ether groups on silica and alumina may reflect that OH groups are more accessible for ether groups than Lewis acid sites. Ether groups in the main chain of adsorbate molecules are less exposed than functional end groups and are therefore more sterically hindered to find optimal orientations on the substrate. This sterical hindrance will be more effective for Lewis acid sites than for hydroxyl groups, as explained earlier.

The diagram of Figure 6 can predict which polymers will and which will not adsorb on a substrate from a particular solvent when the adsorption energy of this solvent is inserted into the diagram. For instance, the adsorption energy of benzene calculated by Eq. (3) lies above the level of PS and below the levels of the other polymers. Hence, benzene is only a displacer for PS and not for the other polymers. On the other hand, the diagram may be indicative for the adsorption energy of a solvent when it is known which polymers can and which cannot be displaced by this solvent. Poly(ethylene oxide) adsorbs on silica from pure water.[45,46] Hence, the adsorption energy of water is probably smaller than that of PEO.

Adsorption energies of displacers can be determined from critical points and polymer adsorption energies with the help of either Eq.

Table 10. Values for χ_s^{do} of various displacers on both silica and alumina relative to carbon tetrachloride

displacer	silica						alumina					
	PS	PBMA	PTHF	PMMA	PEO	Av.	PS	PBMA	PTHF	PMMA	PEO	Av.
toluene	1.1	-	-	-	-	**1.1**	0.7	-	-	-	-	**0.7**
chloroform	1.1	-	-	-	-	**1.1**	1.0	-	-	-	-	**1.0**
benzene	1.3	-	-	-	-	**1.3**	0.8	-	-	-	-	**0.8**
methylene chloride	1.6	-	-	-	-	**1.6**	1.1	-	-	-	-	**1.1**
1,2-dichloroethane	1.7	-	-	-	-	**1.7**	1.3	-	-	-	-	**1.3**
isopropyl ether	4.0	-	-	-	-	**4.0**	2.6	-	-	-	-	**2.6**
ethyl ether	4.4	3.7	-	-	-	**4.1**	2.9	-	-	-	-	**2.9**
isopropyl acetate	4.0	4.1	-	-	-	**4.1**	3.4	3.1	3.3	-	-	**3.2**
ethyl acetate	4.5	4.4	-	4.3	-	**4.4**	3.7	3.5	3.7	-	-	**3.6**
tetrahydrofuran	4.6	4.9	4.7	4.7	-	**4.8**	3.5	3.7	3.7	3.7	-	**3.7**
acetone	5.2	5.0	5.0	5.0	-	**5.0**	4.3	4.1	3.8	3.9	-	**3.9**
dioxane	4.0	4.9	5.0	5.0	-	**5.0**	3.3	4.0	3.9	4.1	3.9	**4.0**
acetonitrile	4.8	4.8	-	5.2	-	**5.0**	3.8	4.4	4.8	4.5	-	**4.6**
pyridine		5.5	5.7	5.4	5.6	**5.6**		4.5	4.3	4.5	4.6	**4.5**

(1) or (2). The results for PS have already been discussed. For the other polymer/displacer systems Eq. (2) can be used to calculate these adsorption energies. We have neglected the solute/solvent interaction term of Eq. (2) for these calculations. Table 10 gives the χ_s^{do} values for all our displacer/substrate/polymer combinations. We have to note that the given values include, in principle, only the adsorption on acidic surface sites because we have only considered the displacement of basic polymers. The agreement between displacer adsorption energies determined using different polymers is very good except for some values obtained for PS. Most critical points for PS are very small and therefore less accurate.

We do not observe *localization effects* such as found by Snyder.[7,8] He claims that the solvent strength of a displacer may decrease as the concentration increases because more molecules become *delocalized* on the surface as the adsorbed amount increases. Our adsorption energies (solvent strengths in Snyder's terminology) of displacers become not consistently lower as the concentration of the displacer needed to fully desorb a particular polymer are higher (going from PS to PEO). Hence, solvent localization effects do not play a significant role for the given polymer displacement experiments. We also give in Table 10 the adsorption energies averaged over the values for the different polymers. We excluded for this averaging the χ_s^{do} values for strong displacers obtained with PS (i.e., from ethyl acetate to pyridine) because these values are less accurate.

For the calculation of the adsorption energy difference between PS and PBMA we used only the χ_s^{do} values obtained with PS. This energy difference remains the same when the average (more accurate) χ_s^{do} values are used. Hence, the χ_s^{po} values of the polymers PTHF, PMMA, and PEO, which are based on the χ_s^{po} of PBMA, do not need to be corrected.

It is remarkable that the trends between the different displacer adsorption energies are the same as those found for the polymers. All the displacers have a lower adsorption energy on alumina than on silica. The largest energy difference between adsorption on silica and alumina is again obtained for the ethers. Displacers with larger alkyl groups have smaller adsorption energies.

The displacers acetonitrile and chloroform have the smallest adsorption energy difference between silica and alumina. Acetonitrile is an even stronger displacer than pyridine on alumina, whereas the reverse is the case on silica. The same phenomenon is found for chloroform and benzene. It may be noted that chloroform and acetonitrile are the displacers with the most acidic character. Probably, the interaction between these displacers and basic surface sites on alumina indirectly increase their displacement strength for polymers on acidic surface sites. This may be explained by the steric hindrance of displacer molecules on basic surface sites for polymer adsorption on acidic surface sites.

6.5.3. Work of adhesion

For the calculation of the work of adhesion in vacuum the dispersion force component of the surface tension of the substrate has to be known (see Eq. (14)). The determination of γ_s^D for inorganic hydrophilic surfaces is experimentally difficult. For instance, the amount of physically adsorbed water and the contamination by impurities may drastically change the value of γ_s^D.[47] The value obtained for γ_s^D may also depend on the method used. Fowkes[48] reports for silica a γ_s^D of 78 mJ/m^2. Other values for this parameter from the literature are $44^{[49]}$, $75.5^{[50]}$, $89.7^{[50]}$, and 71.3 $mJ/m^{2\,[51]}$. We have chosen the value reported by Fowkes to calculate the dispersive work of adhesion of a solvent on silica, using Eq. (11).

In this study, we consider the work of adhesion of polymers only with silica as the substrate. Due to the uncertainty in γ_s^D for inorganic substrates it is not very useful to compare the dispersive work of adhesion between a polymer on silica and on alumina. We just mention that Janczuk et al.[50] found γ_s^D for alumina to be about 10 mJ/m^2 larger than that for silica.

We use cyclohexane as the reference solvent for the calculation of W_{sp} for the different polymers on silica. This hydrocarbon has no specific interactions with the silica surface. Since γ_o^D for cyclohexane is equal to 25.5 $mJ/m^{2\,[10]}$ we find, with $\gamma_s^D = 78$ mJ/m^2, from Eq. (11) $W_{so}^D = 89$ mJ/m^2.

The χ_s^{po} values for adsorption from cyclohexane on silica are 0.9 higher than those from carbon tetrachloride on silica (Figure 6).[4] The adsorption energies of the polymers used relative to cyclohexane are given in the second column of Table 11. The term $\chi_s^{po}kT/A$ in Eq. (14), which is mainly determined by specific interactions, can be calculated if the surface area per polymer segment A is known. This surface area can be estimated from the molecular dimension of the polymer segment. We used the procedure described by Snyder,[6] in which molecular areas of common chemical groups, occurring in many relevant compounds, are calculated on the basis of covalent bond lengths and Van der Waals' radii. The molecular area of an arbitrary organic compound is then obtained by the summation of areas of the chemical groups in that compound.

Table 11. *Work of adhesion of several polymers on silica*

polymer	χ_s^{po} [1]	$(1/A)$ [2] (nm^{-2})	$\chi_s^{po}kT/A$ (mJ/m^2)	W_{sp} (mJ/m^2)	% specific interaction
PS	2.0	1.4	11	100	11
PBMA	3.8	1.4	21	110	19
PMMA	5.2	2.0	43	132	33
PTHF	4.8	2.5	48	137	35
PEO	6.0	3.9	97	186	52

[1] Relative to cyclohexane.
[2] Calculated on the basis of the molecular dimension.[6]

The reciprocal molecular area is equal to the number of bound polymer segments per unit area. Values of $(1/A)$ are given in the third column of Table 11 and range from 1.4 nm^{-2} for PS to 3.9 nm^{-2} for PEO. The hydroxyl density for most silicas is between 4 and 8 silanols/nm^2.[21,52] This implies that, in principle, all functional groups may be in contact with an active surface site. The specific work of adhesion, approximated by $\chi_s^{po}kT/A$, for several polymers on silica is given in the fourth column of Table 11.

The last two columns of this table give the total thermodynamic work of adhesion for the polymers on silica and the percentage of this work due to specific interactions. The data should be interpreted carefully because of the assumptions made and the uncertainties in the various input parameters. The percentage of the work of adhesion due to specific interactions increases by 3-7% when γ_s^D as reported by Van Pelt et al.[49] (i.e., 44 mJ/m^2) instead of Fowkes'[48] value of 78 mJ/m^2 is used.

The order of the polymers according to increasing work of adhesion is not the same as for the segmental adsorption energies. PTHF has a higher work of adhesion than PMMA whereas the reverse is the case for the segmental adsorption energies. This effect is due to the size of the polymer segments. When the segments are small the number of specific interactions per surface area increases and so does the work of adhesion.

About half of the work of adhesion for PEO on silica is due to specific interactions. This contribution is even less for the other polymers. Hence, dispersive interactions are very important for the work of adhesion of polymers on silica.

6.6. Conclusions

The segmental adsorption energies relative to carbon tetra-chloride for the polymers PS, PBMA, PTHF, PMMA, and PEO increase in the given order on both silica and alumina. Each individual polymer has a lower adsorption energy on alumina as compared to silica. Polymers with more methylene groups per segment in the main chain or with larger alkyl groups attached to the functional groups have a lower adsorption energy.

Polymers can serve as standards for the adsorption energy of solvents and displacers. Unlike the results reported by Snyder[7,8], the adsorption energies of strongly adsorbing solvents do not depend on the concentration in our experiments.

The work of adhesion of pure polymers on silica is of the order of 100-200 mJ/m^2. The contribution of specific interactions to the total work of adhesion relative to vacuum range from about 10% for

159

PS to about 50% for PEO. The contribution of the specific interactions to the total work of adhesion is not only determined by the segmental adsorption energy but also by the area of a segment.

6.7. References

1. Fowkes, F. M. *J. Adhesion Sci. Technol.* **1987**, 1, 7.
2. Cohen Stuart, M. A.; Fleer, G. J.; Scheutjens, J. M. H. M. *J. Colloid Interface Sci.* **1984**, 97, 515.
3. Cohen Stuart, M. A.; Fleer, G. J.; Scheutjens, J. M. H. M. *J. Colloid Interface Sci.* **1984**, 97, 526.
4. Van der Beek, G. P.; Cohen Stuart, M. A.; Fleer, G. J.; Hofman, J. E. *Langmuir* **1989**, 5, 1180.
5. Silberberg, A. *J. Chem. Phys.* **1968**, 48, 2835.
6. Snyder, L. R. *Principles of Adsorption Chromatography*; Marcel Dekker: New York, 1968.
7. Snyder, L. R. In *High-performance liquid chromatography*, 3rd ed.; Horvath, C., Ed.; Academic Press: New York, 1983, p 157.
8. Snyder, L. R.; Glajch, J. L. *J. Chromatogr.* **1981**, 214, 1.
9. Fowkes, F. M. *Ind. Eng. Chem.* **1964**, 12, 40.
10. Fowkes, F. M.; Riddle, F. L.; Pastore, W. E.; Weber, A. A. *Colloids and Surfaces* **1990**, 43, 367.
11. Drago, R. S.; Wayland, B. B. *J. Am. Chem. Soc.* **1965**, 87, 3571.
12. Drago, R. S.; Vogel, G. C.; Needham, T. E. *J. Am. Chem. Soc.* **1971**, 93, 6014.
13. Tanaka, T.; Donkai, N.; Inagaki, H. *Macromolecules* **1980**, 13, 1021.
14. Inagaki, H. In *Fractionation of synthetic polymers*; Tung, L. H., Ed.; Marcel Dekker: New York, 1977, p 649.
15. Jednacak-Biscan, J.; Pravdic, V.; Haller, W. *J. Colloid Interface Sci.* **1988**, 121, 345.
16. Ghiotti, G.; Garrone, E.; Boccuzzi, F. *J. Phys. Chem.* **1987**, 91, 5640.
17. Kawaguchi, M. Yamagiwa, S.; Takahashi, A.; Kato, T. *J. Chem. Soc. Faraday Trans.* **1990**, 86, 1383.
18. Fontana, B. J; Thomas, J. R. *J. Phys. Chem.* **1961**, 65, 480.

19. Killmann, E.; Fulka, C.; Reiner, M. *J. Chem. Soc. Faraday Trans.* **1990**, 86, 1389.

20. Kobayashi, K.; Araki, K.; Imamura, Y. *Bull. Cem. Soc. Jpn.* **1989**, 62, 3421.

21. Iler, R. K. *The Chemistry of Silica*; John Wiley & Sons: New York, 1979.

22. Zhdanov, S. P.; Kosheleva, L. S., Titova, T. I. *Langmuir* **1987**, 3, 960.

23. Peri, J. B. *J. Phys. Chem.* **1965**, 69, 220.

24. Von Stoltz, H.; Knözinger, H. *Kolloid-Z. u. Z. Polymere* **1971**, 243, 71.

25. Cross, S. N. W.; Rochester, C. H. *J. Chem. Soc. Faraday Trans. 1* **1981**, 77, 1027.

26. Rochester, C. H.; Yong, G. H. *J. Chem. Soc. Faraday Trans. 1* **1980**, 76, 1466.

27. Kiviat, F. E.; Petrakis, L. *J. Phys. Chem.* **1973**, 77, 1232.

28. Morterra, C.; Chiorino, A.; Ghiotti, G.; Garrone, E. *J. Chem. Soc. Faraday Trans. 1* **1978**, 74, 271.

29. Healy, M. H.; Wieserman, L. F.; Arnett, E. M.; Wefers, K *Langmuir* **1989**, 5,114.

30. Morimoto, T.; Suda, Y.; Nagao, M. *J. Phys. Chem.* **1985**, 89, 4881.

31. Snyder, L. R. *J. Chromatogr.* **1967**, 28, 432.

32. Holmes-Farley, S. R. *Langmuir* **1988**, 4, 766.

33. Marshall, K.; Rochester, C. H. *J. Chem. Soc. Faraday Trans. 1* **1975**, 71, 2478.

34. Rochester, C. H.; Trebilco, D.-A. *J. Chem. Soc. Faraday Trans. 1* **1978**, 74, 1137.

35. Nagao, M.; Suda, Y. *Langmuir* **1989**, 5, 42.

36. Glöckner, G. *J. Polym. Sci. Polym. Symp.* **1980**, 68, 179.

37. Fuchs, R.; Peacock, L. A.; Stephenson, W. K. *Can. J. Chem.* **1982**, 60, 1953.

38. Sharma, S. C.; Lakhanpal, M. L.; Rumpaul, M. L. *Indian J. Chem.* **1981**, 20A, 770.

39 Bristow, G. M.; Watson, W. F. *Trans. Faraday Soc.* **1958**, 54, 1742.

40. Orwoll, R. A. *Rubber Chem. Technol.* **1977**, 50, 451.

41. Höcker, H.; Flory, P. J. *Trans. Faraday Soc.* **1971**, 67, 2270.

42. Kawaguchi, M.; Chikazawa, M.; Takahashi, A. *Macromolecules* **1989**, 22, 2195.

43. Kawaguchi, M. *Rep. Chem. Mat. R & D Found.* **1989**, 4, 117.

44. Kamiyama, F.; Inagaki, H. *Bull. Inst. Chem. Res., Kyoto Univ.* **1974**, 52, 393.

45. Van der Beek, G. P.; Cohen Stuart, M. A. *J. Phys. (Paris)* **1988**, 49, 1449.

46. Van der Beek, G. P.; Cohen Stuart, M. A.; Cosgrove, T. *Langmuir,* **1991**, 7, 327.

47. Shafrin, E. G.; Zisman, W. A. *J. Am. Ceram. Soc.* **1967**, 50, 478.

48. Fowkes, F. M. In *Chemistry and Physics of Interfaces, Vol. 1*; American Chemical Society: Washington, D. C., 1965, p 5.

49. Van Pelt, A. W. J.; Weerkamp, A. H.; Uyen, M. H. W. J. C.; Busscher, H. J.; de Jong, H. P.; Arends, J. *Appl. Environ. Microbiol.* **1985**, 49, 1270.

50. Janczuk, B.; Bialopiotrowicz, T. *Clays Clay Miner.* **1988**, 36, 243.

51. Wojcik, W.; Bilinski, B. *Colloids Surfaces* **1988**, 30, 275.

52. Peri, J. B.; Hensley, A. L. *J. Phys. Chem.* **1968**, 72, 2926.

Summary

This thesis describes a method to determine the thermodynamic (reversible) adhesion strength of polymers on inorganic solids.

This adhesion strength of polymers is an important factor in many applications. Examples are the quality and properties of glass fibre reinforced composites, coatings, and adhesives.

The key idea of the method is that the thermodynamic adhesion strength can be obtained from polymer displacement experiments. Polymers adsorbed from solution on an inorganic adsorbent can be desorbed by adding a more strongly adsorbing solvent component (a so-called *displacer*). At a certain critical displacer concentration (the *critical point*) the polymer is entirely desorbed by the displacer. Cohen Stuart *et al.*[1] showed that this critical solvent composition can be related to the effective adsorption energy per segment. Using an apolar solvent, the thermodynamic work of adhesion of a polymer can be estimated from this effective adsorption energy, the segmental cross-section, the solvent surface tension, and the dispersion contribution of the surface free energy of the substrate.

In this study, critical points have been measured for various systems by 5 different methods. Some methods do not only give the critical point, but also specific information about the conformational state of adsorbed polymers. The following procedures were used:
- The adsorbed amount of polymer as a function of the displacer concentration was determined indirectly by measuring the free polymer concentration in solution (see chapters 2, 4, and 5). From the mass balance the adsorbed amount can then be calculated. This method is, however, very time consuming and often difficult to carry out because of analytical problems.
- Thin-Layer Chromatography was used to measure the interfacial residence time of polymer on the substrate as a function of the eluent composition. The critical point is found from the (sharp) transition between full retention (where the polymer is immobile on the thin layer) and no retention (where the polymer moves with the eluent front). In adsorption chromatography studies, the *solvent strength* model of Snyder[2] is frequently used. When this model is

applied to polymer adsorption, it turns out to be similar to the model of Cohen Stuart *et al.*[1] Solvent strength data, which are available in the chromatographic literature, can also serve as a useful source of information for polymer adsorption and adhesion studies. The most important advantage is that the cumbersome procedure to determine separately the displacer energy can now be avoided. Chromatographic experiments are described in chapters 2 and 6.

- Attenuated Total Reflection Infrared Spectroscopy was used to determine critical points and the kinetics of polymer desorption (chapter 3). The advantages of this technique are that the measurements can be done *in situ*, and that different species on the surface can be detected simultaneously. The rate of polymer desorption by a low molecular weight displacer is much more rapid (i.e., within a few minutes) than the rate of desorption by a displacing polymer. The latter process may have time scales of the order of weeks. Polymer desorption by a more strongly adsorbing polymer seems to occur segment-by-segment.

- Dynamic Light Scattering was used to measure the hydrodynamic thickness of adsorbed polymer layers (chapter 4). This thickness is dominated by the free chain ends (*tails*). The results show that the hydrodynamic layer thickness δ_h is constant or increases slightly with increasing amount of displacer up to the critical point and then drops sharply to zero. The adsorbed amount decreases much more gradually as a function of the amount of displacer added. All data agree with most earlier measurements on different substrates, and corroborate the theoretical result that the segmental adsorption energy has no effect on δ_h until very close to full desorption.

- Chapter 5 describes Proton Magnetic Relaxation measurements of silica dispersions carried out as a function of polymer coverage, solution *pH*, and amount of displacer added. We find that the spin-lattice relaxation rate of the solvent is enhanced as a result of polymer adsorption and that, with proper calibration, this enhancement can be used to obtain the amount of polymer segments directly bound to the surface (the so-called *trains*). It turned out that the number of train segments is affected much more strongly by addition of displacer than the tail segment density, as measured by dynamic light scattering.

By means of the methods described above, we determined adhesion strengths for 5 different polymers on silica and alumina. In order to study the effects of the functional group and the chain structure of the polymer on the adhesion strength we choose the following polymers: polystyrene, poly(butyl methacrylate), poly(tetrahydrofuran), poly(methyl methacrylate), and poly(ethylene oxide). The given order of these polymers corresponds to an increasing segmental adsorption energy on both substrates. We find that polymers with more methylene groups per segment in the main chain or with larger alkyl side groups have a smaller adsorption strength. The adsorption energy for each individual polymer is higher on silica than on alumina.

The displacer concept may also be used to determine the adsorption energy of *solvents* but this time *polymers* are used as a standard. Doing so, we obtained the same trends for the adsorption energy of solvents as for polymers with respect to the functional group and the size of the monomer unit.

In chapter 6 we estimate the reversible work of adhesion for polymers in vacuum from the segmental adsorption energy. For pure polymers on silica, this work is of the order of 100-200 mJ/m^2. It turns out that the contribution of specific interactions to the total work of adhesion ranges from about 10% for polystyrene to about 50% for poly(ethylene oxide). The largest contribution to the work of adhesion on silica with respect to vacuum is thus due to non-specific, dispersive interactions.

References

1. Cohen Stuart, M. A.; Fleer, G. J.; Scheutjens, J. M. H. M. *J. Colloid Interface Sci.* **1984**, 97, 515.
2. Snyder, L. R. *Principles of Adsorption Chromatography*; Marcel Dekker: New York, 1968.

Samenvatting

Verdringing van Geadsorbeerde Polymeren

Een systematisch onderzoek naar de wisselwerking tussen segmenten en een oppervlak

Dit proefschrift beschrijft een methode om de thermodynamische adhesiesterkte (hechting) van polymeren op anorganische materialen te bepalen. In het bijzonder wilden we weten wat het effect is van de functionele groep en de ketenstructuur op deze hechting.

Adhesie tussen polymeer en anorganische materiaal is vooral belangrijk voor de kwaliteit en eigenschappen van coatings, glasvezelversterkte polymeercomposieten en lijmen.

Het centrale idee van de beschreven methode is dat de thermodynamische adhesiearbeid kan worden bepaald door middel van desorptie-experimenten. Polymeer, dat geadsorbeerd is op een vast adsorbens vanuit oplossing, kan worden gedesorbeerd door een oplosmiddelcomponent (een *verdringer*) toe te voegen die een sterkere interactie heeft met het substraatoppervlak dan de segmenten van het betreffende polymeer. Bij een bepaalde verdringerconcentratie is het polymeer juist volledig gedesorbeerd. Deze concentratie wordt de kritische verdringerconcentratie of, kortweg, het *kritisch punt* genoemd en kan gerelateerd worden aan de effectieve adsorptie-energie per polymeersegment met behulp van een model ontwikkeld door Cohen Stuart *et al.*[1] Door gebruik te maken van een oplosmiddel dat geen specifieke interacties heeft met het substraat kan de adhesiearbeid van het polymeer berekend worden uit de effectieve adsorptie-energie per segment, de doorsnede van het segment, de grensvlakspanning van het oplosmiddel en het dispersieve gedeelte van de oppervlaktespanning van het substraat.

In dit onderzoek zijn kritische oplosmiddelsamenstellingen bepaald voor diverse systemen met 5 verschillende methoden. Sommige bepalingsmethoden geven naast het kritische punt ook

specifieke informatie over de conformatie van het geadsorbeerde polymeer.

De bewerkelijkste methode om het kritische punt te bepalen is via *analyse van de evenwichtsoplossing* (zie hoofdstukken 2, 4 en 5). De evenwichtsoplossing (met vrij polymeer) moet hiervoor eerst gescheiden worden van substraatdeeltjes met eventueel geadsorbeerd polymeer. Daarna wordt de concentratie polymeer in de evenwichtsoplossing analytisch bepaald. Via de massabalans wordt de geadsorbeerde hoeveelheid polymeer gevonden als functie van de verdringerconcentratie. Het gebruik van deze methode stuit soms op analytische problemen bij de concentratiebepaling.

Dunne-laag-chromatografie werd gebruikt om de retentie van polymeer op het dunnelaag materiaal te meten als functie van de samenstelling van het elutiemiddel. Het kritische punt wordt gemarkeerd door de (scherpe) overgang tussen totale retentie (polymeer loopt niet) en geen retentie (polymeer loopt mee met het elutiefront). Bij adsorptie-chromatografie wordt vaak gebruik gemaakt van het concept *elutiesterkte*, geïntroduceerd door Snyder.[2] Als dit model wordt toegepast op polymeeradsorptie, blijkt het veel overeenkomst te vertonen met het zojuist genoemde model van Cohen Stuart *et al.*[1] Het voordeel is dat in de literatuur getabelleerde gegevens over de elutiesterkte van oplosmiddelen een nuttige bron van informatie vormt voor de bepaling van de adsorptiesterkte van polymeren. In plaats van zelf de adsorptie-energie van verdringers te meten, hetgeen nogal lastig is, kunnnen nu bekende elutiesterkten gebruikt worden. Chromatografische experimenten worden beschre-ven in de hoofdstukken 2 en 6.

Infraroodspectroscopie, gebruikmakend van *totale interne reflectie*, werd toegepast om zowel kritische punten als de kinetiek van polymeerdesorptie te meten. Hoofdstuk 3 is volledig hieraan gewijd. De voordelen van deze techniek zijn dat de metingen *in situ* kunnen worden uitgevoerd en dat tegelijkertijd verschillende componenten aan het substraatoppervlak kunnen worden gedetecteerd. Polymeer-desorptie door een laag moleculaire verdringer geschiedt binnen enkele minuten. Desorptie door een ander, sterker adsorberend polymeer is daarentegen een veel langzamer proces; het kan dan weken duren voordat de evenwichtstoestand is bereikt. De desorptie

van het ene polymeer en de adsorptie van het andere lijkt segment na segment plaats te vinden.

Met *dynamische lichtverstrooiing* werd de hydrodynamische laagdikte van geadsorbeerd polymeer gemeten (hoofdstuk 4). Deze laagdikte wordt vooral bepaald door de losse einden (*staarten*) van geadsorbeerde polymeermoleculen. De hydrodynamische laagdikte (en dus ook de hoeveelheid staartsegmenten) blijft constant met afnemende adsorptie-energie (toenemende verdringerconcentratie) tot vlak voor het kritische punt, waarna deze dikte zeer sterk afneemt tot nul. De geadsorbeerde hoeveelheid polymeer neemt veel geleidelijker af met toenemende verdringerconcentratie. Dit alles is in overeenstemming met berekeningen op basis van de theorie van Scheutjens en Fleer.

Hoodstuk 5 beschrijft *relaxatiemetingen met (proton)kernspinresonantie* uitgevoerd aan silica dispersies als functie van de concentratie polymeer en de hoeveelheid verdringer. De magnetische relaxatiesnelheid van het *oplosmiddel* neemt toe door polymeeradsorptie aan de silicadeeltjes, doordat meer oplosmiddelmoleculen in de solvatatielaag rond de polymeersegmenten geïmmobiliseerd worden. Het blijkt dat deze toename evenredig is met de hoeveelheid direct aan het oppervlak gebonden segmenten (*treinsegmenten*). Net als de totaal geadsorbeerde hoeveelheid polymeer neemt de hoeveelheid treinsegmenten relatief geleidelijk af met toenemende concentratie verdringer.

Voor de basische polymeren polystyreen, polybutylmethacrylaat, polytetrahydrofuraan, polymethylmethacrylaat en polyethyleenoxide werd de adsorptiesterkte op zowel silica als aluminiumoxide bepaald. De gegeven volgorde van deze polymeren correspondeert met toenemende adsorptie-energie per segment op beide adsorbentia. Polymeren met meer methyleengroepen per segment in de hoofdketen of met grotere alkyl-zijgroepen hebben een lagere adsorptiesterkte, corresponderend met een lagere kritische verdringerconcentratie. Voor elk afzonderlijk polymeer is de adsorptie-energie op aluminiumoxide lager dan op silica.

Het model van Cohen Stuart *et al.*[1] kan ook worden gebruikt om de adsorptie-energieën van oplosmiddelen (verdringers) te bepalen,

maar nu wordt het polymeer als standdaard gebruikt. Voor zowel verdringers als polymeren werden dezelfde trends met betrekking tot het effect van de functionele groep en de monomeergrootte op de adsorptie-energie waargenomen.

In hoofstuk 6 hebben we schattingen gemaakt van de totale reversibele adhesiearbeid voor de genoemde polymeren op silica in vacuüm. De waarden voor deze adhesiearbeid liggen tussen 100 en 200 mJ/m^2. De bijdrage van specifieke interacties tot de totale adhesiearbeid loopt van 10% voor polystyreen tot ongeveer 50% voor polyethyleenoxide. Het grootste deel van de totale adhesiearbeid van de polymeren (behalve voor polyethyleenoxide) is derhalve het gevolg van niet specifieke, dispersieve interacties.

Referenties

1. Cohen Stuart, M. A.; Fleer, G. J.; Scheutjens, J. M. H. M. *J. Colloid Interface Sci.* **1984**, 97, 515.
2. Snyder, L. R. *Principles of Adsorption Chromatography*; Marcel Dekker: New York, 1968.

Curriculum Vitae

Gerrit van der Beek werd op 28 september 1964 geboren in Genderen (Land van Heusden & Altena). In 1982 behaalde hij het diploma Atheneum B aan het Willem van Oranje College te Waalwijk. In datzelfde jaar ging hij scheikunde studeren aan de Rijksuniversiteit te Utrecht. Het doctoraalexamen met als onderzoeksspecialisatie Fysische en Colloïdchemie en keuzevakken Chemieonderwijs en Fysische Chemie werd in 1987 met succes afgelegd. Van mei 1987 tot mei 1991 was hij als assistent in opleiding (AIO) verbonden aan de vakgroep Fysische en Kolloïdchemie van de Landbouwuniversiteit te Wageningen. Gedurende deze periode is het in dit proefschrift beschreven onderzoek uitgevoerd. Tijdens zijn aanstelling als AIO heeft hij enkele maanden onderzoek verricht aan "The School of Chemistry of Bristol University" in Engeland. Vanaf 1 juni 1991 is hij in dienst bij Philips Forschung in Aken, Duitsland.

Nawoord

Graag wil ik een ieder, die op welke wijze dan ook heeft bijgedragen aan het tot stand komen van dit proefschrift, van harte bedanken. Een paar mensen wil ik in dit verband speciaal noemen.

Mijn moeder heeft mij zolang ik me kan herinneren op allerlei terreinen gesteund en gestimuleerd. Zij heeft me de mogelijkheid gegeven om te studeren. Bedankt ma!

Martien Cohen Stuart, ik ben onder de indruk van jouw kreativiteit. De plastic vaten vol met zand en wc-papier als trillingsdempers voor de optische opstelling is daar een mooi voorbeeld van. Ik vaarde wel bij jouw goede ideeën!

Gerard Fleer, ik ken maar weinig mensen die zo "to the point" zijn als jij. Ik wil je bedanken voor het vertrouwen dat je in me stelde en voor de opbouwende kritiek.

Het was zeer prettig samenwerken met Tetje Jensma uit Canada ("the girl who worked with the *famous* colloid group in Holland"). Tetje, ik hoop dat je inmiddels de dubbele betekenis van het woord "monster" weet.

Met Riet van de Steeg en Marcel Böhmer heb ik lange tijd met veel plezier mijn kamer gedeeld. Riet, de sokken met geborduurde roosjes die ik van je heb gekregen, trek ik nog regelmatig aan. Marcel, je zou altijd nog een taart voor me bakken, die ik in één keer moet opeten.

Ans Hofman heeft veel (soms saaie) experimenten voor mij uitgevoerd. Ans, ik kan me voorstellen dat je geen tlc-plaatje meer kan zien.

Hoewel het werk van de doctoraalstudenten Fried Faassen en Lenie Braks niet expliciet in dit proefschrift is terug te vinden, is het er wel voor van belang geweest. Lenie, tegenwoordig doen we alle lichtverstrooiingsexperimenten met een *gekantelde* horizontaal gepolariseerde laser.

I am grateful to Terence Cosgrove of the Bristol School of Chemistry for helping me with the NMR experiments. Terence, your typical phrases "I am so busy" and "let's make coffee" will keep for ever in my mind. I acknowledge also the hospitality experienced from the group of Bristol.

Ik heb dankbaar gebruik mogen maken van het FTIR apparaat op het RIKILT. Joop Weseman verleende daarbij regelmatig deskundige hulp.

Wat voor werkkring ik ook zal krijgen, een tweede Bert Bouman zal er waarschijnlijk niet rondlopen. Bert, bedankt voor al de dropjes en je hulp.

Alle andere mensen, die ik erkentelijk ben, worden op een speelse wijze genoemd aan het einde van dit nawoord. Mocht u zich tijdens de promotieplechtigheid

vervelen, dan kunt u uitzoeken hoeveel personen (met voor- en achternaam) op deze manier worden bedankt.

Tot slot wil ik al mijn (ex)medewerkers bedanken voor de bijzonder prettige werksfeer waarin ik 4 jaar mocht verkeren. Ik denk met plezier terug aan de volleybalwedstijden, de Veluweloop, het roeien, de prijsuitreiking bij feestjes, etc. Met een traan in m'n oog en een glimlach om mijn mond neem ik afscheid van de vakgroep. Het gaat jullie allen goed!

Gerrit

```
p t a a r t j e n k y w s e e r v n a v t e n a j t a a i
j e j o s e z e e v a t g e e t s e d n a v t e i r f l a
e e t l r c a l l e n o b h k o n i n g n t y d p a a j r
j a b e o o a e m i c h e l m s o b n i t r a m s u r a t
o e l e r u n s h y e n e b n n a m f o h s n a k t e s s
d r o e r g i a m t n g a h a r t e l i j k n m a s r t f
l a a k o t r s l y v l y m g e r a r d f l e e r n s s o
e r a f i n v i v d e o t s r u t a b e m o t r b e r n l
v g r m e e b a f e w r n e b u s s f r a n e e e h e e s
e n t t b l n r n f r e e v r e u j a e b m e u i o k j n
n i s f e b i y e d i h g e n e r b o m h o o q n c a t e
r l l r e t s s e m e t a h s y n t t o c e e i e n m u i
a e y e s a j e r l e r h g l g e c b i p r n n l e r e m
b s k d o s e e r a k r w s e a n l e o r w a o j i e h o
r s n e s t h a j s e l a a g n e i k c u r e m o t e c c
e e a l b e n s p e e l i n l c h a l e o m e s k r l s a
t b h g h a r m j a n a s w r e e d a l k s a g e a s n j
e s o e r n n g n e s s a a f d e i r f u e g n a m n a g
p a j r a k g e o r g e m d b e d a n k t v i r f a a j e
m a t s e i p e t n e l n a v n y w e d u o b m o o r n b
k l o m a e l u t n i a s s u o t e n n o v y o e v f e a
o k c a d n e d n i l r e d n a v a k n i t a k r e e s k
```